Characterization of spermatogenic histone variants with special emphasis on histone H2A.X and double stranded break repair

by

Andra Jia Jia Li
B.Sc., University of Victoria, 2004

A Thesis Submitted in Partial Fulfillment
of the Requirements for the Degree of

DOCTOR OF PHILOSOPHY

in the Faculty of Science, Department of Biochemistry and Microbiology

Supervisory Committee

Characterization of spermatogenic histone variants with special emphasis on histone H2A.X and double stranded break repair

by

Andra Jia Jia Li
B.Sc., University of Victoria, 2004

Supervisory Committee

Dr. Juan Ausió, (Department of Biochemistry and Microbiology)
Supervisor

Dr. Robert D. Burke, (Department of Biochemistry and Microbiology)
Departmental Member

Dr. Claire G. Cupples, (Department of Biochemistry and Microbiology)
Departmental Member

Dr. John S. Taylor, (Department of Biology)
Outside Member

Abstract

Supervisory Committee
Dr. Juan Ausió, (Department of Biochemistry and Microbiology)
Supervisor
Dr. Robert D. Burke, (Department of Biochemistry and Microbiology)
Departmental Member
Dr. Claire G. Cupples, (Department of Biochemistry and Microbiology)
Departmental Member
Dr. John S. Taylor, (Department of Biology)
Outside Member

The fundamental subunit of chromatin, known as a nucleosome, is comprised of DNA wrapped around two H2A-H2B dimers and one H3-H4 tetramer. This structure perpetuates itself and together with linker histones (histone H1) give rise to the chromatin fibre. This causes compaction of DNA within the nucleus of a eukaryotic cell, which have inhibitory effects in terms of both its accessibility and metabolism. By modifying chromatin structure, cells can regulate and fine-tune different cellular processes, such as DNA repair, replication, transcription and spermatogenesis. Chromatin structure can be modulated by three main mechanisms: covalent post-translational modification of histone tails, incorporation of histone variants and recruitment of chromatin remodelling complexes. In this thesis, the contribution of histone variants and their post-translational modifications to chromatin structure will be discussed.

In Chapter 1, I review the role of H2A.X in DNA double stranded break (DSB) repair and other less studied cellular processes, such as transcription and cell cycle. In addition, this chapter also introduces a putative model for the role of H2A.X phosphorylation in DNA DSB repair. In Chapter 2, our results demonstrate that S139 and T136 of H2A.X are both phosphorylated during DNA DSB repair. These two post-

translational modifications are functionally different in that S139E and T136A/S139E mutants partition to different chromatin fractions. Furthermore, we show that nucleosomes containing H2A.X are less stable compared to nucleosomes with canonical H2A. The destabilizing effect is more prominent in the nucleosomes containing H2A.X phosphorylated by DNA-dependent protein kinase suggesting that the post-translational modifications of histone variants and histone variant itself have a direct structural role in chromatin integrity.

Recombinantly expressed H2A.Bbd has also been shown to modify chromatin structure by destabilizing nucleosomes in a way that resembles that of H2A.X. However, the native form of this H2A.Bbd has never been identified *in vivo*. Chapter 3 provides evidence for the presence of native H2A.Bbd in mammalian testis and human sperm.

Histone variant hTSH2B, which was found in only a fraction of mature human sperm, has been characterized most recently. In Chapter 4, we report the structural characterization of this variant in the context of other core histones (histone octamer) and in a nucleosome. Although an hTSH2B-containing nucleosome did not show structural alterations compared to its canonical counterpart, hTSH2B octamers were shown to be less stable.

Finally, we addressed the disagreement in the literature as to whether or not H1t, a linker histone variant specific to mammalian testis, is phosphorylated during spermatogenesis. Chapter 5 shows that native H1t is phosphorylated. The sites of phosphorylation of H1t were determined. The phosphorylation of histone H1 at the C-terminal domain has been shown to significantly weaken its affinity for the chromatin

fibre thus inferences chromatin structure. It is not surprising that the newly identified phosphorylation sites of H1t within this region also serve similar function.

The four histone variants analyzed in this thesis: H2A.X, H2A.Bbd, hTSH2B and H1t, are all expressed in mammalian germ cells and hence play an important role in spermiogenesis. Their structural contribution may help explain some of the complex chromatin transitions involved in this multifaceted cell differentiation process.

Table of Contents

List of Tables

List of Figures

Acknowledgments

I would like to thank my amazing supervisor, Juan, for his guidance and encouragements through my graduate years. Your passion for science is infectious and you make working in the lab exciting and fun. In addition to your support professionally, I thank you for being a fatherly figure to me through my toughest times in life. Thanks for all of the things that you have done for me and you will always have a special place in my heart.

I thank my supervisory committee, Dr. Clare Cupples, Dr. Robert Burke and Dr. John Taylor, for your suggestions and criticisms through my graduate years.

Thanks to all of the current and past Ausió lab members, Deanna, Lindsay, Toyotaka, Ali, Begonia, Anita, Chema, Wade, Igor, Ron, Lyndsay, Brad, Rodrigo, Corina and Katie. You guys have been a great group and you made coming to work fun.

Special thanks to Dr. Rozanne Poulson for being a great mentor and a great person to talk to when I am lost in life. Thanks to Melinda, Deb and John for all your administrative help and for looking out for graduate students. Last but not least, I would like to thank Albert, Steve and Scott for all of your technical support and the daily hallway giggles.

To my friends, I have been fortunate enough to be blessed with great friends. Hong and Melody, we have been great friends since high school and thanks for your encouragements and mental support through my graduate years. Tina, Kevin, Hao and Johnny, I thank you for being my stress management team through countless smashes in our badminton games and being there for me when I needed you.

Dedication

To my loving husband, Ambrose, I thank you for all your support through the years and stand by me through good times and bad times. I could not have done it without you. You are my best friend, my badminton partner and most importantly, my soul mate. I love you.

To my grandfather, I thank you for checking on me often to make sure that my thesis is getting done. Every little bit of wisdom and encouragement, perhaps a tiny bit of nagging, from you is a motivation for me to reach my goal. Although I am not with you in China, I will always remember the life lessons that you taught me.

To my beautiful auntie, my life would be forever changed if I didn't have your support. You gave me a sense of family by treating me like your children.

To my strong and caring mother, you are the best mom one could ever ask for. Fifteen years ago you brought me to Canada with you. Speaking no English at the time, you managed to raise me and gave me the best study environment that you could provide. Words cannot describe how thankful I am. Thank you, mom, for always believing in me.

General Introduction and overview

In the eukaryotic cell, DNA is organized into dynamic structure called chromatin in the presence of histones. There are two major types of histones: core histones and linker histones. Two copies each of the four core histones, H2A, H2B, H3 and H4, are arranged into a histone octamer, which 146-180 bp of DNA are wrapped (Ausio and Abbott, 2004) forming a structure that is known as the nucleosome core particle (NCP). Each of the four core histones has a central histone fold domain, which consists of three alpha helices connected by two loops (Arents and Moudrianakis, 1995). The core histones interact via the histone fold domain providing stability to the nucleosome (Luger *et al.*, 1997). The histone fold is flanked by regions that have very little secondary or tertiary structure, known as the histone tails, with a less well defined contribution to the stability of the nucleosome (Ausio and Abbott, 2004). These N- or C- terminal tails interact extensively with the DNA. In the chromatin fiber, NCPs are connected by lengths of linker DNA. Linker histones together with some of the core histone tails bind to these linker DNA domains play an important role in the folding of the chromatin fiber.

It was initially thought that histones provided a passive packaging structure for DNA, which prevents DNA from becoming an unmanageable tangle. In recent years, it has become apparent that chromatin structure is a dynamic platform for some of the most important cellular processes that are involved in spermiogenesis, X chromosome inactivation, chromosome segregation, DNA replication, transcription, recombination and repair. All of them involve transient global or local changes in chromatin conformation. Such dynamic properties of chromatin are mediated by the incorporation of histone variants, the introduction of post-translational modification of canonical histones and/or

histone variants and the presence of chromatin remodelling complexes (Thambirajah *et al.*, 2009). In this thesis, I will be focusing on germline-specific histone variants, H2A.X, H2A.Bbd, hTSH2B and H1t, their particular biological functions and unique features, such as their PTMs and their structural contribution to the nucleosome conformation.

Histone variants

From a structural point of view, core histone variants can be grouped into two major classes, homomorphous and heteromorphous (West and Bonner, 1980). The homomorphous class consists of histone variants that differ from their canonical counterpart only by a few residues and they usually cannot be resolved on a sodium-dodecyl-sulfate (SDS)-PAGE gel. In this thesis, two homomorphous core histone variants, H2A.X and hTSH2B, are discussed in Chapter 1, 2 and 4. Although their primary structures are very similar to their canonical counterpart, we found that they both impart alteration to the nucleosome structure and chromatin function. Histone variants from the heteromorphous class exhibit a significant departure in their amino acid sequence from that of their canonical counterpart and they can be resolved on a SDS-PAGE gel. H2A.Bbd discussed in Chapter 3 is considered to be a heteromorphous histone H2A variant, in that it shares only 48 % identity to histone H2A (Chadwick and Willard, 2001).

Histone H1, also referred to as linker histone, represents a highly heterogeneous group of histones. The somatic histone H1 has small variations in amino acid sequence is referred to as microheterogeneity (Cole, 1984). They display their sequence variation mainly at the N- and C-terminal tails. Macroheterogeneous variants of histone H1 are a

group of specialized, tissue-specific linker histones. Histone H1t discussed in Chapter 5 is a H1 variant specific to the testes that belongs to this later group.

Post-translational Modification

The covalent linkage of chemical moieties, such as acetylation, phosphorylation, methylation, poly ADP-ribosylation, and ubiquitination, to core and linker histones are becoming well characterized (Ausio, 2004). A histone code hypothesis has been proposed to explain the complex PTM patterns and their biological consequences (Strahl and Allis, 2000). This hypothesis states that PTMs could serve as a signal for *trans* factors, or act in *cis* to structurally modify the local chromatin region. Histone variants add an extra layer of complexity not only as they allow compositional variation to individual nucleosomes, but also can be further modified through PTMs. Histone acetylation and phosphorylation are the main PTMs in this thesis. Histone acetylation is one of the better characterized histone modifications that involves the covalent linkage of an acetyl group to the Ɛ-amino group of lysine residue mainly at the N-terminal tails of core histones. This PTM has been linked to eukaryotic gene expression (Allfrey *et al.*, 1964), histone deposition during DNA replication (Annunziato and Hansen, 2000) and the removal of histones during mammalian spermiogenesis (Oliva and Dixon, 1991). Like histone acetylation, histone phosphorylation is a dynamic post-translational modification and its functional significance appears to be equally multifaceted ranging from transcriptional inhibition (Zhang *et al.*, 2004) to DNA DSB repair (Li *et al.*, 2005a). Whereas the phosphorylation of mammalian H2A.X at S139 is well-known marker for DNA double stranded breaks

(DSBs) (Rogakou *et al.*, 1998), the phosphorylation of H1t during spermiogenesis has been in the centre of a controversy (Khadake *et al.*, 1994; Meistrich *et al.*, 1994).

Histone Variants in the Testis

Mammalian spermatogenesis is a dramatic chromatin remodelling processes that takes place in testis. Spermatogenesis is the process during which male spermatogonia differentiate into mature spermatozoa, also known as sperm. During the post-meiotic maturation of male haploid germ cells, or spermiogenesis, histones are actively replaced by different, testis-specific histone variants (Meistrich, 1989) and then by small basic proteins, which in mammals are transition proteins and protamines (Govin *et al.*, 2004). Curiously, human sperm retains 10-15% of histone variants (Tanphaichitr *et al.*, 1978) whereas replacement of histones variants by protamines is almost complete in mice (Churikov *et al.*, 2004). This process results in the packaging of the haploid genome into a genetically inert nucleus, in which the DNA is at least sixfold more highly condensed than in mitotic chromosomes of somatic cells (Frehlick *et al.*, 2007; Ward and Coffey, 1991). However, the mechanism underlying the histone to protamines transition is elusive. Evidence supports the model that histone removal during spermiogenesis is preceded by a massive incorporation of histone variants and post-translational modifications of these histones (Govin *et al.*, 2004; Meistrich *et al.*, 1985). All of the histone variants studied in this thesis are enriched in the mammalian testis compared to their canonical counterparts and they are synthesized and replace their canonical counterparts during pre-meiotic, meiotic and post-meiotic stages of spermatogenesis. H2A.X and its phosphorylated form are highly enriched in testis, specifically in the

spermatogonia, probably due to the presence of DNA DSB during homologous recombination of germ cell differentiation (Meistrich *et al.*, 1985). Phosphorylated H2A.X peaks in leptotene spermatocytes that correlate with initiation of meiotic DSBs (Mahadevaiah *et al.*, 2001b). The determination of the role of H2A.X in DNA DSB repair could shed some lights on its involvement in spermiogenesis. Chapter 1 reviews the recent developments in H2A.X. In Chapter 2, I hypothesize that the phosphorylation at S139 and possibly at S/T136 of H2A.X has structural and signalling functions that may allow chromatin to adopt a conformation accessible to recruitment of DNA DSB complexes to the site of DNA damage or DNA recombination. Although the expression of H2A.Bbd is found to take place mainly in mouse testis (Eirin-Lopez *et al.*, 2008) and its ectopically expressed form has been shown to be deficient in the inactive X chromosome, the occurrence of the native form of H2A has never been previously documented. In Chapter 3, I undertook the challenge to isolate and characterize the native form of H2A.Bbd. hTSH2B is expressed exclusively in human spermatogenic germ cells and present in a subpopulation of mature sperm cells (Singleton *et al.*, 2007a; Zalensky *et al.*, 2002). In Chapter 4, the hTSH2B is shown to be incorporated into nucleosome structures and the hTSH2B-containing octamer is less stable compared to that of its canonical counterpart. In Chapter 5, I study H1t, which is first synthesized in primary spermatocytes, and it is the predominant form of linker histone in round spermatids (Bucci *et al.*, 1982). Because, phosphorylation of H1t has been a centre of debate, I set out to determine the presence and the sites of this modification. Taken together, the structural and functional differences of the histone variants in testis compared to their somatic counterparts could facilitate the adoption of specific chromatin conformations at

different stages of spermatogenesis or at specific cellular events, such as DNA DSB repair.

Chapter 1. H2A.X: tailoring histone H2A for chromatin dependent genomic integrity

Li A's contribution to the work: writing and preparing figures and table. Eirín-López JM's contribution to the work: writing and preparing figures for the section on the phylogenetic perspective of H2A.X. Adapted from Li *et al.* and Thambirajah *et al.* for the purpose of this thesis (Li *et al.*, 2005a; Thambirajah *et al.*, 2009).

Abstract

During the last decade, chromatin research has been focusing on the roles of histone variability as a modulator of chromatin structure and function. Histone variability can be the result of either post-translational modifications or of intrinsic variation at the primary structure level. In this chapter, I center attention to one of the most extensively characterized histone variants, histone H2A.X. The molecular phylogeny of this variant seems to have run in parallel with that of the major canonical somatic H2A1 in eukaryotes. Functionally, H2A.X appears to be mainly associated with its participation in maintaining the genome integrity by participating in the repair of the double stranded DNA breaks exogenously introduced by environmental damage, or in the process of homologous recombination during meiosis. At the structural level, these processes involve the phosphorylation of serine at the SQE motif, which is present at the very end of the C-terminal domain of H2A.X. It is also possible that these processes also involve other PTMs, some of which have recently started to be defined. I discuss a model to account for how these H2A.X PTMs in conjunction with chromatin remodeling complexes, such as INO80 and SWRI, can modify chromatin structure to support the DNA unraveling required for DNA repair. In addition to its involvement in DNA repair, it is clear from recent publications that H2A.X also participates in many other cellular processes. Its role in other non-DNA damage related processes will also be discussed.

Introduction to H2A.X

Histone H2A.X is a unique, heteromorphous, core histone H2A variant (Ausio and Abbott, 2002), which represents 2-25% of the mammalian histone H2A population depending on the cell line or tissue examined (Rogakou *et al.*, 1998). Its amino acid sequence was first determined in 1989 (Mannironi *et al.*, 1989). This H2A variant is evenly distributed throughout the genome based on immunofluorescent experiments (Siino *et al.*, 2002a). H2A.X is characterized by a unique and invariant SQE motif at the C-terminal tail, which is a consensus sequence for phosphatidylinositol-3 kinase-like family of kinases (PIKK). Immediately upstream of the SQE motif, mammalian H2A.X variants also contain a second phosphorylatable motif: SQ in mouse and TQ in human (Rogakou *et al.*, 2000a). Therefore, it is possible that both of T136 and S139 in human H2A.X are phosphorylated (Rogakou *et al.*, 2000a). In mammalian cells, three PIKKs are known to phosphorylate the serine residue in the SQE motif of H2A.X. These PIKK members, which play an important role in double stranded break (DSB) repair, are Ataxia telangiectasia mutated (ATM), DNA-dependent protein kinase (DNA-PK) and ATM and Rad3-related kinase (ATR) (Stiff *et al.*, 2004b). Because a lot of DSB repair research has been carried out in yeast, *Saccaromyces cerevisiae,* it is important to note that the major histone H2A variant (which is encoded by genes *HTA1* and *HTA2*) in this organism contains the SQE motif (Celeste *et al.*, 2002). This SQE motif can be phosphorylated by the mammalian homologs of ATR and ATM, Mec1p and Tel1p, respectively (Downs *et al.*, 2000). The HTA1 and HTA2 isoforms contribute 95% of the H2A complement in yeast (Pilch *et al.*, 2003a), the rest corresponding to HTZ1/HTA3 (the H2A.Z homolog in yeast) (Downs *et al.*, 2000).

Histone H2A.X. A phylogenetic perspective

The evolution of the H2A.X variant, in the context of other histone H2A variants, is shown in Fig. 1. With few exceptions such as in the nematode, *Caenorhabditis elegans,* which does not have H2A.X, and the fruit fly *Drosophila,* which contains a chimeric H2AZ/H2A.X variant (H2AvD), histone H2A.X is evenly distributed throughout the eukaryotic kingdom with one gene per species. As pointed out above, in *S. cerevisiae*, the major H2A component is H2A.X and similarly, H2A.X also replaces the canonical H2A in *Giardia* and fungi. Therefore, as it can be seen in Fig. 1, the canonical H2A.1 and H2A.X appear to have co-evolved in different eukaryotic lineages, having had multiple evolutionary origins (Malik and Henikoff, 2003). This evolution is in contrast to that of other histone variants such as, H2AZ, H2ABbd and macroH2A, where the diversification has been the result of single differentiation events along the phylogenetic tree. The single evolutionary origin of macroH2A has been the most recent (Fig. 1). At the protein level, the evolutionary process involves the alteration and extension of a region of over 20 amino acids at the C-terminal domain of H2A (see Fig. 2A) with the appearance of a highly conserved SQE phosphorylatable motif (Fig. 2B). At the gene level, the unique gene encoding this variant in higher eukaryotes is transcribed as two different mRNAs. Although both transcripts contain the 3' stem loop characteristic of the replication-dependent histone mRNAs, one of them consists of a 3'UTR extension with a polyA signal which is characteristic of replication-independent histone genes. The occurrence of these two different RNA populations is the result of alternative splicing. This allows a fraction of H2A.X to be expressed during S phase, while another fraction is expressed during G1 (Alvelo-Ceron *et al.*, 2000). This later fraction exchanges with the canonical

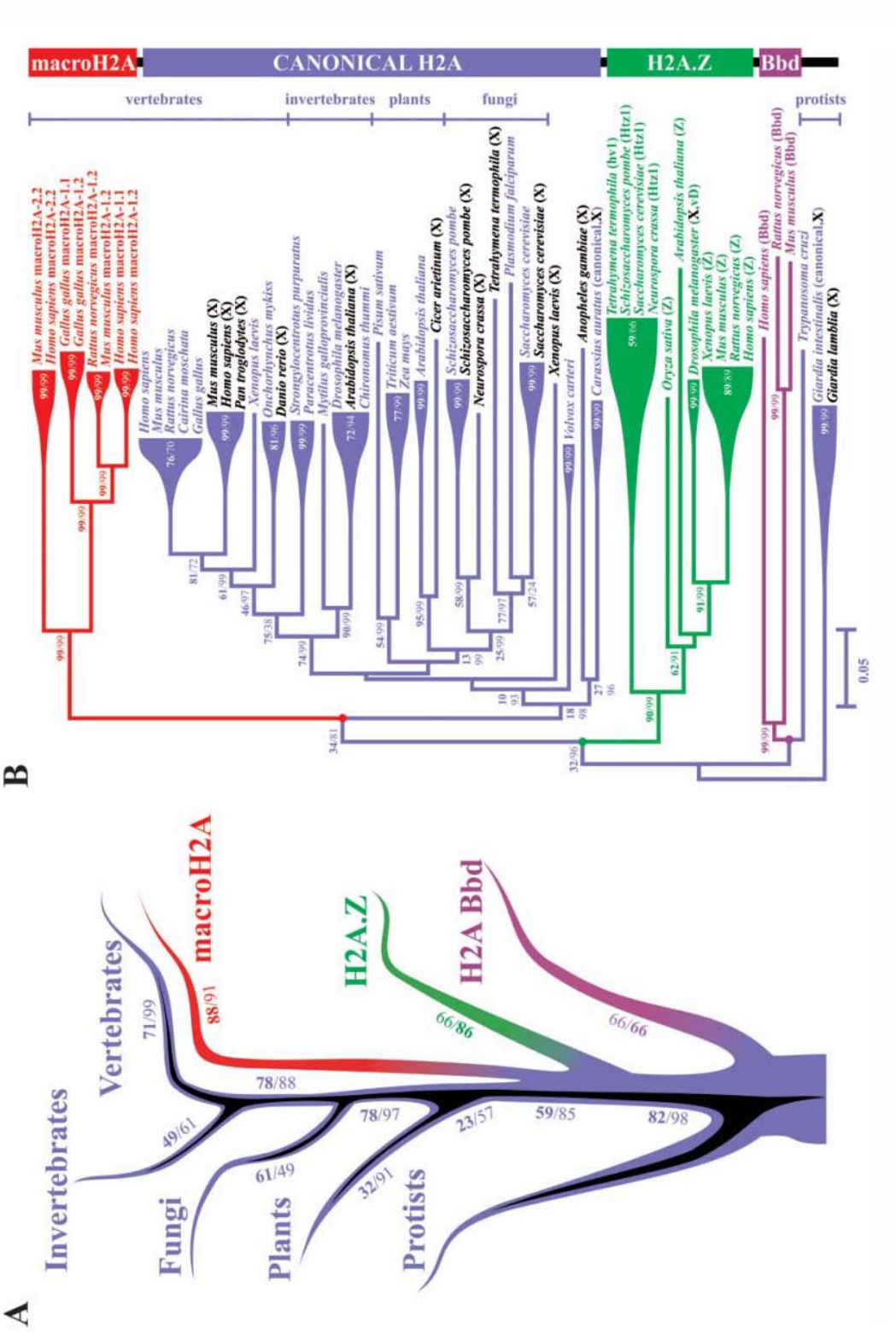
A
Invertebrates
Vertebrates
Fungi
Plants
Protists
macroH2A
H2A.Z
H2A Bbd
71/99
88/91
66/86
66/66
78/88
49/61
78/97
23/57
59/85
82/98
61/49
32/91
B
macroH2A
CANONICAL H2A
H2A.Z
Bbd
vertebrates
invertebrates
plants
fungi
protists
0.05

Figure 1. Schematic representation and neighbour-joining tree of the phylogenetic relationships of H2A histones from different species.

A) Schematic representation of the phylogenetic relationships among different H2A histones in eukaryotes based on the neighbour-joining tree shown in (B). The canonical H2A lineage is represented in blue and H2A.X is in black. The Barr body deficient H2A, H2A.Bbd (purple), the H2A.Z (green), and the macroH2A (red) lineages stem from the main trunk through single differentiation events taking place during histone H2A evolution. The numbers for interior branches represent bootstrap (boldface) and interior-branch test (normal) values, both based on 1000 replications and only shown when greater than 50%. B) Phylogenetic neighbour-joining tree reconstructed from uncorrected *p*-distances showing the relationships among H2A genes from representative organisms of the *Eukarya* superkingdom. The topology reveals the early differentiation as well as the monophyletic origin for the three variant lineages mentioned previously. The H2A.X variants (black and in boldface) are otherwise ubiquitous in the major eukaryotic groups, arising through multiple differentiation events from canonical H2A histones (blue), with the unique exception of *D. melanogaster* H2A.X variant.

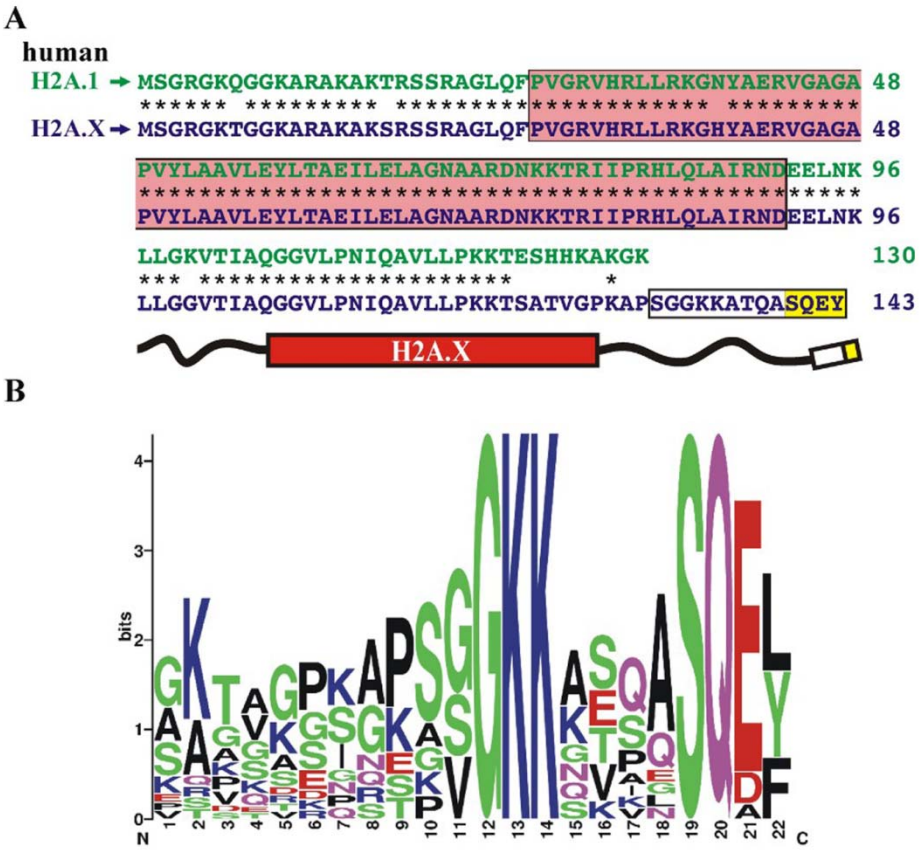

Figure 2. Sequence alignment of the full length humanH2A1 and H2A.X and sequence comparison of the last 22 amino acids of H2A.X from different organisms in a Logos format.

A) Sequence alignment of human histone variants H2A.1 and H2A.X. The stars identify the identical amino acids and the pink box corresponds to the histone fold. A schematic representation of H2A.X is also shown. B) The last C-terminal 22 amino acids of histone H2A.X from different organisms (see Fig. 1B) were sequence aligned and displayed in a Logos format (Schneider and Stephens, 1990). In this representation, the size of the letters is proportional to the frequency with which an amino acid appears at a given position in the sequence alignment. The overall height of all of the letters at any given position is proportional to the conservation of the site. The letters are colour coded according to the physical and chemical structural characteristics of the amino acids they represent.

H2A and probably with phosphorylated H2A.X in the process of DSB DNA repair during the G phase of the cell cycle, as it will be discussed later. Sequence comparison of the protein sequence extension of H2A.X beyond the protein sequence of the canonical H2A for different representatives within the eukaryotes (Fig. 2B) provides some interesting information. Firstly, as already described, an SQE phosphorylation motif appears to be conserved. In addition, it reveals the presence of a conserved GKK motif. The conservation of this motif suggests that in addition to phosphorylation, the C-terminal extension of H2A.X may be subject to other PTMs at these lysine residues that may also participate in the DSB repair process (Moore and Krebs, 2004; Wyatt *et al.*, 2003) or in other important nuclear metabolic processes.

The protein extension at the C-terminal end that occurred during the evolutionary diversification of H2A.X from the main canonical H2A components is a region that is very close to the binding site of histone H1 in the nucleosome, and hence, can in itself or through its PTMs, such as phosphorylation, have a structural effects of its own (Abbott *et al.*, 2001; Arents and Moudrianakis, 1995).

H2A.X phosphorylation triggered by different double stranded break origins

H2A.X is phosphorylated extensively in response to a specific type of DNA damage called DSB. DSB, as the name implies, takes place when both strands of DNA are broken exposing free DNA ends. If improperly repaired, DSB can have deleterious consequences for the cell. These include chromosomal aberrations such as chromosomal breaks, translocations and aneuploidy (Fernandez-Capetillo *et al.*, 2004). DSB repair can

be achieved by two different pathways: non-homologous end joining (NHEJ) and homologous recombination (HR). NHEJ involves the direct joining of the broken DNA ends. HR takes the advantage of the homologous DNA sequence from other parts of the genome to repair the broken ends. DSBs are mainly repaired by NHEJ in mammalian cells (Drouet *et al.*, 2004). However, HR is found to be predominant in yeast in diploid cells and the S-phase of haploid cells (Moore and Krebs, 2004) and during meiosis. HR is used whenever a sister chromatid or a homologous chromosome is available.

In eukaryotic cells, DNA DSBs can have diverse origins. DSBs are induced accidentally by chemical agents, such as bleomycin, camptothecin, hydroxyurea (HU) and methyl methanesulfonate (MMS), and ionizing radiation (Balajee and Geard, 2004; Millar *et al.*, 2002; Nazarov *et al.*, 2003; Ward and Chen, 2001). DSBs can be replication fork associated when a replication fork collides with an unrepaired DNA single-stranded break (Arnaudeau *et al.*, 2001). Viral agents such as retroviruses also induce DSBs in host DNA by an integrase-mediated process (Daniel *et al.*, 2004). Bacterial toxins, cytolethal distending toxins (CDT), produced in some Gram negative bacteria are able induce DSBs (Thelestam and Frisan, 2004). In addition to accidental damage, DSB occur in normal environments within the cell, such as during V(D)J, apoptosis and meiotic recombination (Chen *et al.*, 2000; Mahadevaiah *et al.*, 2001b; Rogakou *et al.*, 2000b). These programmed DSBs are all essential processes for the survival of the cell or the organisms themselves. The existence of a mechanism of DSB detection and repair in both environmental and physiological conditions are essential for genomic integrity. Phosphorylation of H2A.X is a marker for environmental and natural DNA DSB (Rogakou *et al.*, 1998). Immediately after occurrence of DSBs, numerous DNA repair

factors are recruited and modified at the DSB site. Amongst them, H2A.X is extensively phosphorylated over approximately 2 Mb immediately to the DSB (Rogakou *et al.*, 1999). The phosphorylated form of H2A.X is commonly denoted as γ-H2A.X.

In what follows next, I am going to briefly review the occurrence of γ-H2A.X triggered by DSB DNA damage and other physiologically relevant processes involving DSBs.

1) DSB damage induced by external agents

Time-dependent phosphorylation of H2A.X in response to DSB damage induced by extracellular agents has been studied extensively due to the availability of reagents and controllable experimental conditions. These studies have allowed the examination of the role of γ-H2A.X in DSB repair. It has been shown that γ-H2A.X are generated with 1 min and γ-H2A.X foci appeared within 3 min after irradiation (Rogakou *et al.*, 1999). The phosphorylation of H2A.X rapidly increases and peaks at around 30 min after irradiation (Rogakou *et al.*, 1998). At this point, γ-H2A.X starts being dephosphorylated with a half-life of approximately 2 hours (Celeste *et al.*, 2002).

Ionizing radiation (IR)-induced γ-H2A.X foci formation had been initially shown to be ATM dependent in ATM knockout cell lines (Burma *et al.*, 2001). However, later it was observed that both ATM and DNA-PK appear to be able to phosphorylate H2A.X redundantly after IR exposure (in actively growing and plateau phase human fibroblasts, growing MEFs and LCLs, and in chicken cells), although there are kinetic and growth conditions where ATM predominates (Stiff *et al.*, 2004b). Thus, ATM may play the dominant role of phosphorylating H2A.X. ATM is critical at least at the early time post

irradiation (Stiff *et al.*, 2004b). ATM is activated by DNA damage through a process that involves autophosphorylation and dimer dissociation, presumably as a result of the chromatin alteration caused by DNA DSB (Bakkenist and Kastan, 2003). The ATM-mediated H2A.X phosphorylation represents an important step that determines subsequent events in the signal transduction pathway that participates in the DNA repair process. However, DSB repair factors such as Nbs1, Mre11, 53BP1 and Brca1 (see Table 1) are also phosphorylated in response to IR by ATM (Balajee and Geard, 2004; Taylor *et al.*, 2004). Thus, besides H2A.X phosphorylation, ATM and DNA-PK are also required for the repair of IR-induced DSBs because cells deficient for either of these factors are hypersensitive to IR and exhibit DNA repair defects (Bassing *et al.*, 2003). Indeed, deletion of the ATM and DNA-PK genes has more severe consequences to the cells than H2A.X deletion (Kurimasa *et al.*, 1999; Xu *et al.*, 1996) because besides H2A.X phosphorylation, these PIKK members are also involved in other cellular mechanisms. For instance, ATR has been known to participate in the initiation of G_2 arrest signalling and phosphorylation of cellular proteins that are not related to DNA damage response (Zimmerman *et al.*, 2004).

The dephosphorylation of H2A.X is just as important as the phosphorylation process. Indeed, the H2A.X homolog in *D. melanogaster,* H2AvD, is also phosphorylated during DSB repair. The removal of the phosphorylated form of H2AvD involves the dTip60 chromatin-remodelling complex (Kusch *et al.*, 2004). This chromatin-remodelling complex mediates the acetylation of the phosphorylated H2AvD and further exchange of this acetylated and phosphorylated H2AvD with an unmodified H2AvD (Kusch *et al.*, 2004). However, this finding does not preclude the involvement of other

mechanisms. Protein phosphatase 1 has been shown to remove the phosphate group from γ-H2A.X containing chromatin *in vitro* and *in vivo* (Nazarov *et al.*, 2003).

The existence of a γ-H2A.X replacement mechanism raises the issue of the existence of a replication-independent H2A.X variant. As described in the evolution section, the H2A.X gene can be transcribed as mRNA with or without a polyadenylated tail (Alvelo-Ceron *et al.*, 2000). It is possible that the polyA- form is involved in the replication dependent deposition of H2A.X every 5 nucleosomes during S phase of the cell cycle (Pilch *et al.*, 2003a). However, only one in 10 of the H2A.X containing nucleosomes are phosphorylated during DSB repair (Pilch *et al.*, 2003a). The fraction of the replication independent H2A.X (polyA+) may be responsible for the unmodified H2A.X, which replaces this γ-H2A.X after the DSB is repaired.

2) Apoptosis

Apoptosis or programmed cell death is an essential process for multi-cellular organisms which involves an important alteration of chromatin. Phosphorylation of H2A.X is also associated with apoptosis. The initiation of DNA fragmentation during apoptosis induces DSB and thus, induces the formation of γ-H2A.X (Rogakou *et al.*, 2000a). γ-H2A.X was detectable as soon as the DNA DSB occurred during this process and it was observed in all apoptotic systems examined (Rogakou *et al.*, 2000a). An indirect effect of apoptosis is the localization of γ-H2A.X at telomeres. This is due to the apoptotic events resulting from the loss of telomere function. Mice lacking the RNA component of telomerase ($mTR^{-/-}$) are unable to express a functional telomerase which contains both RNA and catalytic protein subunits. Therefore, telomere sequence loss

during replication is not compensated in these mutants and the $mTR^{-/-}$ mice telomere are gradually shortened resulting in the loss of the telomere function. These mice have a decrease in fertility and an increase in T cell apoptosis (Zhao *et al.*, 2004). The loss of telomere function or the critically short telomeres are recognized as DSBs (Zhao *et al.*, 2004). Not surprisingly, γ-H2A.X is localized to the shortened telomeres (Zhao *et al.*, 2004).

3) V(D)J recombination

V(D)J recombination induces programmed DSB formation in cells of the mammalian immune system, such as developing thymocytes (Chen *et al.*, 2000). This programmed DSB from V(D)J cleavage is mediated by RAG and repaired by NHEJ. Repair of DSBs by NHEJ in mammals requires DNA-PK and DNA ligase IV/XRCC4 protein complex (Drouet *et al.*, 2004). DNA-PK is activated by nucleosomes and the activated DNA-PK is capable of phosphorylating H2A.X within the nucleosome (Park *et al.*, 2003a).

Nbs1 and γ-H2A.X are known to associate with the V(D)J recombination-induced DSBs site. In developing thymocytes, Nbs1 and γ-H2A.X are associated with the T cell receptor alpha locus in response to RAG protein-mediated V(D)J cleavage (Chen *et al.*, 2000). Although the γ-H2A.X foci formation is universal in T cell receptor recombination, it has been shown that γ-H2A.X is dispensable for this process (Chen *et al.*, 2000).

4) Meiosis

Programmed DSB formation also occurs in germ cells during meiotic recombination (Hunter *et al.*, 2001; Mahadevaiah *et al.*, 2001a) where DSB are repaired by HR. Indeed, phosphorylated H2A.X has been shown to be temporally and spatially linked to Spo11, a topoisomerase II-like protein responsible for DSB formation during meiosis (Mahadevaiah *et al.*, 2001a). Moreover, more H2A.X are phosphorylated in testis than in any other unirradiated mouse tissues, possibly due to the extent of DSB formation during meiosis in the male germinal cells (Mahadevaiah *et al.*, 2001a). The distribution of phosphorylated H2A.X varies during spermatogenesis. γ-H2A.X foci can be observed in intermediate and B spermatogonia and in preleptotene to zygotene spermatocytes, whereas γ-H2A.X exhibits a more homogeneous nuclear distribution in type A spermatogonia and round spermatids, and coalesce in the sex body in pachytene spermatocytes (Hamer *et al.*, 2003). The overall relevance of H2A.X to meiosis and in particular to spermatogenesis (Lewis *et al.*, 2003c) is underscored by the observation that H2A.X expression in mice is required for fertility and maturation of male testis but expendable in females (Celeste *et al.*, 2002) (see also (Scherthan, 2003) for a review) . The role of H2A.X in the meiotic process goes beyond DSB repair. As stated previously, phosphorylated H2A.X has been also shown to accumulate in the highly condensed chromosomal sex body during meiotic prophase. This event has been shown to happen in a way which is independent of meiotic recombination-associated DSB (Fernandez-Capetillo *et al.*, 2004). Furthermore, there is evidence to suggest that H2A.X has a critical role in controlling the topological distribution and movement of telomeres during meiosis (Fernandez-Capetillo *et al.*, 2004).

5) Stalled replication forks

During replication, DSBs also are present at stalled replication forks (Ward and Chen, 2001). This damage signal is initiated by ATR and the activation of this pathway prevents entry into mitosis to allow for either DNA repair or apoptosis (Zimmerman *et al.*, 2004). H2A.X is phosphorylated by ATR in response to DNA replication stress, such as stalled replication forks (Ward and Chen, 2001). The specificity of ATR in this process is underscored by the fact that it does not show a significant contribution to the phosphorylation of H2A.X after DSB induced by IR (Stiff *et al.*, 2004b; Zimmerman *et al.*, 2004).

The different sources of DSBs described above result in the activation of different PIKKs. However, γ-H2A.X is found at the sites of all DSBs regardless of their origin. Therefore, H2A.X phosphorylation is considered to be a marker for the site of DNA DSBs. In addition to DSB repair, γ-H2A.X may play a supporting role in checkpoint control of the cell after DNA damage (Fernandez-Capetillo *et al.*, 2004; Stewart *et al.*, 2004). Therefore, the cell cycle does not proceed until DNA damage is repaired. The sequential events and the different components involved during each of the DSB repair process are yet to be elucidated.

H2A.X Foci: H2A.X modifications and its partners, their role in DSB repair

H2A.X modifications and modified nucleosomal partners

Immediately after the induction of DNA DSB, S139 of human H2A.X becomes phosphorylated. Recently, other DNA DSB-related PTMs of H2A.X have been identified. This potentially allows for an additional layer of epigenetic regulation that could

contribute to the H2A.X histone code. Histone H2A.X is acetylated at K5 by TIP60, a histone acetyltransferase (Ikura *et al.*, 2007), preceding its ubiquitination at K119 (Huen *et al.*, 2007; Ikura *et al.*, 2007). TIP60 regulates the poly-ubiquitination of H2A.X via the ubiquitin-conjugating enzyme UBC13 in a way that is independent of γ-H2A.X (Ikura *et al.*, 2007). The simultaneous presence of acetylation and ubiquitination of histone H2A.X could facilitates its release from DNA at damaged sites (Ikura *et al.*, 2007). Since both modifications occur within the first 5 minutes after irradiation (Ikura *et al.*, 2007), the release of the post-translationally modified histone H2A.X may allow for the reconfiguration of chromatin and thereby facilitate the recruitment of DNA DSB repair factors. Interestingly, K119 ubiquitination can occur in ways that are dependent or independent of S139 phosphorylation (Fig. 3).

Ubiquitination of histone H2A.X by UBC13 via interactions with Ring Finger Protein 8 (RNF8) is dependent on the phosphorylation at S139 of human H2A.X (Huen *et al.*, 2007). Histone H2A.X phosphorylation at S139 recruits RNF8 to the site of DNA damage via an adaptor protein, mediator of DNA damage checkpoint protein 1 (MDC1) (Huen *et al.*, 2007). In contrast to the S139 phosphorylation–independent poly-ubiquitination of H2A.X by UBC13 via TIP60 interaction, the interaction of UBC13 and RNF8 allows for the S139 phosphorylation–dependent di-ubiquitination of γ-H2AX (Huen *et al.*, 2007). The different number of ubiquitin adducts present on histone H2A.X adds a new layer of complexity to the PTMs involved in DNA DSB repair regulation.

It is important to emphasize that both K5 and K119 residues are conserved in the canonical histone H2A. Therefore, the possibility exists that H2A is also acetylated and ubiquitinated during DNA DSB repair. It has been shown that the ubiquitin-conjugating

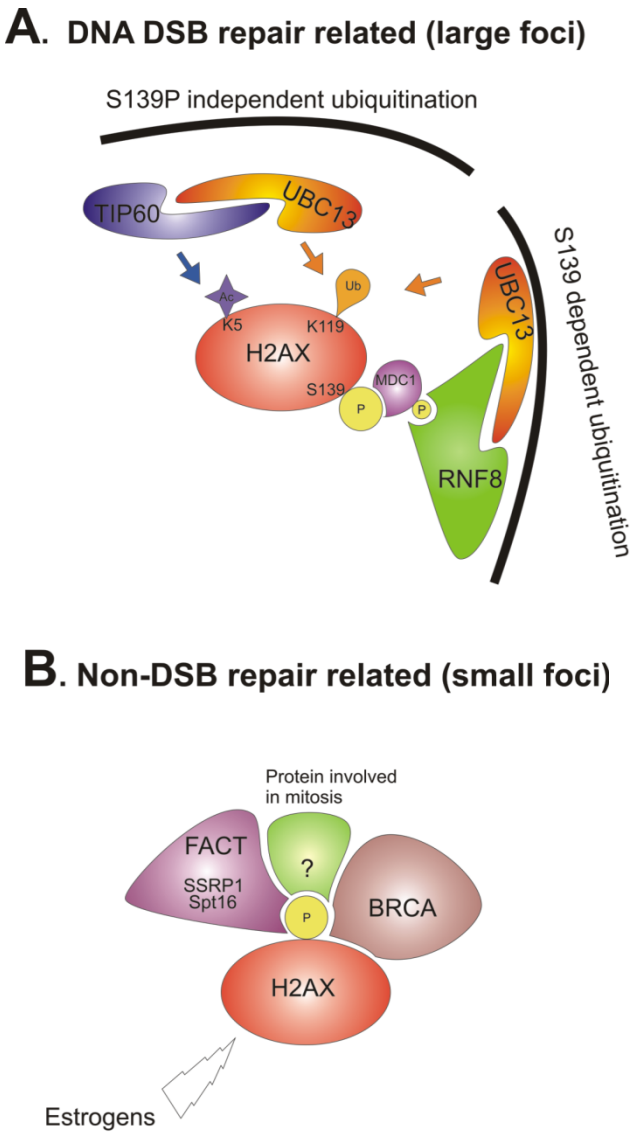

Figure 3. Schematic diagram showing the potential involvement of histone H2A.X in DNA DSB repair-related and in non-DSB repair-related processes.

A) the post-translational modifications of histone H2A.X and its interacting partners during DNA DSB repair. B) the interactions of histone H2A.X and other proteins participating in non-DSB repair related mechanisms.

E3 enzyme RNF8 is able to ubiquitinate histone H2A and histone H2A.X (Mailand *et al.*, 2007). K119 is the only site that can be ubiquitinated for histone H2A (Osley, 2004). Sites on histone H2A.X other than K119 can also be ubiquitinated during DNA DSB repair as histone H2A.X with a K119R mutation can still be ubiquitinated (Ikura *et al.*, 2007). Hence, other lysines in the C-terminal tail of histone H2A.X, which are not present in histone H2A, are also ubiquitination targets. The ubiquitination of the lysine residues could potentially be present at the conserved GKK motif discussed in the evolution section. It has been shown that H2A ubiquitination enhances the binding of the linker histones to nucleosomes and H2A deubiquitination might cause the dissociation of linker histones from core nucleosomes (Jason *et al.*, 2005). Therefore, the epigenetic contribution resulting from the combinatorial modifications of histone H2A or histone H2A.X may regulate DNA DSB repair or other cellular processes, such as transcription, by directly altering chromatin structure.

Whereas H2A.X is extensively modified during DSB repair, modifications on other histone have also been shown to have an important role during DSB repair. For instance, methylated K79 of histone H3 is involved in targeting 53BP1 to DSBs in mammalian cells (Huyen *et al.*, 2004). 53BP1 is a DNA DSB response protein. Its tandem tudor domain binds to the methylated K79 of histone H3. This domain is sufficient for targeting 53BP1 to DSBs initially, but it does not allow the retention of 53BP1 at DSB. A different domain of 53BP1 located N-terminal to the tandem tudor domain binds to γ-H2A.X (Ward *et al.*, 2003). Since 53BP1 needs to interact with both γ-H2A.X and methylated histone H3 to function properly, it is reasonable to hypothesize that the γ-H2A.X and the methylated histone H3 are close, possibly in the same

nucleosome. There might be a designated nucleosome that has a modified H2A.X and a modified canonical H3 that act synergistically in the initiation of DSB repair as a part of a DSB histone code. A related event has been described in *Schizosaccharomyces pombe*. In this instance, Crb2, a homolog of 53BP1 in mammalian cells, is recruited to DSB by methylated histone H4 at lysine 20 (Sanders, 1978).

Histone H2B has been found to be phosphorylated at the N-terminal S14 at the DSB site (Fernandez-Capetillo *et al.*, 2004). Furthermore, histone H2B is not a direct target for PIKK (Fernandez-Capetillo *et al.*, 2004). The formation of phosphorylated H2B is γ-H2A.X independent, which does not require the presence of γ-H2A.X. However, the recruitment of proteins to phosphorylated H2B requires the presence of γ-H2A.X (Fernandez-Capetillo *et al.*, 2004). This indicates that the formation of irradiation-induced $H2B^{Ser14P}$ foci is downstream of the γ-H2A.X signal.

Another post-translational modification of histones that has been shown to contribute to DSB repair is acetylation. H4 acetylation in yeast by Esa1, an acetyl transferase (HAT) subunit of NuA4 chromatin remodeling complex, is necessary for DSB repair (Millar *et al.*, 2002). Also, in mammalian cell lines, histone deacetylase 4 (HDAC4) is associated with 53BP1 at the IR-induced foci and HDAC 4 inhibition increased sensitivity to IR (Kao *et al.*, 2003).

These modified nucleosomal partners are likely to act synergistically to transiently alter chromatin structure and function, as well as providing an initiation histone code that triggers the repair events.

Non-nucleosomal partners

The phosphorylation of H2A.X represents an early response to DSBs (Stiff *et al.*, 2004b). In addition, H2A.X foci colocalize with IRIF consisting of 53BP1, Brca1, MRN complex and ATM in mammalian cells (Fernandez-Capetillo *et al.*, 2004; Paull *et al.*, 2000). The generation of γ-H2A.X foci triggering the recruitment of numerous proteins to the DSB site indicates that DSB repair is an amplified process in the cell. However, the initial recruitment of factors, such as Nbs1, 53BP1 and Brca1, does not require the phosphorylation of H2A.X while the retention of these factors to form IRIF requires H2A.X (Celeste *et al.*, 2003). Furthermore, the recruitment of the IRIF components is a sequential event. γ-H2A.X and 53BP1 foci form very rapidly (within minutes) in response to IR, followed by the appearance of Brca1 foci (within hours) (Celeste *et al.*, 2003). HR repair factors either Rad50 or Rad51 were found, by immunoprecipitation experiments, to colocalize with γ-H2A.X foci after the recruitment of the product of the tumor suppressor gene BRCA1 and the formation of the Brca1 foci (Paull *et al.*, 2000). The HR repair is mediated by the recruitment of HR repair proteins, Brca1, Rad50 and Rad51, via γ-H2A.X (see Table 1).

After the exposure to IR, the recruitment of NHEJ repair factors is also observed in human cells (Drouet *et al.*, 2004). In addition, the recruitment of these repair factors is a dose- and time-dependent process (Drouet *et al.*, 2004). These proteins include DNA-PK (Ku70/80, DNA-PKcs), XRCC4 and DNA ligase IV proteins (see Table 1) (Drouet *et al.*, 2004). As shown in the yeast system, both repair factors from HR and NHEJ repair pathway are recruited within the first 2 hours of IR exposure. These proteins included

Table 1. The DSB repair factors in human and their yeast homologs (Krogh and Symington, 2004).

Human	Yeast	DSB repair pathway and function
Rad51	Rad51	HR, involved in strand exchange.
Rad52	Rad52	HR, indispensable DNA end/single-strand-binding protein, stimulates complementary single-strand adhesion.
Mre11/Rad50/ Nbs1 (MRN complex)	Mre11/Rad50/ Xrs2 (MRX complex)	Recruitment to DSB site, yeast MRX complex involved in both HR and NHEJ, but mammalian MRN complex only involved in HR
Ku70	Yku70/HDF1	NHEJ, a component of DNA-PK in human
Ku80	Yku80/HDF2	NHEJ, a component of DNA-PK in human
DNA-PK (Ku70/80 and DNA-PKcs)	--	NHEJ, kinase complex recruited to DSB site
Ligase IV	DNL4	NHEJ ligases
XRCC4	LIF1	NHEJ
ATM	Tel1	PIKK kinase
ATR	Mec1	PIKK kinase
Brca1	--	HR, it associates with SWR
RPA	--	HR and NHEJ, single stranded DNA binding protein

Rad51, Rad52, Rad54, Rad55 and Yku80 (see Table 1) (Morrison *et al.*, 2004). The difference in preference of the repair pathways between mammalian cells and yeast is still unclear. One might speculate that the histone code is different due to the different levels of H2A.X and H2A phosphorylation in mammalian cells and in yeast. The relevance of phosphorylation in the overall repair process is underscored by the fact that wortmanin, a PIKK inhibitor, when added before DSB induction, eliminates focus formation by Rad51 and Brca1 (Paull *et al.*, 2000). As well, it reduces the colocalization of RPA, a protein involved in HR and NHEJ repair (see Table 1), that has also been shown to be associated with γ-H2A.X in a time-dependent manner after DNA damage (Balajee and Geard, 2004). All of the DNA repair factors discussed have also shown to play a role in DNA DSB repair pathways (Morrison and Shen, 2005; Paull *et al.*, 2000).

In addition to DNA repair factors, three chromatin remodelling complexes were found to associate with the phosphorylated S129 of histone H2A (γ-H2A) in yeast. They are NuA4 HAT, INO80 and SWR1 chromatin remodelling complexes (Downs *et al.*, 2004b; Morrison *et al.*, 2004; van Attikum *et al.*, 2004b) (Fig. 4). The recruitment of these chromatin remodelling complexes to the DSB site via γ-H2A is a time-dependent process. The NuA4 HAT complex with acetyltransferase activity is recruited prior to the association of the ATP-dependent chromatin remodelling complexes, INO80 and SWR1 (Downs *et al.*, 2004a). The NuA4 HAT complex is responsible for the acetylation of N-terminal tail of histones H2A and H4 (Boudreault *et al.*, 2003). All three chromatin remodelling complexes contain one common subunit, Arp4 (Downs *et al.*, 2004a). This subunit directly binds to γ-H2A. However, the interaction of INO80 and γ-H2A is mediated by the Nhp10 subunit of the INO80 complex (Morrison *et al.*, 2004). Evidence

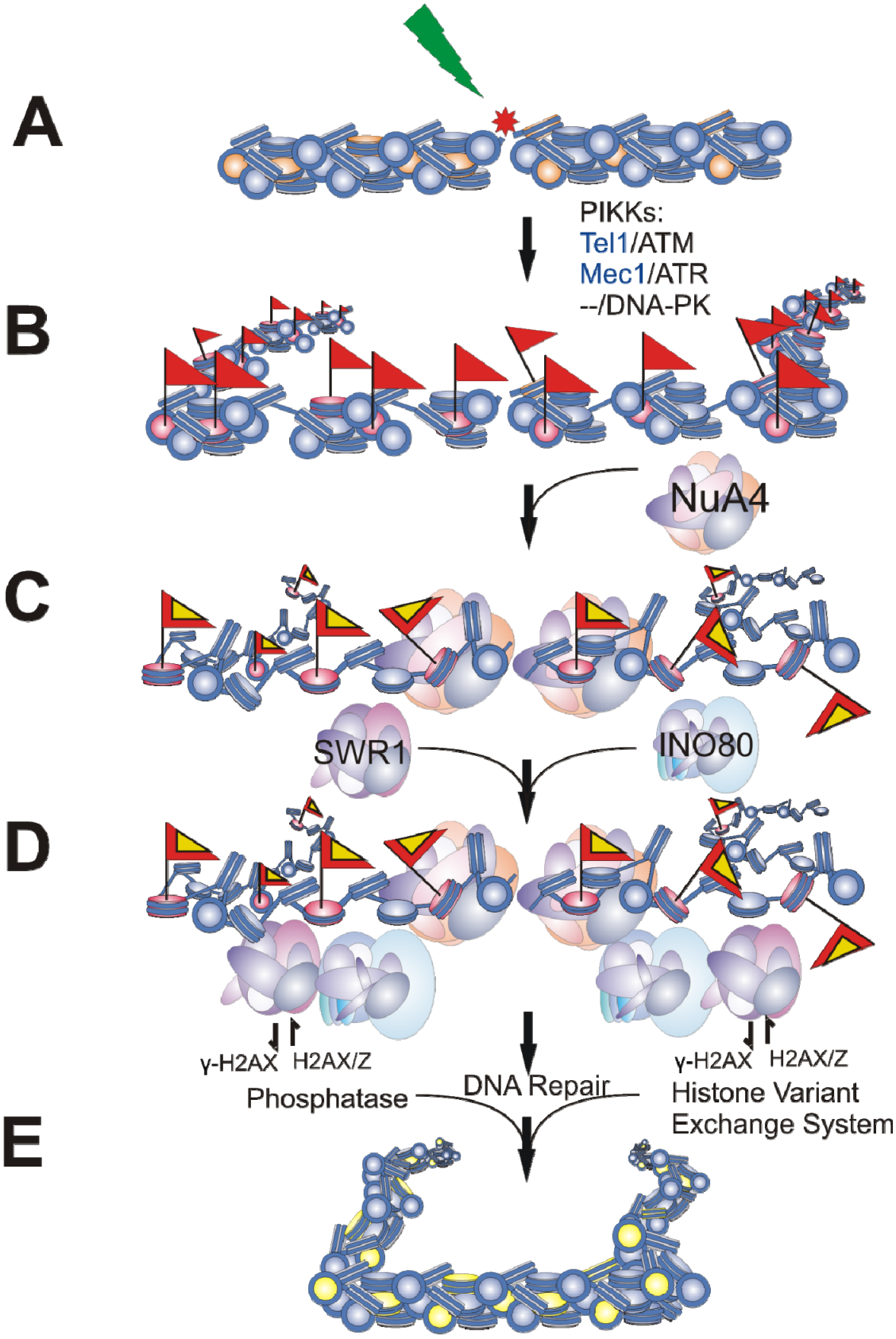
A
PIKKs:
Tel1/ATM
Mec1/ATR
--/DNA-PK
B
NuA4
C
SWR1
INO80
D
γ-H2AX
H2AX/Z
γ-H2AX
H2AX/Z
Phosphatase
DNA Repair
Histone Variant
Exchange System
E

Figure 4. A putative model for the role of H2A.X phosphorylation in DSB repair. A) The induction of DSB in chromatin results in a rapid recruitment of HR or NHEJ proteins followed by the activation and the recruitment of PIKK members. Homologs are written in blue (yeast) and black (human). In our chromatin representation, the circular discs in blue represent histone octamers and the darker bands represent the DNA wrapping around the octamer. The orange discs represent H2A.X-containing octamers. B) PIKK kinases phosphorylate targets including H2A.X. The phosphorylation of H2A.X (red flags) by PIKK members marks the chromatin for recruitment of DNA DSB repair factors and remodelling complexes. The presence of γ-H2A.X spanning a large region of the chromatin may alter the chromatin structure (Downs *et al.*, 2000). C) This, in combination with HAT activities, such as those of the NuA4 complex that acetylate H2A.X (yellow flags), may further alter chromatin structure and/or provide the signalling for the recruitment of the ATP-dependent chromatin remodelling complexes, INO80 and SWR1 (Downs *et al.*, 2004b; Morrison *et al.*, 2004; van Attikum *et al.*, 2004b) (D). D) INO80 is a multi-subunit complex that binds directly to γ-H2A.X through one of its constitutive subunits (see text). The activity of INO80 is presumably responsible for the appearance of single stranded DNA. The presence of RuvB-like protein subunits in INO80 suggests that this complex in collaboration with SWRI, which mediates the exchange of γ-H2A.X by non-phosphorylated H2AZ/H2A.X, may play an important role in HR repair. However, as pointed out in the text the presence of phosphatases that hydrolyzed the γ-phosphate cannot be ruled out. E) Upon repair by either NHEJ or HR the chromatin fiber reverts to its folded organization.

has shown that the conserved yeast chromatin remodelling complex, INO80, from the SWI/SNF super family is involved in the DSB repair in addition to the well established function in transcription (Morrison *et al.*, 2004). As mentioned earlier, this 12 subunit complex is recruited to the DSB site through the physical interaction between the Nhp10 protein subunit of the complex and γ-H2A (Morrison *et al.*, 2004). In addition, the Rvb1/Rvb2 protein subunits of the complex are similar to the RuvB helicase in bacteria, which is involved in DNA recombination and repair. This implied the involvement of INO80 complex in DSB repair (Morrison *et al.*, 2004). The finding of the recruitment of this chromatin remodelling complex to the DSB site provides evidence for the unfolding of chromatin during DSB repair. Perhaps the remodelling/unfolding of the chromatin requires the assistance of chromatin remodelling machineries. In yeast, the INO80 complex is either directly involved in the Rad52 DNA repair pathway (HR) or might be part of the NHEJ pathway.

In addition to INO80, another remodelling complex, SWRI, which probably mediates the exchange of H2A.X by non-phosphorylated H2A.X (Zhang *et al.*, 2005) (Fig. 3D) can also participate in the chromatin remodelling process (Downs *et al.*, 2004a). In *Drosophila,* where this exchange has been shown to take place (Kusch *et al.*, 2004) and possibly in humans, this role is played by Tip60. Mammalian homologs of some of the protein subunits from these chromatin remodelling complexes are well documented. For example, almost all of the protein subunits from yeast NuA4 HAT complex are conserved in human (Doyon *et al.*, 2004). The yeast NuA4 catalytic subunit Esa1 is very similar to the higher eukaryotic Tip60 (Kusch *et al.*, 2004). The mammalian homolog of Arp4 is Baf53 (Downs *et al.*, 2004a). Therefore, the mechanism by which γ-

H2A.X mediates DSB repair in mammalian cells is expected to be similar to that of the yeast.

The hypothetical roles of γ-H2A.X during DNA DSB repair

Numerous pieces of evidence suggest the role of H2A.X within the cell in particular as it pertains to DSB DNA repair. Three hypotheses have been proposed in attempt to explain the role of γ-H2A.X in this process.

In the first hypothesis, the protein complexes formed at the DSB site may facilitate repair by holding the broken ends in position by themselves (Pilch *et al.*, 2003a). Studies in support of this hypothesis have shown that γ-H2A.X is dispensable for the DNA strand joining in V(D)J recombination and retroviral DNA integration (Daniel *et al.*, 2004). Cells respond to retroviral DNA integration in a similar way to DSB induction during V(D)J recombination by NHEJ. Both V(D)J recombination and retroviral DNA integration involve enzymes, the RAG1/2 protein complex or the viral integrase complex, that hold the broken DNA ends together (Daniel *et al.*, 2004). The presence of these protein complexes may be redundant with H2A.X phosphorylation and hence, H2A.X could be dispensable in these two systems. Because no proteins have been found to hold the broken ends of DNA together in DSBs induced by IR and chemical agents, γ-H2A.X is hypothesized to hold DNA ends together during DSB repair.

A second hypothesis proposes that γ-H2A.X can act as a component in the signal transduction pathway or is part of the histone code that recruits DSB repair factors. In support of this, DNA repair factors, such as Nbs1, 53BP1 and Nhp10 (part of the INO80 complex in yeast), have been shown to interact directly with γ-H2A.X (Celeste *et al.*,

2003). Furthermore, the accumulation, but not the initial recruitment, of the repair proteins requires γ-H2A.X (Celeste *et al.*, 2003).

In the third hypothesis, it has been proposed that γ-H2A.X directly affects the chromatin structure in the region surrounding a DSB making the region accessible to repair factors. Accordingly, histone H2A.X is implicated in the alteration of the chromatin structure in *S. cerevisiae* (Downs *et al.*, 2000). Because the C-terminal tail of H2A.X is located near the entry and exit sites of DNA in the nucleosomes, the phosphorylation of this tail could relax the chromatin fiber by altering the linker DNA trajectory (Abbott *et al.*, 2001). This change in chromatin conformation may be the result of the presence of the two or more negative charges introduced by one or more phosphates at this location. Conversely, histone H1, which binds to the same nucleosomal location, could have an inhibitory role in the process. Indeed, it has been experimentally shown that Hho1p linker histone suppresses HR (Dalton *et al.*, 1989; Downs *et al.*, 2003). The opening of the chromatin fiber would allow the recruitment of the H2A.X dependent DSB repair proteins to the chromatin forming IRIF.

These hypotheses are not mutually exclusive. Indeed, it is possible that several of these mechanisms may act synergistically to facilitate DNA repair. For example, repair factors could be directly recruited to DSB by the phosphorylation of SQE motif at the C-terminal tail of H2A.X, which could also be involved in the alteration of chromatin conformation. In Chapter 2, we will investigate the role of H2A.X during DNA DSB repair.

A working model for the role of H2A.X during DNA DSB

The histone modifications and the recruitment of the chromatin remodeling complexes and DNA repair factors are essential parts of repairing DSBs. The phosphorylation of H2A.X precedes most of the repair mechanisms. It is possible to envisage a model in which γ-H2A.X's role in DSB repair is that of a signal mediator and DSB repair facilitator. γ-H2A.X could act as part of the histone code which flags the region of DNA damage. This would allow the activation and recruitment of the critical DNA repair factors in both HR and NHEJ pathways as well as the recruitment of chromatin remodeling complexes. γ-H2A.X could also directly, or in combination with histone acetylation by NuA4 complex, alter the conformation of chromatin facilitating the recruitment of DNA repair factors. The subsequent recruitment of chromatin remodeling complexes could additionally alter the conformation of the chromatin fiber for further facilitation of the DSB repair process (see Fig. 4).

Although H2A.X sequence and function have been conserved through evolution (see Fig. 1 and 2), the mode of action of this histone H2A variant might be slightly different in different species. The role of H2A.X in the yeast and mammalian systems has been studied extensively. However, there are major differences between the two systems. First, yeast has a much smaller genome than mammals. Also, because the yeast orthologs (HTA1, HTA2) of H2A.X make up 95% of the H2A population the involvement of chromatin modification through phosphorylation at the C-terminus might be more significant than that observed in the mammalian systems. Therefore, the frequency of γ-H2A.X-containing nucleosomes in the yeast chromosome is different from that of the mammalian chromosome. Another major difference is that yeast employs HR as the

predominant pathway to repair DSB whereas the mammalian systems, including human, mainly use NHEJ. After IR exposure, yeast contains a large amount of phosphorylated H2A-containing nucleosomes due to the large occurrence of these H2A.X orthologs in the yeast genome. This most likely results in a major alteration of the chromatin folding (Downs *et al.*, 2000) which probably facilitates the HR repair pathway. In mammals, the more subtle changes in the chromatin folding may simply reflect the preferential use of the NHEJ DSB repair pathway by these organisms.

Other roles of γ-H2A.X not related to DNA DSB

After the introduction of DNA DSBs, IRIFs form and can be observed as large foci using confocal microscopy when stained with a γ-H2A.X antibody. However, in the absence of DNA DSBs, small γ-H2A.X foci that are distinct from the larger foci are visible (Ismail and Hendzel, 2008). Furthermore, there is no DNA DSB repair recruitment at these small γ-H2A.X foci (McManus and Hendzel, 2005). These two clearly distinct populations of γ-H2A.X raise the question: does γ-H2A.X participate in other cellular processes in addition to its role in DNA DSB repair and if so, what are they?

The large DNA DSB-associated γ-H2A.X foci were found to be excluded from heterochromatin regions (Kim *et al.*, 2007; McManus and Hendzel, 2005). In contrast, the more abundant, small γ-H2A.X foci that occur independently of DNA DSB seemed to partition equally within euchromatin and heterochromatin (McManus and Hendzel, 2005). Co-localization of DNA DSB repair factors (Mre11, Rad51, NBS1, Brca1, Ku80,

53BP1, XRCC4 and DNA ligase IV) are visualized at the sites of the large γ-H2A.X foci (McManus and Hendzel, 2005) in contrast to small γ-H2A.X foci, which lack these DNA DSB repair factors (McManus and Hendzel, 2005). Under normal growth conditions (*i.e.* in the absence of any DNA damaging agents), the microscopic signal intensity of γ-H2A.X was observed to be under cell cycle regulation. It reaches maximal levels at G_2/M in an ATM-dependent manner and begins to decrease, reaching basal steady-state levels immediately after cytokinesis (McManus and Hendzel, 2005). Although a small number of large γ-H2A.X foci are always present due to endogenous DNA DSB, most of this observed signal dependence is due to the abundant small γ-H2A.X foci. However, the nature of the involvement of histone H2A.X in these small foci and the participation of other mitotic proteins is not clear.

FACT (facilitates chromatin transcription) is a histone chaperone that consists of two subunits, Spt16 and SSRP1 (Sims *et al.*, 2004). Recently, FACT has been shown to interact with H2A.X in a way that is dependent on DNA-PK H2A.X phosphorylation (Fig.3). FACT catalyzes the incorporation and the dissociation of H2A.X from the nucleosome (Heo *et al.*, 2008). DNA-PK phosphorylation enhances the exchange of H2A.X in the nucleosome by altering its stability (Heo *et al.*, 2008). Furthermore, poly-ADP-ribosylation of the Spt16 subunit of FACT significantly reduces its H2A.X exchange activity (Heo *et al.*, 2008). Thus, the phosphorylated form of histone H2A.X selectively contributes to the exchange of this variant during transcription.

In addition to transcription factors, steroid hormones, such as estrogens, also contribute to histone H2A.X metabolism (Fig.3). Estrogens (E2) play critical roles in the initiation, development and metastasis of breast and uterine cancers (Yager and

Davidson, 2006). The breast and uterine cancer cells respond to estrogens via estrogen receptor-α (ER- α), a ligand-activated transcription factor that regulates transcription of target genes by binding to recognition DNA sequences (Hua *et al.*, 2008). Estrogens are shown to upregulate the expression of H2A.X (Hua *et al.*, 2008). Such an enhanced expression may play important roles in the regulation of transcription during tumorigenesis and cancer progression.

Finally, the phosphorylation of H2A.X has been shown to be coupled with the late replication of the inactive X chromosome (Xi) (Abbott *et al.*, 2005). Furthermore, both Brca and γ-H2A.X co-localize within facultative heterochromatin of the Xi during late S-phase (Abbott *et al.*, 2005). Although the mechanism by which γ-H2A.X participates in Xi replication still needs to be elucidated, it is possible that like macroH2A, it may also contribute to maintaining gene silencing.

The involvement of γ-H2A.X in DNA DSB repair has been the focus of intense research in recent years. However, it is clear from the above that γ-H2A.X participates in many other cellular processes and shifting the research attention in this direction may prove to be very rewarding.

Conclusion

At present, the detailed molecular mechanisms of DSB DNA repair, NHEJ or HR in yeast and in metazoans, are not completely understood. As well, the structural and the functional implications of γ-H2A.X in DNA DSB repair and in the more recently described non-DSB related cellular mechanisms await further investigation. Despite the many remaining unanswered questions, γ-H2A.X exhibits a ubiquitous occurrence in

DSB repair throughout the eukaryote kingdom regardless of the DSB origin and the different pathways used for its repair. There is no doubt that the co-evolution of H2A.X with the canonical H2A counterpart has played an important role in the maintenance of the eukaryotic genome integrity. Its emerging role in non-DSB related processes, such as transcription, is a new and exciting field, which is also very important in deciphering the role of H2A.X in the cell.

Chapter 2. Phosphorylation of T136 and S139 of histone H2A.X by DNA-PK is not affected by core histone acetylation and it alters nucleosome stability and histone H1 binding

Li A's contribution to the work: performed and analysed all of the experimental data except for the mass spectrometry data and prepared figures.

Abstract

Phosphorylation of the C-terminal end of histone H2A.X is the most characterized PTM in DNA DSB. DNA-PK is one of the three PIKK members, which is known to phosphorylate histone H2A.X during DNA DSB repair. There is a growing body of evidence supporting a role for histone acetylation in DNA DSB repair but the mechanism or the causative relation remains largely unknown. Using bacterially expressed recombinant mutants and stably and transiently transfected cell lines, we find that DNA-PK can phosphorylate T136 in addition to S139 both *in vitro* and *in vivo*. Furthermore, the phosphorylation reaction is not inhibited by the presence of H1, which is itself a substrate for DNA-PK. We also show that, in contrast to previous reports, the ability of the enzyme to phosphorylate these residues is not affected by the extent of acetylation of the core histones. *In vitro* assembled nucleosomes and HeLa S3 native oligonucleosomes consisting of non-acetylated and acetylated histones are equally phosphorylated by DNA-PK. We demonstrate that the apparent differences in the extent of phosphorylation previously observed can be accounted for by the differential chromatin solubility under the $MgCl_2$ concentrations required for the phosphorylation reaction *in vitro*. Finally, we show that while H2A.X does not affect nucleosome conformation, it has a de-stabilizing effect that is enhanced by the DNA-PK- mediated phosphorylation and impairs histone H1 binding.

Introduction

As described above, DNA DSB repair is an important cellular process that is critical for the maintenance of genome integrity. In the eukaryotic cell, the repair mechanism requires the participation of chromatin components. One of the chromatin hallmarks involved is the phosphorylation of histone H2A.X at its highly conserved C-terminal SQE motif (Fig. 5A) (Li *et al.*, 2005a; Pilch *et al.*, 2003b; Rogakou *et al.*, 1998). This phosphorylated form of H2A.X is commonly denoted as γ-H2A.X (Rogakou *et al.*, 1998). As described in Chapter 1, it is well known that histone H2A.X is phosphorylated ubiquitously at DNA DSB regardless of the source of the damage and of the pathway used in its repair: homologous recombination (HR) or non-homologous-end joining (NHEJ). The enzymes responsible for the DSB-induced H2A.X phosphorylation are all members of the PIKK family, such as the DNA-dependent protein kinase (DNA-PK), ataxia telangiectasia mutated (ATM) and ATM and Rad3-related (ATR) (Li *et al.*, 2005a; Stiff *et al.*, 2004a).

In the yeast H2A.X ortholog, T126 and S129 can both be phosphorylated during DSB in a way that appears to depend on the repair pathway. It has been shown that T126 is important for HR but dispensable for NHEJ (Moore *et al.*, 2007). The early identification of γ-H2A.X in vertebrates (Rogakou *et al.*, 1998), hinted to the possibility that S/T136 could also be phosphorylated . However, experimental evidence for this suggestion has been lacking. Determining whether or not this residue is also phosphorylated is important as, in contrast to yeast, where HR is the preferred mechanism of DSB repair, mammalians preferentially use NHEJ (Mahaney *et al.*, 2009) where DNA-PK plays a critical role (Meek *et al.*, 2008).

In addition to the phosphorylation of the histone H2A.X, there is a growing body of evidence supporting a role for histone acetylation in DNA DSB repair. Cells with DNA breaks have a transient increase in histone H3 and H4 acetylation (Tamburini and Tyler, 2005). Defects in the acetylation of K56 in histone H3 result in sensitivity to genotoxic agents that cause DNA DSBs during replication (Masumoto *et al.*, 2005). It has been found that mutation of multiple acetylatable lysine residues in the H4 tail (Bird *et al.*, 2002) or mutations of the TIP60 (human HAT complex that mediate H4 acetylation) (Ikura *et al.*, 2000; Murr *et al.*, 2006) and NuA4 (yeast homologue of TIP60) (Downs *et al.*, 2004a) complexes confer sensitivity to agents that create DSBs. Although acetylation of histones is one of the most studied histone modifications and evidence has been provided that histone acetylation enhances phosphorylation of H2A.X by DNA–PK (Park *et al.*, 2003b), the concerted structural effect, if any, of this histone PTM with that of γ-H2A.X remains to be elucidated.

The structural and functional involvement of this highly characteristic H2A.X phosphorylation is not clearly understood. It is yet unclear whether it elicits a change in chromatin structure allowing for access of DNA repair machineries or if it acts as part of the histone code that recruits repair machineries (Li *et al.*, 2005a; Morrison and Shen, 2005). These two possibilities need not be mutually exclusive. As an example of the former, it has been shown that γ-H2A.X promotes rapid Rad9 recruitment to DSBs in yeast (Javaheri *et al.*, 2006). A direct role on chromatin conformation was suggested by the decrease in chromatin compaction by the serine/glutamic phosphorylation mimics of yeast H2A.X at S129 (Ausió *et al.*, 2001; Downs *et al.*, 2000). Arguing against this, and against a general role for the C-terminal tail of H2A.X, it was recently shown that the

yeast S/E mutants had no effect on either chromatin stability and supercoiling or on nucleosome positioning (Fink *et al.*, 2007).

In this chapter, I show that T136 and S139 of human H2A.X are both substrates of DNA-PK and are phosphorylated in cells. Acetylation of core histones does not influence the ability of the phosphorylating enzymes to phosphorylate H2A.X and neither does the presence or absence of linker histones. Finally, we observe that H2A.X de-stabilizes the nucleosome and its DNA-PK- mediated phosphorylation slightly impairs linker histone binding.

Materials and Methods

Histone plasmid constructs

A plasmid containing human H2A.X prepared as in (Siino *et al.*, 2002b) was kindly provided to us by Joe Siino and it was subcloned into a pET11a bacterial expression plasmid. Similar expression vectors consisting of the mutant forms of H2A.X: S139A, T136A/S139E and A138E/S139E were prepared using the appropriate 3'end primers encompassing these mutations (see Table 1). Constructs containing GFP at the N-terminal end of H2A.X and its mutants were prepared by inserting the coding regions (320 nt to 737 nt) of the previous plasmids into pEGFP-C1 mammalian expression vector (BD Biosciences Clontech, San Jose, CA).

Table 2. Table of primer sequences used to construct H2A.X and H2A.X mutant expression vectors.

	Primer sequences
H2A.X	Forward 5' GGAATTCCATATGTCTGGACGTGGAAAA Reverse 5' CGGGATCCTTAGTATTCCTGGGAAGCCTGGG
S139A	Forward 5' GGAATTCCATATGTCTGGACGTGGAAAA Reverse 5' CGGGATCCTTAGTATTCCTGAGCAGCCTGGG
T136A/S139E	Forward 5' GGAATTCCATATGTCTGGACGTGGAAAA Reverse 5' CGGGATCCTTAGTATTCCTGCTCAGCCTGGGCAGCTTTTTT
A138E/S139E	Forward 5' GGAATTCCATATGTCTGGACGTGGAAAA Reverse 5' CGGGATCCTTAGTATTCCTGCTCAGCCTGCTCAGCTTTTTT

Histone Expression and Purification

Recombinant human H2A.X and all mutants, were expressed in *Escherichia coli* BL21(DE3) cells. The bacterial pellet was homogeneized with a dounce in 6 M guanidium hydrochloride, 1 mM EDTA, 1 mM DTT and 50 mM Tris-HCl (pH 7.5) buffer. The cell lysate was dialyzed against 2 L of 0.1 M NaCl, 50 mM Tris-HCl (pH 7.5) and 1 mM EDTA buffer for 2 hr at 4˚C. The recombinant histone was extracted by 0.5N HCl. The solubilized histones were precipitated overnight at – 20 °C with six volumes of cold acetone, pelleted, dried and resuspended in water. The HCl extracted histones were further purified using a Macro-Prep CM Cation Exchange resin (BioRad, Hercules, CA) with a 0 to 1M NaCl gradient in 7M urea, 10mM NaOAc (pH 5.2), 5mM β-mercaptoethanol and 1mM EDTA buffer. The eluted histone was dialyzed lyophilized and further purified by reversed-phase HPLC (Grace Vydac, St. Hesperia, CA) using a a 4.6 x 250 mm Vydac C_4. Elution is carried out using a linear acetonitrile gradient (0-60% in 40 mins) in 0.1% TFA at 1 ml/min (Ausió and Moore, 1998). Native histone H2A-H2B dimers and H3-H4 tetramers and histone H1 were purified by salt gradient hydroxyapatite fractionation of HeLa S3 (Simon and Felsenfeld, 1979). Histone H2B was isolated from histone H2A by a Vydac C_4 reverse-phase HPLC as above.

DNA fragments

A 146 bp random sequence DNA was obtained from chicken erythrocyte nucleosome core particles prepared as described elsewhere (Ausió *et al.*, 1989). A sequence-defined 208 bp DNA fragment was obtained by *Rsa*I digestion of a 208-12 DNA construct consisting of 12 identical copies of a 208 bp fragment of the 5S rRNA

gene of the sea urchin *Lytechinus variegatus* (Simpson *et al.*, 1985). After digestion with *Rsa*I, the 208 bp DNA was HPLC purified using a 75 x 7.5 mm Bio-Gel DEAE-5-PW (Bio-Rad, Hercules, CA) in 0-1M NaCl gradient in 100 mM Tris-HCl (pH 7.5) buffer.

Western Blot and Antibodies

Approximately 2 µg of proteins was loaded onto SDS-PAGE and transferred to a PVDF membrane at 100V for 3 hrs at 4 °C in 25 mM Tris-HCl (pH 7.5) and 192 mM Glycine. The membrane was prepared by dipping into 100% methanol for 5 sec followed by rinses in dH_2O and transfer buffer. Transferred membranes were blocked in 3% skimmed milk overnight at 4 °C. An antibody against γ-H2A.X was prepared by Dr. Sheng-Chung Lee (Academia Sinica, Taiwan). H2A.X antibody was from Applied Biological Materials (abm, Richmond, BC). GFP antibodies were from Abcam (Abcam, Cambridge, MA).

Transient and Stable Transfections

The H2A.X/T136A/T136A-S139E GFP constructs were transfected into HeLa cells using Polyfect Transfection Reagent (Qiagen, Mississauga, ON). Transient transfected HeLa cells were cultured at 37 °C, 5% CO_2 and collected after incubating for 24 hours. H2A.X/T136A/T136A-S139E with an N-terminal FLAG tag was cloned into the pcDNA 3.1 (-) mammalian expression vector. The H2A.X/T136A/T136A-S139E FLAG constructs were transfected into H2A.$X^{-/-}$ MEFs (kindly provided to us by Andre Nussenzweig) (Celeste *et al.*, 2002). Transfection was carried out using Effectene Transfection Reagent (Qiagen, Mississauga, ON). The transfected H2A.$X^{-/-}$ MEFs were

cultured at 37 °C and 5% CO_2. After 24 hour incubation, media were replaced with fresh media containing 800 μg/ml geniticine. The media was replaced again after one week with fresh media containing 400 μg/ml geniticine. After one week of incubation, stably transfected MEFs were then collected and expression of the protein constructs was checked by Western Blot analysis using GFP and H2A.X antibodies.

Cell irradiation

Cell irradiation was performed by Dr. Wayne Beckham (BC Cancer Agency, Victoria). HeLa cells or stably transfected MEF cells were subjected to 10 Gy irradiation at room temperature, using a Varian 6EX medical linear accelerator (Varian Medical Systems, Palo Alto CA). Maximum uncertainty in the radiation dose was estimated to be ±5%.

Chromatin Preparation from Butyrate-treated and Non-treated HeLa S3 Cells

HeLa S3 cells were grown in 10 % fetal calf serum in Dublbecco's modified Eagle's medium supplemented with 2 mM glutamax, 0.11 mg/ml sodium pyruvate and 0.5 mg/ml penicillin/streptomycin. The cells were grown to a density of 5-10 x 10^5 cells/ml. The cells were then harvested or incubated in the presence of 5 mM sodium butyrate for 21 hrs before harvesting. Cell pellets were resuspended in buffer A (0.25 M sucrose, 60 mM KCl, 15 mM NaCl, 10 mM MES (pH 6.5), 5 mM $MgCl_2$, 1 mM $CaCl_2$, 0.5% Triton X-100, with or without 5 mM sodium butyrate) at a ratio of 5 ml/g of pellet as described previously (Wang *et al.*, 2000);(Howe and Ausió, 1998). The suspension was then centrifuged at 3000 x *g* for 10 min at 4°C. This step was repeated and the

pellets (nuclei) were then resuspended in buffer B (50 mM NaCl, 10 mM Pipes (pH 6.8), 5 mM $MgCl_2$, 1 mM $CaCl_2$, with or without 5 mM sodium butyrate) at a ratio of 2.5 ml/g of pellet and centrifuge under the same condition as above to obtain nuclei. Nuclei from butyrate-treated and non-treated HeLa S3 cells were digested with micrococcal nuclease (MNase) (Worthington Biochemical Corp., Lakewood, NJ). The digestion was carried out at 30 units/mg DNA for 7 min at 37 ºC in buffer B (with or without 5 mM sodium butyrate). The supernatant obtained after centrifugation for 10 min at 10,000 x *g* (4ºC), was designated as fraction S1. The pellet was then resuspended and lysed in 0.25 mM EDTA (pH 7.5) to produce, after a subsequent centrifugation, a supernatant (SE) and a pellet (P) fractions. Histone H1 from the SE fraction was stripped from chromatin by treatment with CM Sephadex C-25 resin in the presence of 0.35 M NaCl. All the buffers used for the chromatin preparation of butyrate-treated HeLa S3 cells contained 5 mM sodium butyrate.

Nucleosome Reconstitution

Native H2A or recombinant human H2A.X, A138E-S139E or H2A.X phosphorylated with DNA-PK (P-H2A.X) were mixed with HeLa S3 H2B, H3 and H4 histones, and reconstituted onto nucleosomes in the presence of either 146 bp or 208 bp DNA. More specifically, histones in stoichiometric amounts were lyophilized and resuspended at 2 mg/ml in a 6 M guanidinium-hydrochloride, 20 mM β-mercaptoethanol, 50 mM Tris-HCl (pH7.5) buffer. After incubation for 30 min at room temperature, the samples were dialyzed against dsH_2O for 2 hours at 4°C. The dialysis bag was then transferred to another container containing 2 M NaCl, 50 mM Tris-HCl (pH 7.5), 1 mM

EDTA, 1 mM DTT buffer and dialyzed overnight at 4°C. For the reconstitution of nucleosomes consisting of cold DNA, the histone mixture thus prepared was mixed with either 146 bp or 208 bp DNA at a histone to DNA ratios of (1.12:1 w:w) or (0.79:1 w:w), respectively, in 2 M NaCl, 50 mM Tris-HCl (pH 7.5) , 0.1 mM EDTA buffer. For the γ^{32}P-ATP –labelled nucleosome reconstitution, γ^{32}P-ATP –labelled 208 bp DNA was mixed with an approximately 10 fold amount of cold 208 bp DNA and mixed with histones at a (0.79:1 w:w) histone: DNA ratio in the same 2M NaCl buffer (Maffey *et al.*, 2007). In all instances, nucleosome reconstitution was achieved by a 2 to 0 M NaCl stepwise salt gradient dialysis in 10 mM Tris-HCl (pH 7.5) and 0.1 mM EDTA buffer (Ausió and Moore, 1998). Nucleosomes reconstituted in this way, were purified with as described below, and used for subsequent experiments: H1 binding assay, DNA-PK reaction and analytical ultracentrifuge analysis.

Sucrose Gradient Purification of Reconstituted Nucleosomes and Native Nucleosomes Isolated From HeLaS3 Cells

Nucleosomes in 10 mM Tris-HCl (pH 7.5) and 0.1 mM EDTA were loaded onto a 5-20% sucrose gradient in 25 mM NaCl, 10 mM Tris–HCl (pH 7.5), 0.1 mM EDTA buffer and centrifuged at 111,081 x *g* for 19.6 hr in a Beckman SW41Ti rotor at 4˚C. Fractions (0.5 ml) were collected and analyzed by 4% native PAGE.

Gel Electrophoresis and Western blots

SDS-polyacrylamide gel electrophoresis (PAGE) was performed as described by Laemmli (Laemmli, 1970). Native 4% acrylamide PAGE was carried out according to

Yager and van Holde (Yager and van Holde, 1984). Acetic acid/urea (AU) gel electrophoresis was performed as previously described (Saperas *et al.*, 2006). Western blots were carried out as described previously (Abbott *et al.*, 2005; Abbott *et al.*, 2004). H2A.X, γ-H2A.X, GFP, and FLAG antibodies were used at 1:5,000, 1:3,000, 1:1,000, 1:5,000 dilutions, respectively.

Histone H1 Binding

Purified H2A, H2A.X, A138E-S139E or H2A.X phosphorylated with DNA-PK (P-H2A.X) nucleosomes (300 ng) were titrated with increasing amounts of HeLa S3 histone H1. The H1 to mononucleosomes molar ratios used were 0, 0.25, 0.5, 1.0, 1.5 and 2.0. The H1 binding reaction was performed in 50 mM NaCl, 2 mM EDTA and 20 mM Tris-HCl (7.5) buffer. The mixture was incubated at room temperature for 30 min. The electrophoretic mobility shift resulting from histone H1 binding was analyzed by agarose gel electrophoresis in 45 mM Tris-HCl (pH 7.5), 45 mM boric acid, 1 mM EDTA (0.5 x TBE).

Analytical Ultracentrifuge

Nucleosomes reconstituted with 208 bp or 146 bp DNA and histone octamers consisting of H2A.X or γ-H2A.X were dialyzed against buffers of varying ionic strength, 0, 0.1, 0.2, 0.4 and 0.6 M NaCl and analyzed by sedimentation velocity using a Beckman XL-I analytical ultracentrifuge (Beckman-Coulter, Fullerton, CA). Samples were loaded in double-sector cells with aluminum-filled Epon centerpieces and runs were performed at 20 ºC on an An-55 Al aluminum rotor and at 40,000 rpm. UV scans were collected at

260 nm and analyzed by the van Holde and Weischet method (van Holde, 1978) using the XL-A Ultra Scan version 9.3 (Demeler, 2005) sedimentation data software (Borries Demeler, Missoula, MT). A value of 0.650 cm^3/g was used for the partial specific volume of the nucleosome (Ausió *et al.*, 1989).

DNA-PK Assay

The DNA-PKcs and Ku70/80 subunits of DNA-PK were purified from HeLa cells by Dr. Susan Lees-Miller (Goodarzi and Lees-Miller, 2004). Purified DNA-PKcs (38.1 ng) and Ku (11.9 ng) were incubated in 35 µl of reaction mixture containing 50 mM Tris-HCl (pH 8.0), 4 mM or 10 mM $MgCl_2$, 10 ug/ml of sonicated calf thymus DNA and 0.25 mM ATP containing approximately 10 µCi ^{32}P- γ-ATP. The substrates, either histones (0.5 µg) or nucleosomes (1 µg), were also added to the reaction mixture. The reaction mixture was incubated for 15 min at 30˚C. Reactions were terminated by the addition of SDS loading buffer for SDS-PAGE or loading immediately after the reaction for 4% native gel. To prepare P-H2A.X on a large scale, the reaction was performed in the same way as above except for scaling up substrates and enzymes proportionally and using cold ATP instead of radioactive ^{32}P- γ-ATP. After the reaction, P-H2A.X was filtered through a 0.45 µm Nanosep centrifugal device (Pall, Ann Arbor, MI) and purified with a 4.6 x 250 mm Vydac C_{18} reversed-phase HPLC column using a gradient as described above.

Mass Spectrometry

Mass spectrometry analysis was performed by Darryl Harding (University of Victoria, Genome BC Proteomics Centre, Victoria). DNA-PK phosphorylated H2A.X

was analysed by an Applied Biosystems/MDS Sciex QStar Pulsar I fitted with a Protana/Proxeon Nanospray source. Two microliters of DNA-PK phosphorylated H2A.X (1 μg/μl) were mixed with 2 μl of 60%methanol/3% formic acid and pipetted into a fused silica Au/Pd coated nanoES spray tip (Proxeon). Spray was established by applying a tip voltage of 1200V and collecting a TOFMS survey scan.

Magnesium Chloride Titration

Chromatin solubility analysis in the presence of $MgCl_2$ (Perry and Chalkley, 1982) was carried out in 50 mM Tris-HCl (pH 7.5) buffer. The chromatin samples had an approximate A_{260} = 0.8. The different $MgCl_2$ concentrations were achieved by mixing equal volumes of the chromatin sample in the 50 mM Tris-HCl buffer with an equal volume of a 2× $MgCl_2$ in the same buffer while vortexing. The sample mixtures were incubated for 1 hr at 4˚C. The chromatin aggregates were centrifuged at 16,000 x *g*. The absorbance of the supernatant at 260 nm were measured and related to the absorbance of the starting sample in the absence of $MgCl_2$.

Results

Mammalian H2A.X T136 and S139 are both phosphorylated in vitro and in vivo

Phosphorylation of mammalian H2A.X of the SQE motif at the C-terminal end of vertebrate H2A.X (S139 in mammals) represents one of the best characterized PTM landmarks associated with double strand DNA repair. However, other phosphorylatable residues (S/T) are present in close proximity of the SQE motif targeted by the ATM/ATR and DNA-PK enzymes in many different species. In many vertebrates, the SQE

sequence is preceded by another potential DNA-PK target motif (S/T Q) which is highly conserved (Fig. 5A). Although the potential for phosphorylation of this secondary residue within γ-H2A.X was hinted in the early paper from the Bonner's lab (Rogakou *et al.*, 1998), the demonstration of its existence has remained elusive.

To test whether this site is amenable to DNA-PK phosphorylation *in vitro*, several human recombinant H2A.X histone versions were created in which the phosphorylatable residues of this histone C-terminal end (TQASQEY) were individually or globally mutated to non-phosphorylatable amino acids and subjected to DNA-PK phosphorylation (Fig. 5B). As can be seen, the TQA motif preceding SQE can be phosphorylated by the enzyme at a lower activity. From here on, the *in vitro* doubly phosphorylated form of H2A.X will be referred to as P-H2A.X to distinguish it from the in vivo phosphorylated form referred to as γ-H2A.X (Rogakou *et al.*, 1998). The ability of the TQA motif to be phosphorylated *in vivo* was assessed using HeLa cells transfected with GFP versions of the same constructs used for the *in vitro* characterization. As shown in Fig. 6A, TQA is phosphorylated in non-irradiated transiently transfected HeLa cells although to a lesser extent than the SQE counterpart. Fig. 6B shows the reactivity of the γ-H2A.X antibody for DNA-PK phosphorylated versions of the different constructs. The slightly different reactivity of the antibody towards H2A.X selectively phosphorylated at T136 can in part account for the lower phosphorylation observed with the corresponding transfected version. Irradiation of these transiently transfected cells resulted in the complete disappearance of the H2A.X-GFP constructs (results not shown), most likely as a result of DNA damage impinged by the radiation on the expressing plasmids.

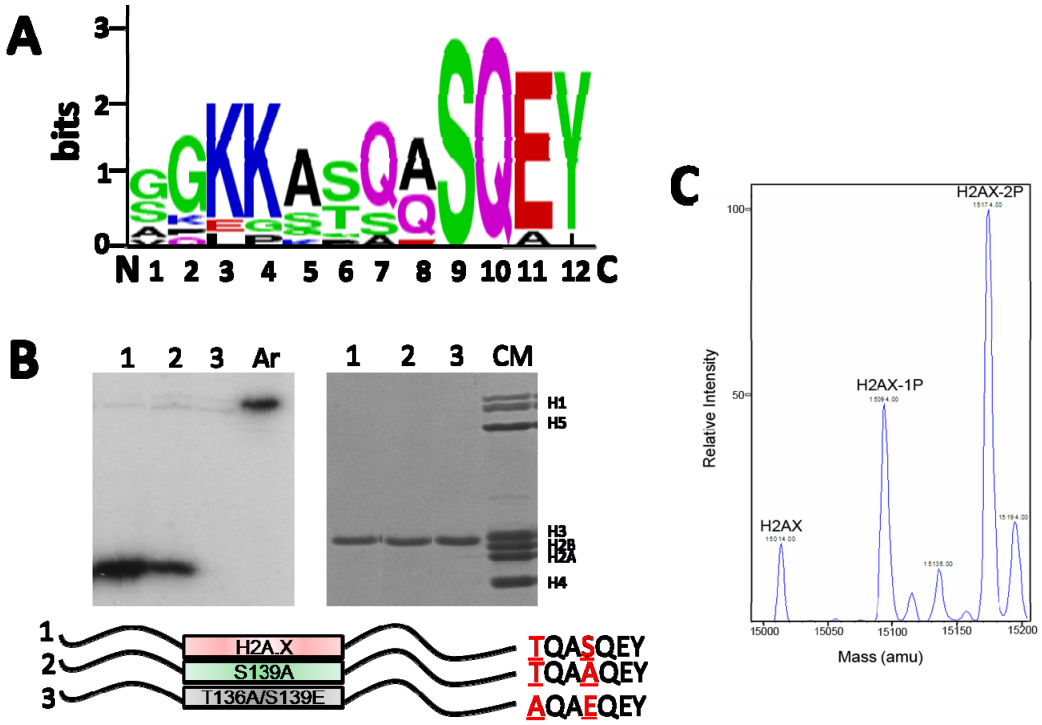

Figure 5. Phosphorylation of human H2A.X-T136 by DNA-PK in vitro.

A) Logos representation of the alignment of the last C-terminal 22 amino acids of histone H2A.X from different vertebrates: (*Homo sapiens (*NP_002096.1)*, Macaca mulatta (*XP_001101949.1)*, Canis familiaris (*XP_853256.1)*, Mus musculus (*NP_034566.1)*, Gallus gallus (*NP_002096.1*), Anolis carolinensis* (AAWZ01044401), *Xenopus tropicalis (*NP_001015968.1)*, Rana catesbeiana (*ACO51989.1)*, Danio rerio (*NP_957367.1) and *Salmo salar (*ACI66032.1)). B) DNA-PK phosphorylates both S139 and T136 of human recombinant H2A.X *in vitro*. Left panel corresponds to radioactive DNA-PK reaction carried out with purified H2A.X mutants: H2A.X (lane 1), S139A (lane 2) and T136A/S139E (lane 3), as substrates. Ar (Artemis) was used as a substrate for DNA-PK to serve as a positive control. Proteins were resolved in SDS-PAGE followed by autoradiographic analysis. The right panel shows an SDS-PAGE analysis of H2A.X (lane 1), S139A (lane 2) and T136A/S139E (lane 3). CM is a chicken erythrocyte histone marker. Bottom panel is a schematic representation of the different H2A.X mutants used in the radioactive DNA-PK reaction with mutations highlighted at the C-terminal tail. C) Deconvoluted nanospray mass spectrum of human recombinant H2A.X phosphorylated with DNA-PK.

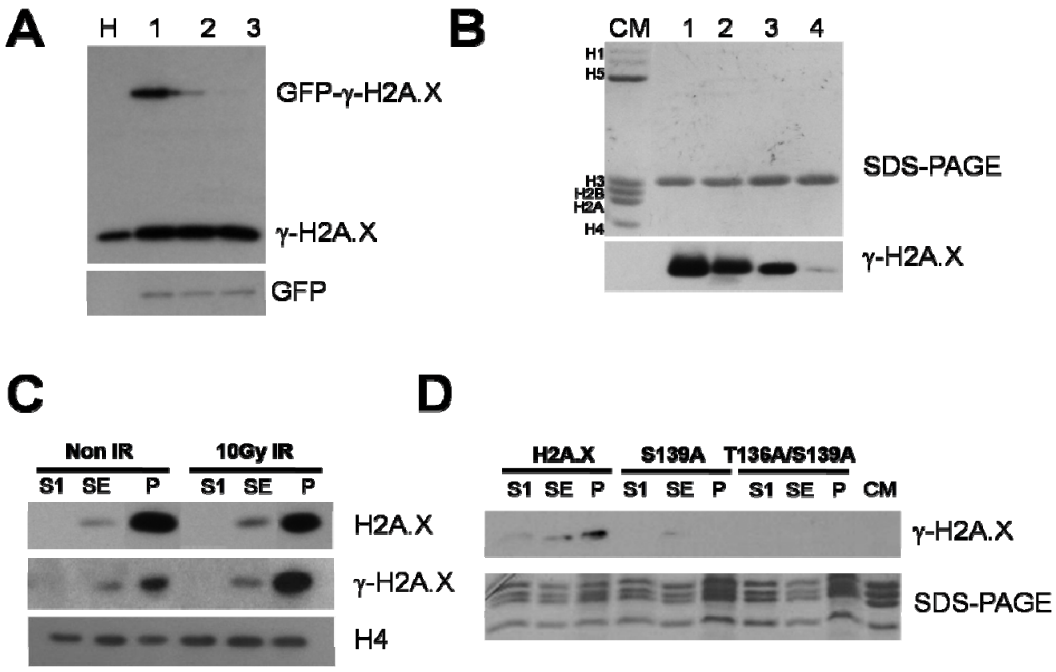

Figure 6. Phosphorylation of human H2A.X-T136 in vivo.

A) HeLa cells were transiently transfected with GFP-H2A.X constructs, H2A.X (lane 1), S139A (lane 2) and T136A/S139E (lane 3). The presence of phosphorylated H2A.X and transfected GFP-H2A.X were identified by western blot using antibody against γ-H2A.X (upper panel) and GFP (lower panel). Non-transfected HeLa cells (lane H) was used as a marker for endogenous H2A.X. B). H2A.X (lane 1), T136A (lane 2), S139A (lane 3) and T136A/S139E (lane 4), phosphorylated by DNA-PK *in vitro* were analysed by western blot using antibody against γ-H2A.X. Top panel corresponds to SDS-PAGE and the bottom panel corresponds to the western showing that the γ-H2A.X antibody is able to detect both phosphorylated T136 and phosphorylated S139. CM are chicken erythrocyte histones used as a marker. C) Western blot analysis of different chromatin fractions (S1, SE and P) obtained from HeLa S3 cells using antibodies against γ-H2A.X, H2A.X and H4 (as a loading control) before and after ionizing irradiation. D) MEF H2A.X-/- cells were stably transfected with different H2A.X mutant constructs and subjected to 10 Gy ionizing irradiation. The presence of phosphorylated H2A.X mutants and transfected FLAG-tagged H2A.X mutants in different chromatin fractions (S1, SE and P) was detected by western blot using γ-H2A.X antibodies (upper panel). The bottom panel shows an SDS-PAGE analysis of the protein loadings for each lane.

Given our inability to recover the transiently expressed GFP versions of H2A.X, stable versions of the different FLAG-H2A.X mutants were produced in MEF H2A.X$^{-/-}$ cells (Celeste *et al.*, 2002) and the chromatin from these cells was digested with MNase and fractionated into S1 (euchromatin), SE (facultative heterochromatin) and P (insoluble) fractions. Interestingly, native H2A.X in HeLa cells exhibits an uneven distribution in this fractionation which is more pronounced in the case of γ-H2A.X in irradiated cells and which fractionates with the highly insoluble P fraction in a way that is highly dependent on irradiation (Fig. 6C). This is probably due to the rearrangement γ-H2A.X from small microfoci into larger foci that takes place in the nucleus of cultured mammalian cells upon irradiation (Ismail and Hendzel, 2008; McManus and Hendzel, 2005).

After irradiation, γ-H2A.X of the MEF H2A.X$^{-/-}$ cells stably transfected with H2A.X exhibits the same distribution. Interestingly, a phosphorylated version of the S139A mutant could be observed in the same cells when transfected with this construct. The phosphorylation signal was low (due in part to the lesser efficiency of the antibody, see above) and interestingly, it was detectable only in the chromatin fraction SE which has been ascribed to facultative heterochromatin (Henikoff *et al.*, 2008; Ishibashi *et al.*, 2009a) .

The DNA-PK-dependent phosphorylation of H2A.X is not affected by histone acetylation

A tri-nucleosome fraction was prepared from HeLa cells that had been grown in the presence or in the absence of sodium butyrate in order to increase the extent of histone acetylation. Native (N) and acetylated (A) tri-nucleosomes containing or lacking

histone H1 were prepared by sucrose gradient fractionation before or after extraction of the histone H1 complement. The DNA and histone composition of these fractions is shown in Fig. 7A-B. The samples thus obtained were phosphorylated by DNA-PK in the presence of either 4 mM or 10 mM $MgCl_2$ (Fig. 7C-D). As can be seen in Fig.7C, native and acetylated nucleosomes in the absence of H1 (N and A, respectively) exhibit an almost identical extent of phosphorylation that increases slightly when the magnesium concentration was increased from 4 to 10 mM. However, in the presence of histone H1 (NH, AH), acetylated nucleosomes are more phosphorylated than the native counterpart both in 4 and 10 mM $MgCl_2$.

This enhanced DNA-PK phosphorylation of H1-containing acetylated oligonucleosomes contrasts with the results observed when H1 is not present and is in agreement with previously published results (Park *et al.*, 2003a). However, when a $MgCl_2$ solubility analysis was carried out with these samples, the results shown in Fig. 7E suggest that the increase in phosphorylation observed in the acetylated oligonucleosomes may simply reflect an increase in solubility at 4 mM and 10 mM $MgCl_2$. At these $MgCl_2$ concentrations, the H1-containing tri-nucleosomes are almost completely insoluble.

DNA-PK can phosphorylate histone H1 in vitro and in a chromatin template

Careful analysis of the phosphorylation assays carried out with oligonucleosomes containing H1 revealed that a band with an electrophoretic mobility corresponding to that of histone H1 was phosphorylated in addition to H2A.X (Fig. 7D). The same result was obtained when a mononucleosome fraction was used (Fig. 8, lanes 1-2). To corroborate that indeed H1 was being phosphorylated, purified HeLa H1 and H3-H4 as well as

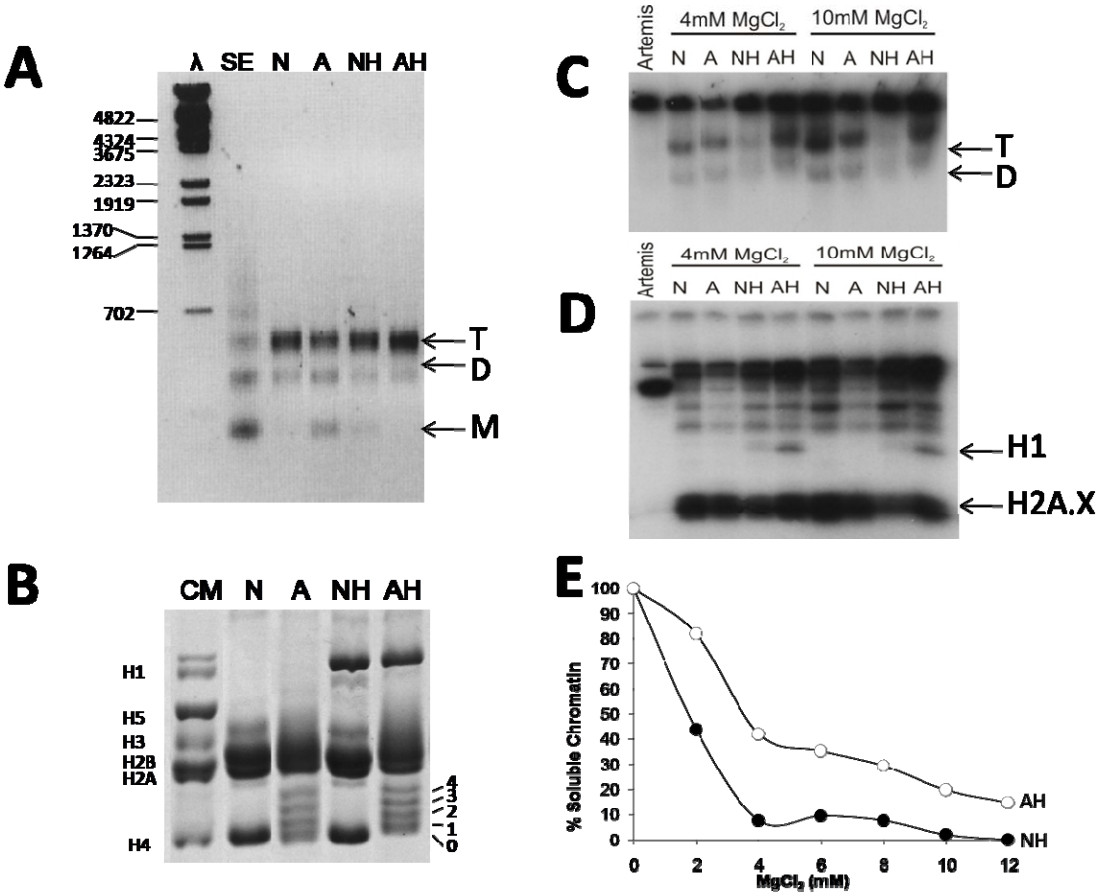

Figure 7. Histone acetylation and H2A.X phosphorylation.

Oligonucleosome DNA and proteins were resolved in 1% agarose (A), and in SDS-PAGE (B). Radioactive DNA-PK reaction was carried out with oligonucleosomes as substrates. Labeled nucleosomes and proteins were resolved in 4% native PAGE (C), and in SDS-PAGE (D). Artemis was used as a substrate to serve as a positive control. E) Solubility of native and acetylated oligonucleosomes with histone H1 in different concentrations of $MgCl_2$. N, native oligonucleosome; A, acetylated oligonucleosome; NH, native oligonucleosome with H1; AH, acetylated nucleosomes with H1; T, tri-nucleosome; D, di-nucleosomes; M, mono-nucleosomes.

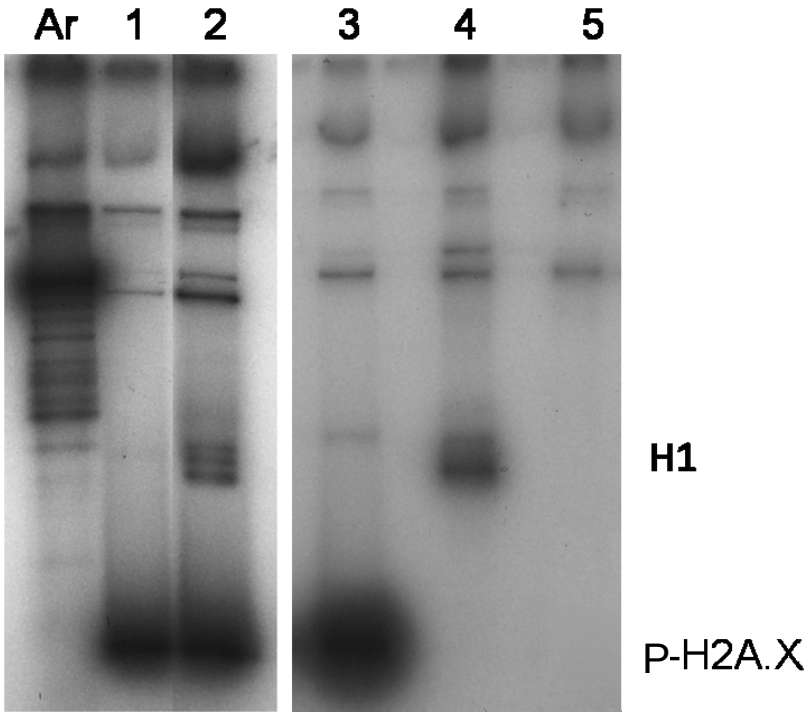

Figure 8. DNA-PK phosphorylates linker histones in vitro and in a nucleosome setting.

Lanes 1 and 2 show an autoradiograph of an SDS-PAGE of HeLa mononucleosomes lacking (lane 1) or containing histone H1 (lane 2) upon phosphorylation by DNA-PK using γP^{32}-ATP. Lanes 3-5 shows an autoradiograph of an SDS-PAGE of purified HeLa histone H2A.X, histone H1 and H3-H4 tetramers phosphorylated by DNA-PK using γP^{32}-ATP. Artemis (Ar) was used as a substrate to serve as a positive control for these reactions.

recombinant H2A.X were phosphorylated *in vitro* using DNA-PK. In Fig. 8, lanes 3 to 5 show that while the phosphorylation reaction is highly specific for H2A.X, histone H1 is also a substrate for DNA-PK albeit to a lower extent.

Histone H2A.X decreases the stability of the nucleosome and alters histone H1 binding

Next we wanted to look at the potential structural effects of the DNA-PK-mediated phosphorylation of H2A.X on nucleosomes. Fig. 9A shows a native PAGE of native NCPs and NCPs reconstituted with 146 bp random DNA sequence and native core histones with recombinant H2A.X or DNA-PK-phosphorylated H2A.X (P-H2A.X). These particles were next analysed in the analytical ultracentrifuge using sedimentation velocity (Ausió, 2000). Native NCPs exhibit a homogeneous sedimentation coefficient distribution with the main peak centered about12 S at low salt and at around 10.5 S at 0.6 M NaCl, as it has been previously described (Ausió *et al.*, 1989) (Fig. 9B). At NaCl concentrations equal to or above 0.4 M NaCl, minor peaks with smaller sedimentation coefficients are observed, which correspond to NCPs with different extent of dissociation. The peak observed at approximately 6 S corresponds to naked (fully dissociated) DNA. In contrast, H2A.X NCPs exhibit a much less stable pattern as a large fraction of the NCPs is fully dissociated by 0.6 M NaCl. A higher dissociation was observed when H2A.X was fully phosphorylated (Fig. 9C). Furthermore, the $s_{20,w}$ values of the undissociated NCP fraction at each NaCl concentration analysed were slightly lower than those of the native NCPs suggesting that H2A.X and P-H2A.X NCPs adopt a different conformation.

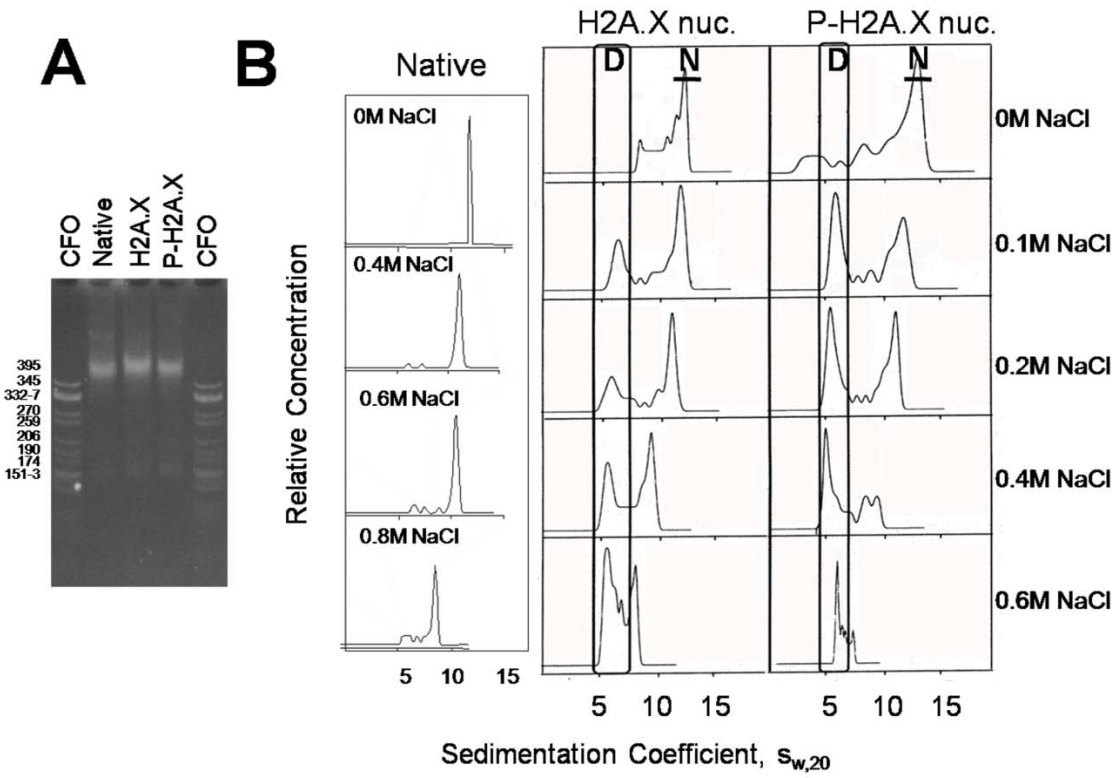
A
CFO
Native
H2A.X
P-H2A.X
CFO
395
345
332-7
270
259
206
190
174
151-3
B
Native
H2A.X nuc.
P-H2A.X nuc.
D
N
0M NaCl
0.4M NaCl
0.6M NaCl
0.8M NaCl
0.1M NaCl
0.2M NaCl
Relative Concentration
5 10 15
Sedimentation Coefficient, $s_{w,20}$

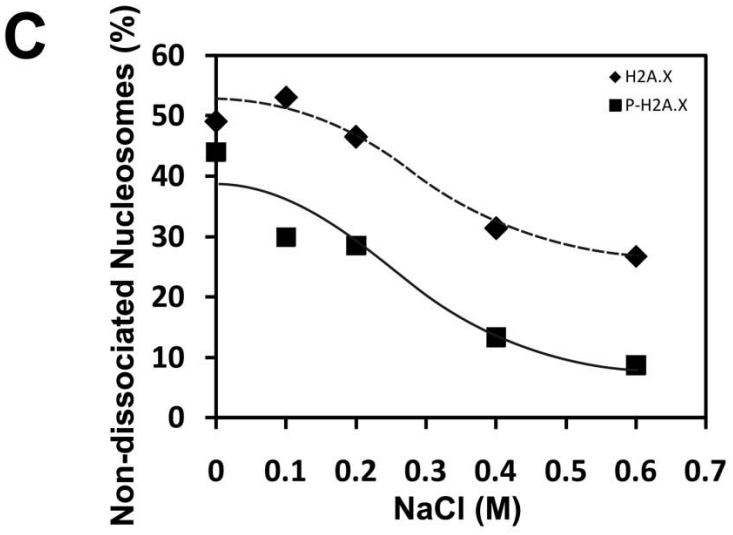
C
Non-dissociated Nucleosomes (%)
60
50
40
30
20
10
0
H2A.X
P-H2A.X
0 0.1 0.2 0.3 0.4 0.5 0.6 0.7
NaCl (M)

Figure 9. DNA-PK γ-H2A.X nucleosome core particles are less stable compared to the H2A.X or H2A nucleosome core particles.

A) Native 4% PAGE analysis of NCPs, in comparison to NCPs reconstituted with H2A.X or with P-H2A.X and 146 bp random senquence DNA. CFO is a *Cfo*I digested pBR322 plasmid DNA used as a marker. B) NaCl dependence of the sedimentation coefficient ($s_{20,w}$) of native NCPs and NCPs reconstituted with H2A.X or with P-H2A.X. Sedimentation velocity experiments were carried out at 40,000 rpm at 20°C in different NaCl concentrations in 10 mM Tris-HCl and 0.1 mM EDTA (pH 7.5) buffer. D: area of the scan corresponding to material sedimenting as free DNA; N: peak in the scan corresponding to NCPs. C) Percentage of non-dissociating H2A.X/P-H2A.X-containing nucleosomes at different NaCl concentrations calculated from the relative area under peak N of the sedimentation velocity profile shown in B)

I wondered if a potential change in NCP conformation of the H2A.X nucleosomes could affect the binding of histone H1. To this end, I reconstituted H2A.X and P-H2A.X containing nucleosomes using a longer 208 bp DNA template (Simpson *et al.*, 1985). Increasing amounts of H1 were then added to these reconstituted nucleosomes and the gel shift obtained is shown in Fig. 10A. As it can be seen, the H2A.X nucleosomes bind less well to H1 and this effect is enhanced by T136/S139 phosphorylation. A similar result was obtained when the S139 of H2A.X was replaced by two glutamic acids to mimic the double negative charge introduced by a phosphate at this position. As seen in Fig.10B, this impaired H1 binding similar to that observed with P-H2A.X in Fig. 10A.

To gain some insight in the potential mechanism involved in the impaired H1 binding, we analysed the 208 bp reconstituted nucleosomes using the analytical ultracentrifuge. Similar to Fig. 9B, a decrease in $s_{20,w}$ of the undissociated nucleosome fraction was observed at any given salt concentration (Fig. 10C). Such decrease is reminiscent of the decrease in the sedimentation coefficient of the NCPs when core histones become acetylated (Ausió and van Holde, 1986) and the effect of destabilization is enhanced by the presence of 208 bp DNA.

Such decrease in the sedimentation coefficient suggests an unfolding of the particle likely resulting from a release of the DNA ends at the entry and exit sites into the nucleosome core particle. Such an alteration in the trajectory of DNA would be consistent with the impaired binding ability of linker histones observed in Fig. 10A-B.

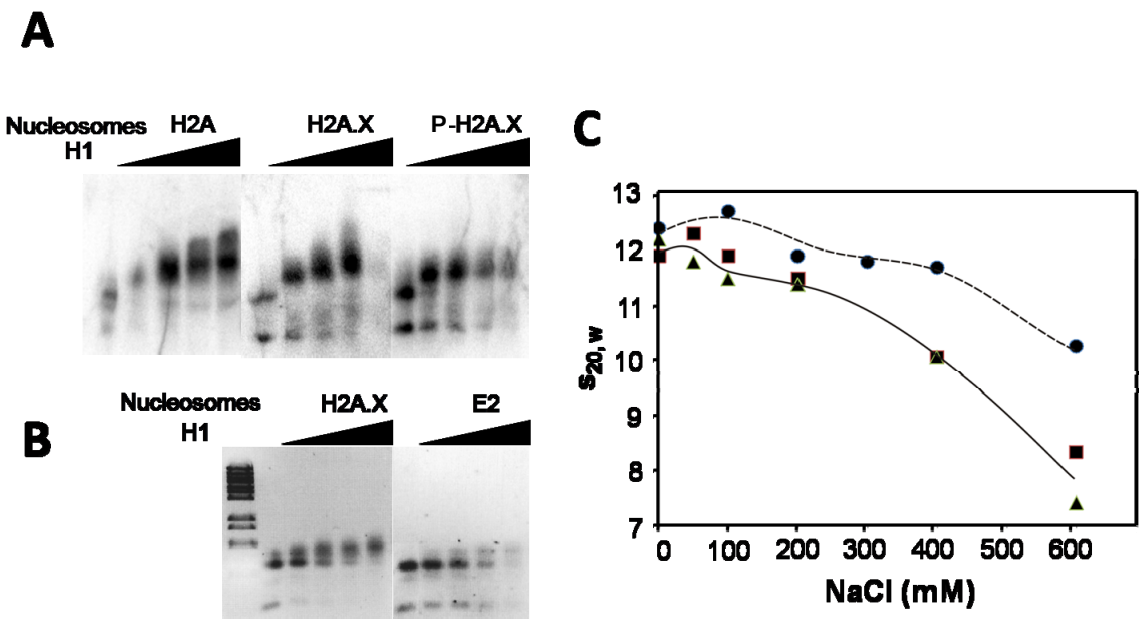

Figure 10. Impaired binding of linker histones to nucleosomes by H2A.X and γ-H2A.X.

A) Nucleosomes reconstituted with H2A, H2A.X and P-H2A.X and γP^{32}-ATP-labelled 208 bp DNA were titrated with increasing amounts of histone H1 and analysed by 1% agarose gel electrophoresis. The histone H1 to nucleosome molar ratios used were 0, 0.5, 1.0, 1.5 and 2.0. The image shows an autoradiograph of the gel. B) Ethidium bromide stain image of a similar H1-dependent gel shift carried out in a 1% agarose gel using 208 bp reconstituted nucleosomes consisting of H2A.X and A138E/S139E. C) Sodium chloride concentration dependence of the sedimentation coefficient ($s_{20,w}$) of 208 bp reconstituted nucleosomes consisting of native H2A (black circles), H2A.X (black squares) and P-H2A.X (black triangles).

Discussion

Presence of several acetylation-independent damage-response phosphorylatable sites at the C-teminus of H2A.X

Vertebrate H2A.X histone variants contain two PIKK target sites at their C-terminus and also, in many instances, contain a phosphorylatable tyrosine at the very end of the molecule (Fig. 5A). The C-terminal tyrosine has been recently shown to be phosphorylated by the Williams-Beuren syndrome transcription factor (WSTF), which is also involved in DNA repair (Xiao *et al.*, 2009). It has been speculated that one of the putative roles for such phosphorylation may be needed to alter chromatin structure for further maintenance of S139 phosphorylation (Xiao *et al.*, 2009). Interestingly, a set of H2A.X having phenylalanine instead of tyrosine at their very C-termini (H2A.X-F) has been identified in *Xenopus laevis* eggs (Shechter *et al.*, 2009). In this instance, an additional SQE motif has been shown to be present (Shechter *et al.*, 2009) . Yet, its C-terminal end has a sequence (…122-SAKATKASQEL-129) where DNA-damage dependent phosphorylation of S122, T126 and S129 has been reported (Harvey *et al.*, 2005; Moore *et al.*, 2007). Therefore, the presence of several phosphorylatable sites at the end of the C-terminal tail of H2A.X appears to be a general feature of the molecule.

Our results show that, as suspected earlier (Rogakou *et al.*, 1998), human T136 is able to be phosphorylated by DNA-PK *in vitro* and *in vivo* (Fig. 5B-C and Fig. 6A-D). Of note, T126 in yeast is important for HR but indispensable for NHEJ (Moore *et al.*, 2007). Since NHEJ is the main repair pathway in vertebrates, it is not surprising that T136 phosphorylation is also important in these organisms (Li *et al.*, 2005a).

In contrast to what was earlier reported, our results show that the phosphorylation process is unaffected by histone acetylation (Fig.7). This result is not surprising as it has been shown in yeast and other organisms that while H2A.X phosphorylation happens relatively quickly upon DSB damage, histone acetylation is a downstream event that occurs later (Krebs, 2007) upon recruitment of the chromatin remodelling complexes INO8, SWRI and NuA4 (Downs *et al.*, 2004b; Morrison *et al.*, 2004; van Attikum *et al.*, 2004a).

Histone H2A.X partitions with insoluble chromatin fractions in HeLa cells

In HeLa cells and in other mammalian tissues (results not shown), H2A.X is preferentially distributed in the chromatin insoluble fraction P (Fig. 6C). Under the experimental digestion conditions used here, fraction P accounts for approximately 65% of the overall chromatin. A smaller amount is detected in SE and not detected in S1. These two fractions respectively correspond to 25% and 10% of the starting chromatin before digestion. The S1 fraction corresponds to nucleosomes from transcriptionally active chromatin (Henikoff *et al.*, 2008), while the SE fraction is enriched in facultative heterochromatin (Ishibashi *et al.*, 2009a) . The P fraction corresponds to insoluble material, which is resistant to MNase digestion. This fraction is not associated with facultative heterochromatin markers (Ishibashi *et al.*, 2009a), but it contains large macromolecular complexes including transcriptionally engaged chromatin and constitutive heterochromatin (Henikoff *et al.*, 2008; Ishibashi *et al.*, 2009a). As shown here, it includes the micro- and macro-foci that are cytologically visualized in cultured

mammalian cells before and after ionizing irradiation, respectively (Bewersdorf *et al.*, 2006; McManus and Hendzel, 2005).

This observation has important implications for the yet unresolved issue of chromatin distribution of histone H2A.X in somatic tissues (Pilch *et al.,* 2003b; Pinto and Flaus, 2010). It has long been proposed that H2A.X distributes itself homogeneously throughout the genome with approximately one molecule every five nucleosomes assuming that only heteromorphic (H2A.X-H2A) nucleosomes are present (Pilch *et al.*, 2003b). Our data (Fig. 6C) are more consistent with a non homogeneous H2A.X chromatin distribution in which either small "islands" of highly H2A.X-enriched nucleosomes are interspersed within more extensive regions with a lower density of the variant or a clustering of the H2A.X nucleosome is present, as it has been recently suggested (Pinto and Flaus, 2010) . Furthermore, the phosphorylation resulting from irradiation affects mainly the P fraction (compare the distribution of γ-H2A.X in irradiated versus non irradiated cells in Fig. 6C). An uneven distribution of the ionizing irradiation induced γ-H2A.X formation towards preferentially transcribing chromatin has been recently documented [(Cowell *et al.*, 2007; Vasireddy *et al.*, 2009), see (Costes *et al.,* 2010) for a recent review].

Finally, the differential chromatin distribution of the phosphorylated forms of the S139A H2A.X mutant (fraction SE) and H2A.X wild type (fraction P) in transfected $H2A.X^{-/-}$ MEF cells (Fig. 6C-D) come in support of their reinforcing structural nature. In the latter instance, it is possible that recruitment of DNA repair complexes to phosphorylated S139 site could render the phosphorylated H2A.X-containing nucleosomes insoluble. This would suggest that, in the absence of S139 phosphorylation,

T136 phosphorylation is not sufficient to recruit such complexes to the site of DNA damage. Therefore, phosphorylation of H2A.X at T136 is likely to act as an enhancer to the structural contribution by phosphorylated H2A.X during DNA DSB repair rather than a signalling factor. As has been earlier demonstrated, phosphorylation of histone H1 (Fig. 8) may also have an important contribution to these processes (Kysela *et al.*, 2005). Indeed, DNA-PK-mediated phosphorylation of H1 has been shown to decrease its affinity within the DNA repair context (Kysela *et al.*, 2005).

H2A.X deposition has important structural consequences for chromatin

The issue on whether the histone H2A phosphorylation resulting from PIKKs has any effect on chromatin structure has been elusive. An early study carried out in *S. cerevisiae* demonstrated that substitution of serine by glutamic acid (a mutation that is aimed to mimic phosphorylation) at position 129 of yeast H2A.X resulted in chromatin relaxation of the yeast minichromosome (Downs *et al.*, 2000). This was not an unexpected result as the C-terminal tail of H2A exits the nucleosome at a position near the pseudo-dyad axis of symmetry where the DNA enters and exits the particle. Therefore, the introduction of negative charges (two per phosphate) at such location has the potential for an alteration of the path followed by DNA (Ausió *et al.*, 2001). However, a recent publication has challenged these results and shown that S129E does not have any effect on the DNA supercoiling nor in nucleosome stability as determined by nucleosome positioning and nuclease accessibility assays (Fink *et al.*, 2007). In contrast to these results, we have observed that the presence of histone H2A.X has a very significant ionic-strength dependent destabilization effect on the nucleosome, which is

enhanced by the presence of DNA-PK mediated phosphorylation (Fig. 9B). This latter result is in agreement with recently published data that showed a γ-H2A.X-mediated structural destabilization of the nucleosome, which appears to primarily affect the ends of the nucleosomal DNA (Heo *et al.*, 2008).

The salt-dependent instability of the H2A.X-containing nucleosome was quite unexpected. However, as pointed out in (Pinto and Flaus, 2010), several important amino acid differences in the histone fold of H2A.X and the divergent sequence of the C-terminal tail could account for de-stabilization. In particular, the change from N38 to histidine and from K99 to glycine between human H2A.1 to H2A.X could be potentially involved. The first substitution which is located in the loop connecting the α1 and α2 helices of the H2A histone fold deserves special attention as this amino acid is in the H2A region (N38-E41) of the H2A-H2B dimer, which makes direct contact with the equivalent region of the second H2A.H2B dimer within the protein core of the nucleosome (Luger *et al.*, 1997; Marino-Ramirez *et al.*, 2005). Furthermore, histidine has long been shown to play an important role in the stability of the histone octamer (Eickbush and Moudrianakis, 1978). Of note, the ionic-strength-dependent instability of the H2A.X nucleosome is very similar to that of the yeast nucleosome, where a histone H2A.X ortholog is present, and represents encompasses 95% of the overall H2A complement (Pilch *et al.*, 2003a). Yeast nucleosomes have been shown to be less stable than those containing canonical H2A and dissociate completely by 0.5 M NaCl (Pineiro *et al.*, 1991). The instability of such nucleosomes would be consistent with a dynamic chromatin designed to accommodate the high levels of transcriptional activity. A similar dynamic chromatin structure is likely to be involved in DNA repair. In terms of the

potential physiological implications, the model proposed in Fig. 11 for the H2A.X containing nucleosome. During DNA DSB repair, it is tempting to speculate that the phosphorylation of both H2AX and H1 provide a dynamic nucleosome environment which prevents histone H1 from binding thus maintaining an open chromatin organization.

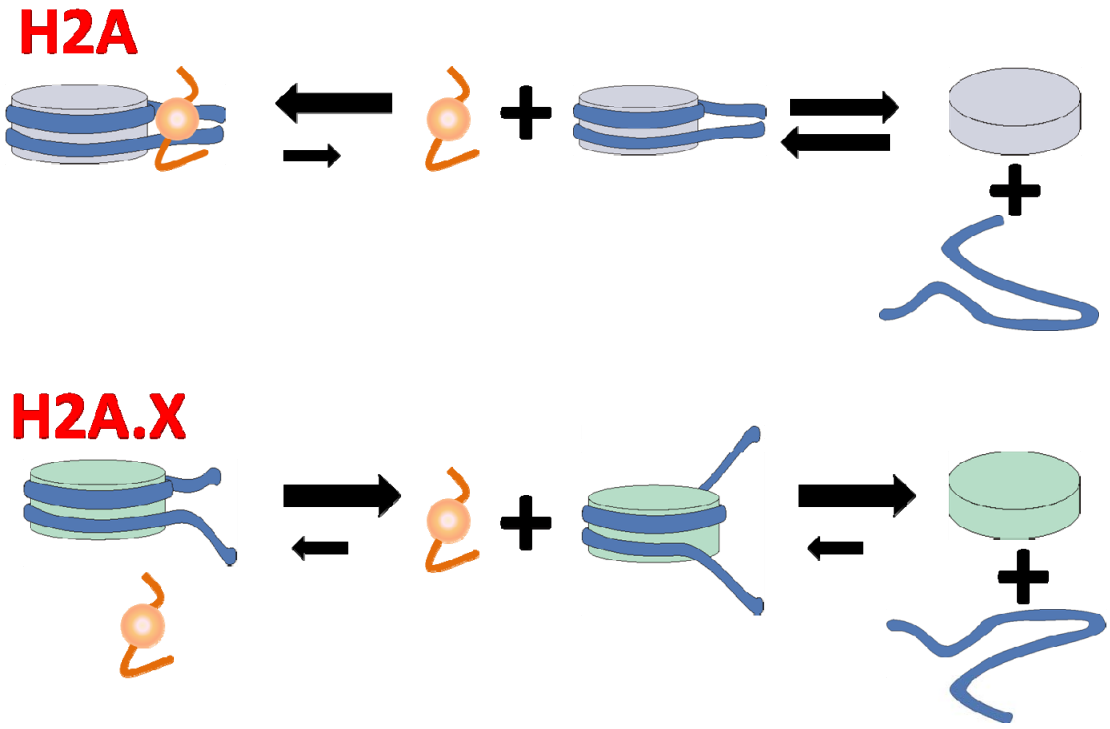

Figure 11. Model proposed to account for the structural implications of histone H2A replacement by H2A.X and its C-terminal phosphorylation.

As indicated in the left hand side of this figure, isolated nucleosomes in solution exhibit a reversible dissociation into its constitutive histone and DNA components that depends on temperature, concentration and ionic strength (Ausio *et al.*, 1984). Histone H2A.X decreases the stability of the nucleosome displacing this equilibrium towards the dissociated state (Fig. 9). In addition, and as shown in the lower part of this figure, histone H2A.X alters the nucleosome conformation (Fig. 10C) in a way that impairs the binding of linker histones (Fig. 10A-B).

Chapter 3. H2A.Bbd: An X-chromosome-encoded histone involved in mammalian spermiogenesis

Adapted from Ishibashi *et al.* for the purpose of this thesis (Ishibashi *et al.*, 2009b). Ishibashi T. and Li A. have contributed equally to this work.

Li A's contribution to the work: transfection, chromatin preparation, histone extraction and purification, western blotting analysis and figure preparation. Ishibashi T contributed the PCR experiments and chromatin preparation. Eirín-López JM contributed the phylogenetic analysis. Meistrich ML contributed the fractionated mouse testis cell. Hendzel M contributed the immunofluorescence analysis.

Abstract

Despite the identification of H2A.Bbd as a new vertebrate-specific replacement histone variant several years ago, and despite the many *in vitro* structural characterizations using reconstituted chromatin complexes consisting of this variant, the existence of H2A.Bbd in the cell and its location has remained elusive. In this chapter, we report that the native form of this variant is present in advanced spermiogenic fractions of mammalian testis at the time when histones are acetylated and being replaced by protamines. It is also present in the nucleosomal chromatin fraction of mature human sperm. The ectopically expressed non-tagged version of the protein is associated with micrococcal nuclease-refractory insoluble fractions of chromatin and in mouse (20T1/2) cells, H2A.Bbd is enriched at the periphery of chromocenters. The exceedingly rapid evolution of this unique X-chromosome-linked histone variant is shared with other reproductive proteins including those associated with chromatin in the mature sperm (protamines) of many vertebrates. This common rate of evolution provides further support for the functional and structural involvement of this protein in male gametogenesis in mammals.

Introduction

It will be nine years since the replacement histone variant H2A.Bbd was first identified from an EST database search using nucleotide sequences of members of the human H2A gene (Chadwick and Willard, 2001). Northern blot identified the presence of its mRNA in human testis and PCR of the cDNA obtained from poly(A)$^+$ RNA fraction revealed its occurrence in different human female tissues (Chadwick and Willard, 2001). Using ectopically expressed myc epitope-tagged and GFP-tagged versions of the protein, it was shown that it was largely excluded from the inactive X-chromosome under these conditions. Furthermore, the ectopically expressed tagged form of the protein co-fractionated in sucrose gradients with the mononucleosome fraction generated from MNase digestion of stably transfected cells (Chadwick and Willard, 2001).

The identification of this new histone H2A variant was followed by many important biochemical studies aimed at the characterization of its role in chromatin organization using mainly *in vitro* reconstituted systems and cells ectopically expressing tagged forms of the protein (Bao *et al.*, 2004; Gautier *et al.*, 2004). In this way, it was shown that H2A.Bbd destabilizes the NCP and it exchanges faster from chromatin than the canonical H2A counterpart (Gautier *et al.*, 2004). The H2A.Bbd-containing reconstituted NCP was shown to have a more relaxed conformation (Bao *et al.*, 2004; Gautier *et al.*, 2004; Montel *et al.*, 2007) and organizes approximately 120-130 bp of DNA (Bao *et al.*, 2004; Doyen *et al.*, 2006), leaving approximately 10 bp at the flanking ends of the NCP free from interaction with the histone core octamer (Doyen *et al.*, 2006; Montel *et al.*, 2007). Also, it was shown that the chromatin remodelling complexes SWI/SNF, ACF and nucleolin are unable to mobilize the variant H2A.Bbd NCP but can

assist the process of NCP assembly (Angelov *et al.*, 2006; Angelov *et al.*, 2004) similarly to what has been observed in the case of the histone chaperone NAP-1 (Okuwaki *et al.*, 2005). From a functional perspective, H2A.Bbd was initially found to co-localize with H4 acetylated at K12 (Chadwick and Willard, 2001) and hence, due to the well known correlation between histone acetylation and active transcription (Calestagne-Morelli and Ausio, 2006; Marushige, 1976), the *in vitro* work has tried to provide support for an involvement of H2A.Bbd in this process. Indeed, transcription appeared to be more efficient for H2A.Bbd nucleosomal arrays than for conventional H2A arrays (Angelov *et al.*, 2004). The lack of an H2A acidic patch (Luger *et al.*, 1997) that regulates chromatin compaction (Chodaparambil *et al.*, 2007) in H2A.Bbd has been shown to be structurally responsible for a 3.5-5.5 fold increase in transcription in the H2A.Bbd nucleosome arrays (Zhou *et al.*, 2007). However, despite the substantial amount of *in vitro* work, the native form of this histone H2A variant has never been identified. Its physiological role has remained elusive and is still completely unknown.

In this chapter, I report the identification of H2A.Bbd in a native setting and its involvement in mammalian spermiogenesis where the protein is found associated with the highly acetylated H4 chromatin fraction that precedes the replacement of histones by protamines (Lewis *et al.*, 2003e; Oliva and Dixon, 1991).

Materials and Methods

Sequence alignment

Histone H2A.Bbd sequences in the evolutionary analysis were retrieved through recurrent BLAST searches on GenBank databases including complete genomes from

human and mouse. Sequences were edited and aligned based on their amino acid sequences using the BIOEDIT (Hall, 1999) and CLUSTAL_X programs using the default parameters of Bioedit. The accession umbers of the sequences used in the analysis were: mBbd.1: NM_001102665; mBbd.2: XM_001476045; mBbd.3: XM_88950, XM_911022; mBbd.4: XM_910275; mBbd.5: XM_001472598; hBbd.1: NM_080720, AF254576, NM_001017991; hBbd.2: NM_001017990.

The rate of H2A.Bbd evolution was estimated by calculating the numbers of amino acid substitutions per site between human and mouse H2A.Bbd proteins taking 112 million years ago (MYA) as a reasonable estimate for human-rodent divergence (Kumar and Hedges, 1998).

PCR

RNA was extracted from mouse testis using RNeasy mini kit (Qiagen). After extraction, cDNAs were synthesized using a Superscript II kit (Invitrogen) following the manufacturer's procedures, and used as templates for PCR. Genomic DNA was extracted from mouse testis using DNeasy tissue kit (Qiagen). cDNA and genomic DNA were subjected to PCR analysis using the following sets of primers: p5 (5' primer: TGATCTTTGCAGTGAGCCTG; 3' primer: GTAGACCTCCAAGTCCAGCG), p4 (5' primer: ATGACAACACCCCCAGAGAG; 3' primer: TAGCTGATGATGAGCAGGGG), p(1-2) (5' primer: GTGGAGCCAAGTCATCCTGT; 3' primer: AGACAGCCAAGTCCAGCAGT) and p3 (5' primer: ATCTTTGCTGTGAGCCTGGT; 3' primer: AAGGCTGGGCAGGACTAACT) of the 5’ and 3’ ends of the coding regions of the corresponding genes. PCR amplification was

carried out by 35 cycles of: 95 °C for 30 sec; 57 °C for 30 sec; 72 °C for 50 sec and final extension: 72 °C for 7 min. The fragments of the PCR product were cloned into pCR2.1-TOPO vector (Invitrogen) and grown clones were amplified by PCR. The PCR products were analyzed by 1.5% agarose electrophoresis and the corresponding gene identification was carried out by digestion with *Hpa* II (New England Biolabs) and analysis on 4% native PAGE in 20 mM sodium acetate, 40 mM Tris-HCl (pH 7.2), 1 mM EDTA buffer. Selected clones from each gene type were also confirmed by the DNA sequencing.

DNA construct and transfection

Total RNA was extracted from mouse tissues and cDNAs were synthesized by reverse transcriptase-PCR (RT-PCR) as described above. The RT-PCR amplicon was identified to be *M. musculus* H2A.Bbd (MmH2A.Bbd) gene isotype 3. The coding region of MmH2A.Bbd was cloned into the pcDNA 3.0 mammalian expression vector (Invitrogen Life Science). The MmH2A.BbD construct was transfected into HeLa cell using Polyfect Transfection Reagent (Qiagen) and cultured at 37 °C, 5% CO_2 for 24 hr. A GFP-version of MmH2A.Bbd isotype 3 was also prepared by cloning its coding region into a pEGFP-N1 vector (Clontech).

Mouse testis cell fractionation

Total cell suspensions were separated by centrifugal elutriation (JE-6B rotor, Beckman Instruments) to obtain Fraction 2 enriched in step 9-12 elongating spermatids (flow rate interval: 12.6 to 18 ml/min, rotor speed: 3000 rpm), Fraction 4 enriched in step 1-8 round spermatids (9.5 to 14 ml/min, 2000 rpm), and Fraction 6 enriched in pachytene

primary spermatocytes (24 to 30 ml/min, 2000 rpm) (Unni and Meistrich, 1992; Zhao *et al.*, 2007).

Chromatin preparation, histone extraction and purification

The testis or liver tissues from mouse were homogenized using a Kinematica Polytron in 150 mM NaCl, 20 mM Tris-HCl (pH 7.5), 0.1 mM EDTA buffer containing a protease inhibitor mixture ("Complete" from Roche Diagnostics at the ratio of 1 tablet per 100 mL buffer). The homogenate was subsequently processed and digested with MNase at 30 unit/mg chromatin for the amount of time indicated, to generate S1, SE and P chromatin fractions as described in Chapter 2. Chromatin fractions from native HeLa cells or from HeLa cells ectopically expressing a non-tagged version of mH2A.Bbd isotype 3 (mH2A.Bbd-3) were prepared in the same way. Mouse testis nuclei were also extensively digested and the digestion product (mainly mononucleosomes) was processed with a modification of the method described elsewhere (Sarcinella *et al.*, 2007). Briefly, nuclei were digested with MNase at 100 units /mg of chromatin at 37 $^{\circ}$C for 30 mins. MNase digest reaction was quenched by addition of EGTA to a final concentration of 1 mM. Nuclei were centrifuged at 600 x *g* for 10 min and the pellets were resuspended in 20 mM Tris-HCl (pH 7.5), 420 mM NaCl, 1.5 mM $MgCl_2$, 0.2 mM EGTA. The resuspended sample was incubated on ice for one and a half hour and then centrifuged at 1000 x *g* for 10 min to produce supernatant and pellet designated as S and P, respectively. Histones from the different chromatin fractions were extracted with 1 N HCl (at approximately 6 µL per milligram of starting tissue), the HCl extracts were precipitated with 6 volumes of acetone at -20 °C and analysed by SDS-/AU-PAGE or RP-HPLC.

Resuspended histones were eluted starting from a 0.1 % trifluoroacetic acid (TFA) solution and an increasing acetonitrile (ACN) shallow gradient: 1-5 % ACN for 1 min, 5-25 % ACN for 10 min, 30-40 % for 40 min. Proteins from mature human sperm samples were analysed by SDS-PAGE. Alternatively, and in order to visualize the protamines, the mouse testis chromatin fractions were dialysed against water, lyophilized, pyridylethylated in the presence of 4M guanidium-HCl, 50 mM Tris-HCl (pH 7.5), 1.25 mM EDTA solution and homogenized. Briefly, 1 µl of β-mercaptoethanol was added to every 250 µl of the guanidinium-HCl suspension and incubated for 1.5 hours at room temperature in the dark followed by addition of 2 µl of vinyl pyridine and further incubation for 30 min vortexing every 5 min. The sample was then dialysed, lyophilized and extracted with 1N HCl as above.

The sperm chromatin was isolated as described elsewhere (Nazarov *et al.*, 2008). In brief, semen samples were washed with ice cold PBS, then cell pellets were treated with PBS containing 0.5% Triton X-100 for 10 min on ice, washed with PBS and resuspended with reaction buffer: 10 mM Tris-HCl, pH 8.0, 2 mM $CaCl_2$, 2 mM $MgCl_2$, 10 mM dithiothreitol. The MNase was added to the suspensions at final concentration of 20 U/mg DNA and samples were incubated for 10 min at 37°C. After centrifugation the supernatants were discarded and the pellets were resuspended with 10 mM Tris-HCl (pH 8.0), 5 mM EDTA, 10 mM dithiothreitol, extracted on ice for 30 min and supernatants (SE) and the pellet (P) were collected.

Western blot analysis

Western blot analysis of SDS-PAGE of the proteins from the different chromatin and RP-HPLC fractions were carried out using a rabbit polyclonal antiserum elicited against recombinant mouse H2A.Bbd in house (Eirin-Lopez *et al.*, 2008) and used at a dilution of 1:1000. Other antibody dilutions used in the Western blots were: H4, 1:5000, pan acetylated H4 (Millipore), 1: 500, and a secondary rabbit horse-radish peroxidase conjugate (Abcam), 1:5000. Protein transfer and detection was performed as described in Chapter 2. Western blot analysis was also used to determine the ratio of histone H2A.Bbd to histone H4 in the mouse spermatogenic fraction 2 obtained by centrifugal elutriation. To this end, the chromosomal proteins from this fraction were run on an SDS-PAGE together with increasing amounts of recombinant mH2A.Bbd and histone H4 followed by a double Western using the mouse H2A.Bbd and H4 antibodies described above. The intensity of the different bands was analysed by densitometry and the relative ratio of H2A.Bbd to H4 in the query sample was determined by interpolation.

Immunofluorescence

Mouse (20T1/2) and human (SK-N-SH) cell lines were grown in DMEM with 10% fetal calf serum, plated on glass cover slips and allowed to attach and grow until between 40 and 80% confluent. They were then co-transfected with GFP-H2A.Bbd using Effectene transfection reagent (Qiagen). The cells were then grown for an additional 16-20 hrs followed by fixation with 4% paraformaldehyde in PBS. The cells were then mounted in PBS containing 90% glycerol, 0.5 mg/ml para-phenylenediamine, and 1 µg/ml DAPI. The cells were then fixed with 4% paraformaldehyde in PBS and imaged by

wide-field fluorescence microscopy. The images were collected with a Zeiss Axioplan II fluorescence microscope using a 63X 1.4 N.A. PlanApo objective and a Photometrics CoolSnap fx 12-bit cooled CCD.

Results and Discussion

Histone H2A.Bbd is located on the X chromosome.

In order to identify the presence of native H2A.Bbd protein in the cell, we used mouse (*M. musculus*) as a biological system. An initial search of the mouse genome indicated that five closely related putative protein isotypes (Fig. 12A) are encoded by 4 different genes, all of which are located on the X-chromosome. Isotypes mH2A.Bbd.1 and mH2A.Bbd.2 are encoded by a single gene referred to here as gene 1-2 (see below). This mouse pattern of gene organization contrasts with that of humans where only two protein isotypes, hH2A.Bbd.1 and hH2A.Bbd.2, are present and are encoded by three different genes also located on the X-chromosome. When these results are translated into evolutionary rates (Fig. 12B), it appears that H2A.Bbd has a rate of evolution that exceeds that of any other histone including histone H1. Furthermore, the rate of H2A.Bbd evolution is even faster than that of human versus mouse P1 protamines (Retief *et al.*, 1993). It is noteworthy that the H2A.Bbd gene is encoded on the X-chromosome (Fig. 13A), since it has been shown that X-linked sperm proteins evolve at faster rates than their autosomal counterparts (Torgerson and Singh, 2003).

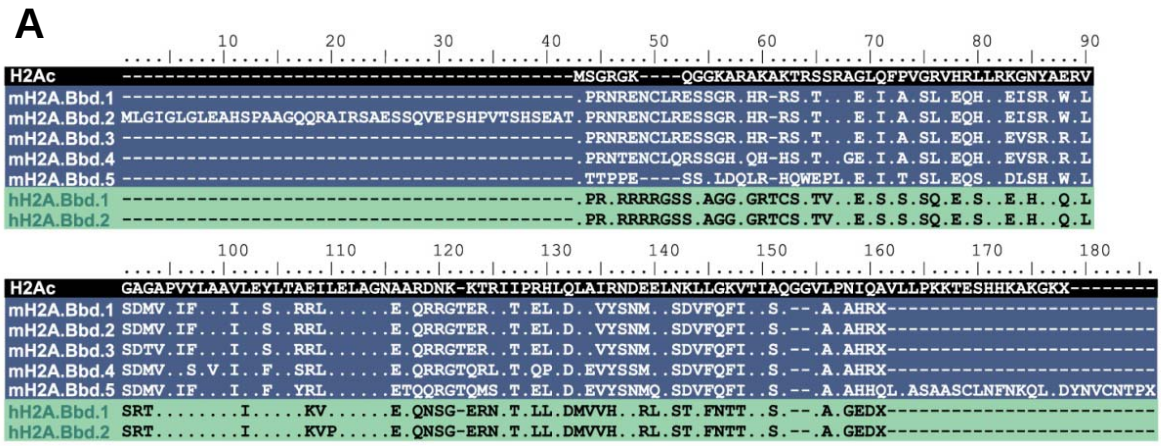

Figure 12. H2A.Bbd sequence alignment.

A) Protein sequence alignment of the mouse mH2A.Bbd isotypes compared to a consensus canonical histone H2A (H2Ac) and to human hH2A.Bbd isotypes. B) Evolutionary rates (amino acid change/100 sites) of mammalian H2A.Bbd compared to P1 protamines, histones and other proteins.

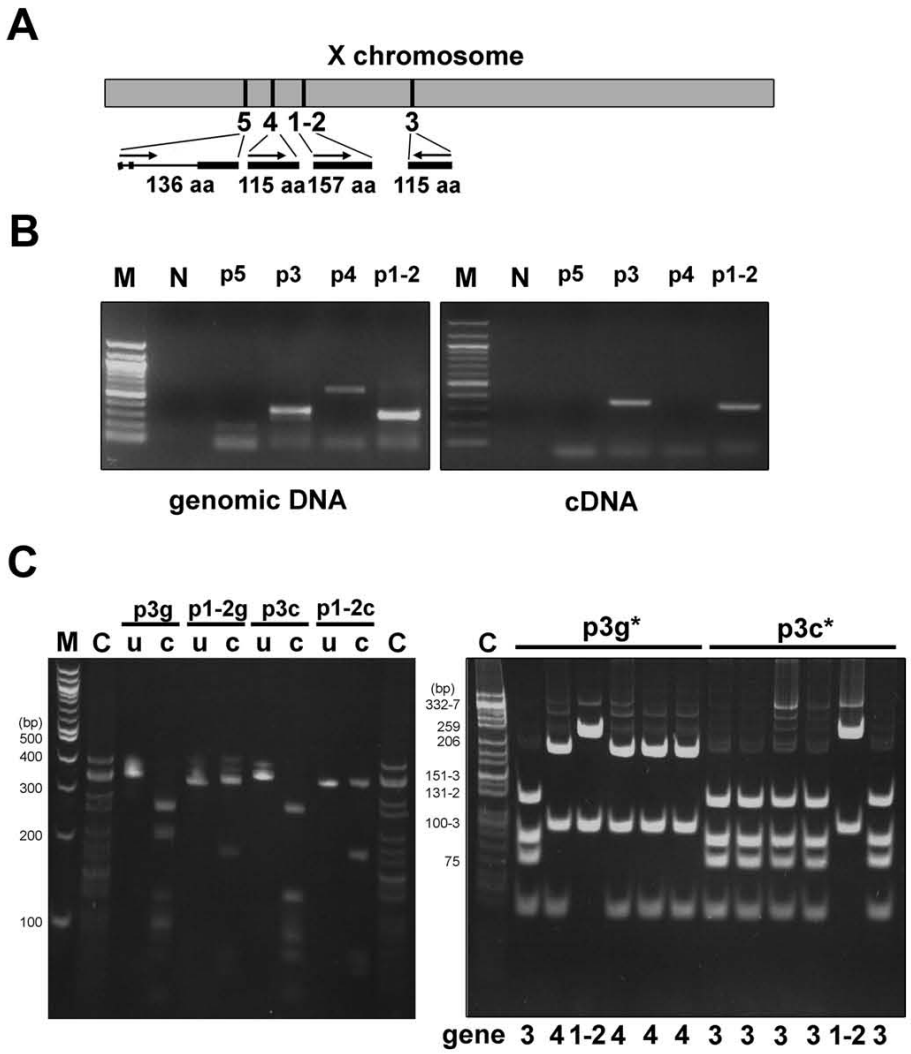

Figure 13. Transcriptional expression of mouse H2A.Bbd.

A) Schematic representation of the H2A.Bbd genes in the mouse X chromosome (grey box) and their organization (arrows depict 5' -3' transcription) and structure (exons, thick line; introns, thin line). B) PAGE of PCR products from mouse genomic DNA and testis cDNA. The primer set number is indicated on top. C) The PCR products of the genomic (p3g, p4g) and cDNA (p3c, p4c) amplification were digested with *Hpa*II restriction enzyme (left panel). Alternatively, the PCR products were cloned and the DNA extracted from genomic (3g*) and cDNA (3c*) colonies was digested with *Hpa*II (right panel). The numbers underneath the gel indicate the genes shown in (A). M is a 100 bp DNA ladder and C is a *Cfo* I digest of pBR322 used as markers; u: uncut; c: cut DNA.

Three of the four histone H2A.Bbd genes in mice are differentially expressed in testis

Previous reports had noted enhanced levels of H2A.Bbd mRNA expression in human and mouse testis (Chadwick and Willard, 2001; Eirin-Lopez *et al.*, 2008). In order to examine this observation, we prepared several primers designed to amplify distinct regions within the coding segments of each of the four mouse genes identified *in silico* as shown in Fig. 13A. Each set of primers was able to generate the expected gene fragments using mouse genomic DNA as a template (Fig. 13B). However, only the cDNAs corresponding to gene 1-2 and gene 3 could be amplified from a mouse testis cDNA library, suggesting that only genes 1-2 and 3 are transcribed in mouse testis. Given the intrinsic similarity between the nucleotide sequences of the cDNAs of the different H2A.Bbd isotypes, it was necessary to expand the analysis in order to corroborate this finding. The fragments amplified with the primers for H2A.Bbd-3, H2A.Bbd-4 and H2A.Bbd-1-2 from testis cDNA template were predicted to have 3, 2 and 1 *Hpa*II restriction sites, respectively, and therefore digestion of the PCR products shown in Fig. 13B with this enzyme (Fig. 13C, left panel) determined that these bands represented a mixed population of PCR amplicons. These amplicons were then cloned and the DNA from the many different colonies obtained was sequenced and digested again with *Hpa*II (Fig. 13C, right panel). The amplified fragments from the cDNA library (*i.e.* p3c*) were able to produce only fragments corresponding to mH2A.Bbd-1-2 and mH2A.Bbd-3, a result that was confirmed by the sequencing analysis. Out of 70 positive colonies obtained from genomic amplification, 43% corresponded to H2A.Bbd-4, 30% to H2A.Bbd-1-2 and 27% H2A.Bbd-3 and from 30 positive colonies obtained from the testis cDNA library, 80% belonged to H2A.Bbd-3 and 20 % to H2A.Bbd-1-2. This

indicates that the primers are approximately equally efficient and that H2A.Bbd-3 is expressed at much greater levels than H2A.Bbd-1-2 in testis. The lack of genomic amplification of gene 5 is not surprising as the coding region of this gene is distributed through 3 exons encompassing 20, 100 and 16 amino acids in the N- to C-terminal direction of the protein, with a 5.2 kilobase intron 2.

Histone H2A.Bbd is present in cells at advanced stage of spermiogenesis and in human sperm.

Since it was clear that mH2A.Bbd isotypes 1-2 and 3 were expressed at the transcriptional level in testis, we decided to look for the protein in testis tissue. Similar protein amounts of HCl nuclear extracts from transfected HeLa cells over-expressing an ectopic version of mH2A.Bbd-3, mouse liver and testis were analysed by RP-HPLC (Fig. 14A-B). The entire volume of each of the HPLC fractions was vacuum-dried and subjected to SDS-PAGE and Western blot analysis with a mH2A.Bbd antibody (Fig. 14B). As shown in Fig.14B, mH2A.Bbd could only be detected in HeLa cells ectopically expressing the protein and in mouse testis. Furthermore, in the almost identical histone elution profiles (Fig. 14A and results not shown), mH2A.Bbd eluted after histone H3. Two bands can be visualized at this position (see arrows in Fig. 14B) in mouse testis: an intense one with identical electrophoretic mobility to mH2A.Bbd-3 and one displaying a lower mobility which presumably corresponds to the less expressed H2A.Bbd-1-2. A Western blot analysis of testis cells at different stages of spermatogenesis is shown in Fig. 14C. The cells were separated by centrifugal elutriation and three fractions, 2, 4 and 6 enriched in elongating spermatids, round spermatids, and pachytene spermatocytes,

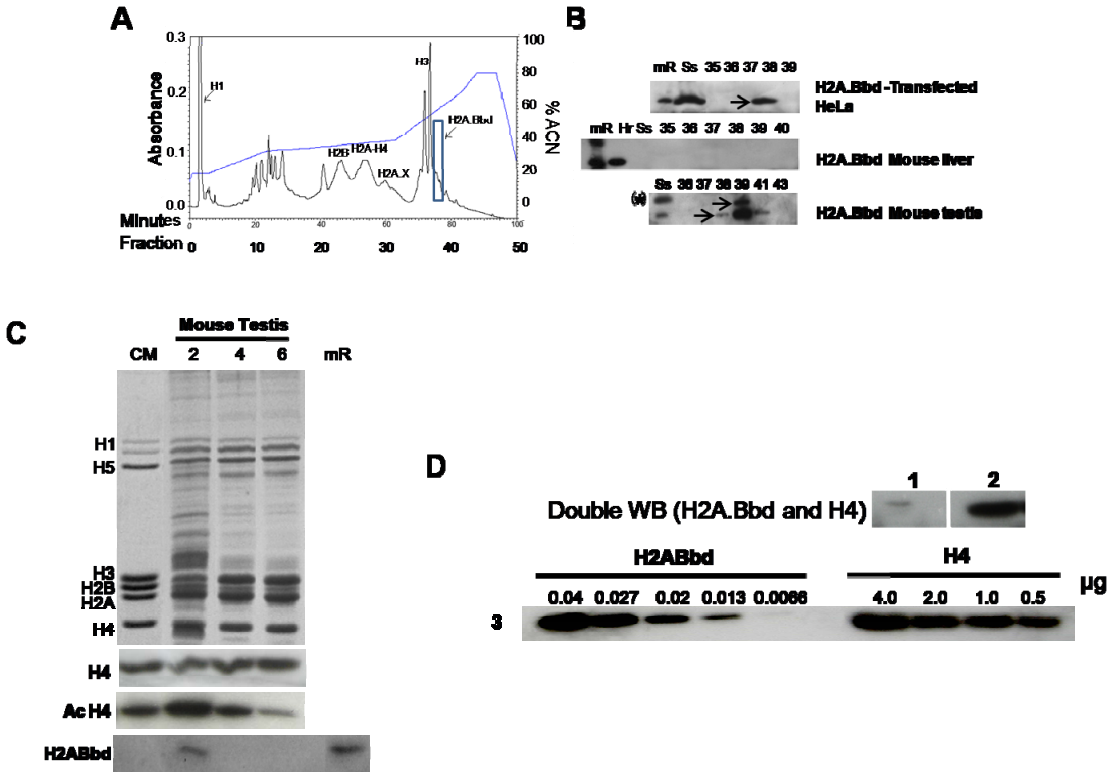

Figure 14. Identification of native H2A.Bbd in mouse testis.

A) Reversed-phase HPLC of a mouse testis HCl extract. B) H2A.Bbd Western blot analysis of some of the fractions shown in (A) and of fractions from similar HPLCs carried out with extracts from HeLa cells over-expressing H2A.Bbd-3 or mouse liver. The arrows point to H2A.Bbd bands. The asterisk shows that in addition to Mm.H2A.Bbd isotype 3, the mouse testis starting sample contains an electrophoretic band with reduced electrophoretic mobility that likely corresponds to the larger isoforms indicated in Fig. 13. C) SDS-PAGE of spermatogenic fractions 2, 4 and 6, and their Western blot analysis using H2A.Bbd, pan-acetylated H4 (Ac H4) and H4 antibodies. CM: chicken erythrocyte histones; hR: human recombinant H2A.Bbd; mR: mouse recombinant H2A.Bbd-3; Ss: starting sample. D) Double Western analysis of spermatogenic fraction 2 using H2A.Bbd antibody (panel 1) followed by H4 antibody (panel 2). Panel 3 shows a similar double Western analysis of increasing amounts of mouse recombinant H2A.Bbd and H4**.**

respectively, were collected. The analysis shows that mH2A.Bbd is present in the elongating spermatid fraction (Fig. 14C) at a time when histone H4 is maximally acetylated and when histones are being replaced by protamines (Lewis *et al.*, 2003e; Oliva and Dixon, 1991). A titration Western blot using different amounts of H4 and mH2A.Bbd and their corresponding antibodies (see materials and methods) indicates that one molecule of mH2A.Bbd is present in approximately every 100 nucleosomes in this spermatogenic fraction (Fig. 14D). Moreover, when human sperm was digested with MNase under strong reducing conditions (to break the inter-protamine disulfide bridges), H2A.Bbd was found to be present in the histone variant-enriched (Churikov *et al.*, 2004; Gatewood *et al.*, 1987), nucleosomally-organized (Nazarov *et al.*, 2008) complement that coexists with protamines in this sperm (Fig.15A-C). This rather unique nucleosome fraction has been described to be associated with telomeres (Zalenskaya *et al.*, 2000). It has been found to be enriched in gene regulatory regions and CTCF binding sequences (Arpanahi *et al.*, 2009), and to include genes that are important for embryo development (Hammoud *et al.*, 2009).

Histone H2A.Bbd is found associated with a chromatin insoluble fraction in cells ectopically expressing the native form of the protein and in mouse (20T1/2) cell line, H2A.Bbd is enriched at the periphery of chromocenters.

MNase digestion analysis of chromatin from mouse testis under non-reducing conditions (Fig. 16A-B and Fig. 16D-E) and from HeLa cells ectopically over-expressing mH2A.Bbd (Fig. 16C) showed that mH2A.Bbd is present in the insoluble fractions regardless of the extent of digestion (Fig. 16D-E). In mouse testis, this is the

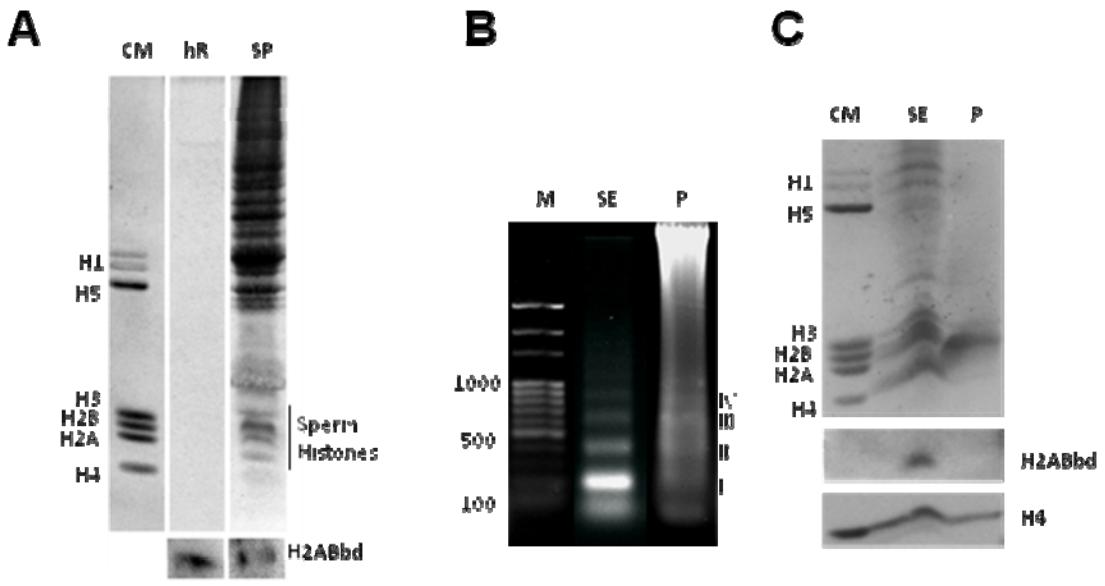

Figure 15. Presence of Native H2A.Bbd in human sperm.

A) SDS-PAGE of human sperm histones and H2A.Bbd Western. Human sperm chromatin fractions obtained from MNase digest are used in (B) and (C). B) Agarose electrophoresis of the DNA fragments of the chromatin fraction soluble upon digestion (SE) and the insoluble protamine-containing (P) fraction. C) SDS-PAGE of the proteins associated with the chromatin fractions and the Western analysis using mouse H2A.Bbd and histone H4 antibodies. CM: chicken erythrocyte histones; hR: human recombinant H2A.Bbd; M: 100 bp DNA marker (New England Biolabs); SP: total human sperm proteins; Ss: starting sample. The roman numerals in (E) denote DNA fragments corresponding to mono-, di-, tri-, and tetra-nucleosomes, respectively.

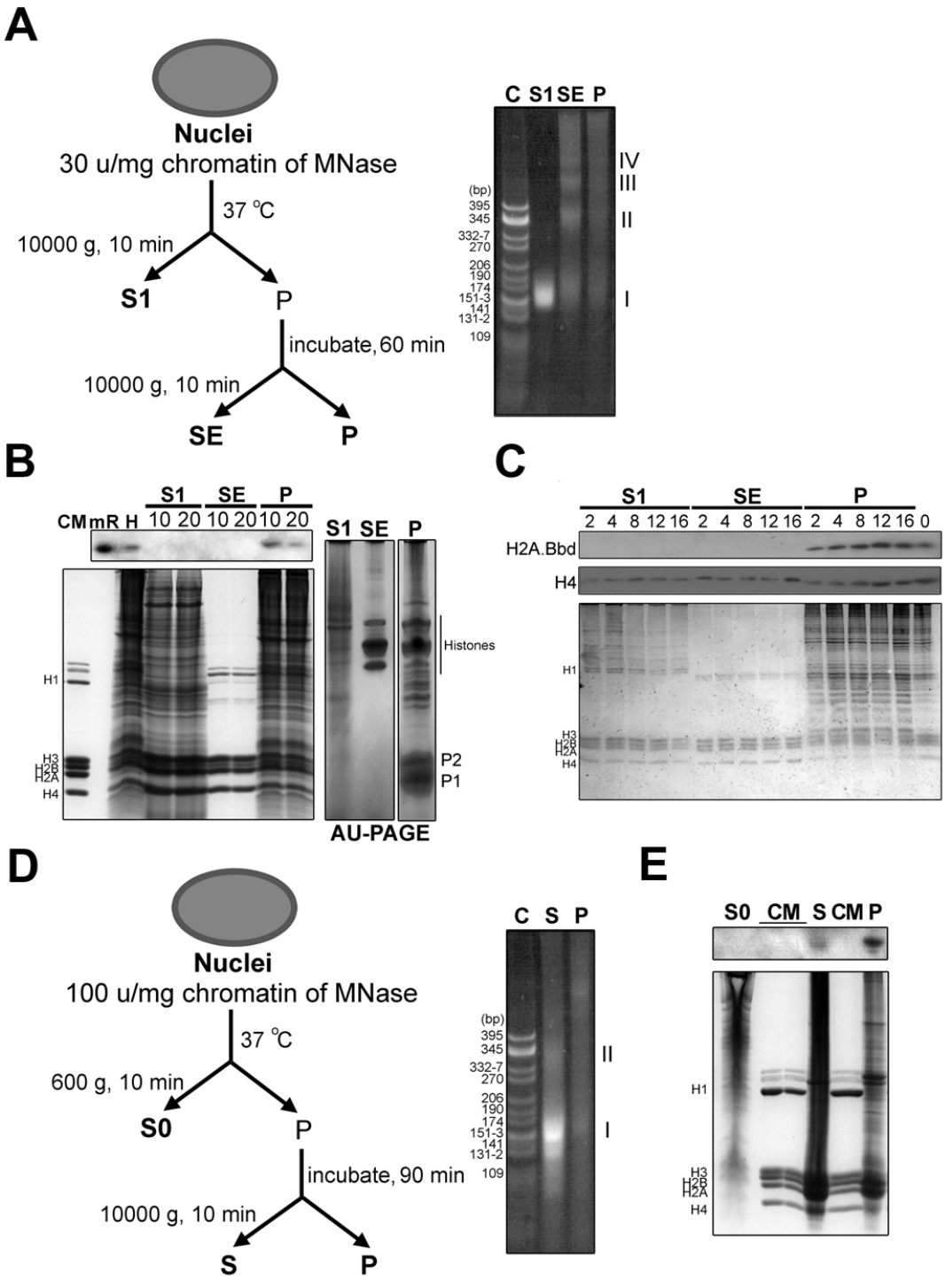
A
Nuclei
30 u/mg chromatin of MNase
37 ℃
10000 g, 10 min
S1
P
incubate, 60 min
10000 g, 10 min
SE
P
C S1 SE P
(bp)
395
345
332-7
270
206
190
174
151-3
141
131-2
109
IV
III
II
I
B
S1 SE P
CM mR H 10 20 10 20 10 20
H1
H3
H2B
H2A
H4
S1 SE P
Histones
P2
P1
AU-PAGE
C
S1 SE P
2 4 8 12 16 2 4 8 12 16 2 4 8 12 16 0
H2A.Bbd
H4
H1
H3
H2B
H2A
H4
D
Nuclei
100 u/mg chromatin of MNase
37 ℃
600 g, 10 min
S0
P
incubate, 90 min
10000 g, 10 min
S
P
C S P
(bp)
395
345
332-7
270
206
190
174
151-3
141
131-2
109
II
I
E
S0 CM S CM P
H1
H3
H2B
H2A
H4

Figure 16. H2A.Bbd is present in MNase-resistant insoluble chromatin.
A) Flowchart of the MNase digestion of mouse testis (left hand) (B) and of HeLa cells ectopically expressing MmH2A.Bbd-3 (C) and a representative PAGE of the DNA extracted from the different chromatin fractions generated in this way (right hand). B) SDS- (left hand) and AU-PAGE (right hand) of the protein composition of the fractions indicated in (A). C) Digestion at different times (in minutes) as indicated on top of the gel. D) Flowchart of an extensive digestion of mouse testis to generate mononucleosome chromatin fragments. E) PAGE of the DNA (left) and SDS-PAGE of the proteins (right) of the fractions thus obtained. Western blots in this figure were carried out with mouse polyclonal H2A.Bbd antibody. C and CM are *Cfo*I pBR322 digested DNA and chicken erythrocyte histone markers, respectively. mR: mouse recombinant H2A.Bbd. The roman numerals (I-IV) in (A) and (E) denote DNA fragments corresponding to mono-, di-. tri-, and tetra-nucleosomes, respectively.

fraction that is enriched in protamines (Fig. 16B). However, in this latter instance, this does not preclude the association of this variant with potential nucleosome structures (see DNA patterns in Fig. 16A and Fig. 16E) which most likely are trapped in the insoluble protamines mesh resulting from the protamines P1/P2 (Fig.16B) intermolecular disulfide bridges (Lewis *et al.*, 2003e).

In order to try to ascertain the potential nature of the genomic regions associated with the MNase insoluble fraction, immunofluorescence studies using mouse and human cell lines transfected with Mm-H2A.Bbd-3-GFP were carried out (Fig. 17). These experiments when carried in combination with FRAP (results not shown) indicated, that like in the case of the human counterpart (Gautier *et al.*, 2004) this histone exhibits an unusually high rate of exchange when compared to any other histone. Human (not shown) and mouse cell lines showed similar distributions. The results with mouse are shown because of the prominent chromocenters that facilitate the assessment of distribution. Two distributions were observed. A minority of the cells showed the distribution shown in Fig. 17A, where there was an unusual enrichment at the periphery of the chromocenters (e.g. arrows in Fig. 17A). This unusual organization has been previously reported for topoisomerase IIα during early G2 (Rattner *et al.*, 1996). The majority of cells showed a more broadly distributed pattern (Fig. 17B). In both cases, the distribution shown in Fig. 17A, where there was an unusual enrichment at the periphery of the chromocenters (e.g. arrows in Fig. 17A). The majority of cells showed a more broadly distributed pattern (Fig. 17B). In both cases, the Mm-H2A.Bbd was largely excluded from heterochromatin. This is an unusual

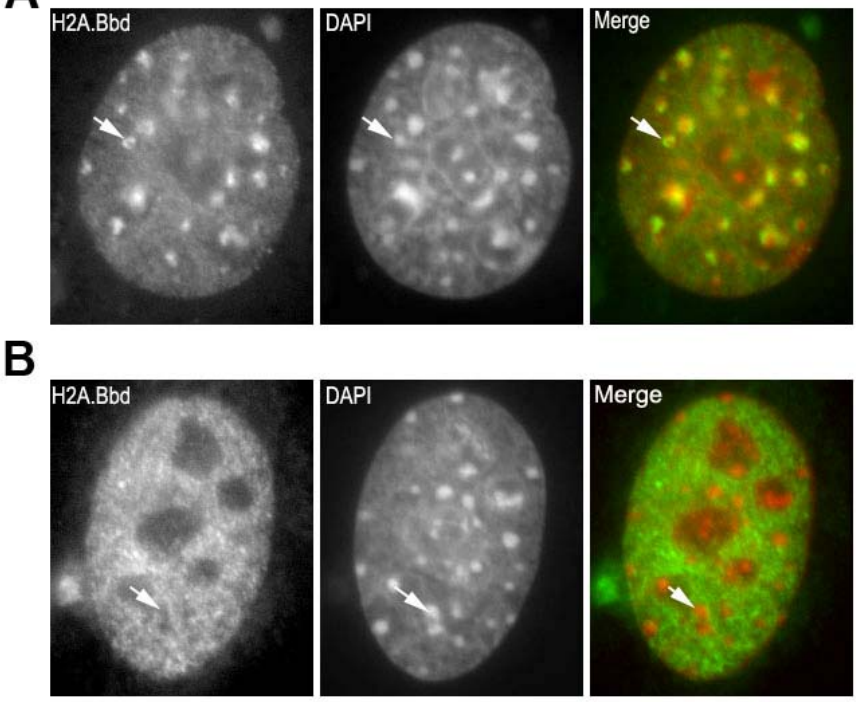

Figure 17. Fluorescence microscopy of MmH2A.Bbd ectopically expressed in mouse 20T1/2 cells.

Examples of the two distributions observed in mouse cell lines are shown. A) A nucleus showing enrichment of MmH2A.Bbd on the periphery of chromocenters. B) A nucleus showing a broad distribution with exclusion from heterochromatin. In these images, the left panel shows H2A.Bbd-GFP, the middle panel is stained with DAPI and the panel on the right is the merged image. Sites that are enriched in H2A.Bbd are green and DNA stained with DAPI is orange. The chromocenters which are clearly visible in the mouse cell line appear yellow.

distribution for a histone. It is possible to speculate that the presence of the native form in the elongating spermatids of fraction 2 of mouse testis (Fig. 14C) has a similar distribution. Interestingly, a murine homologue of HP1 (M31) localizes to the centromeric chromocenter of mice round spermatids. Like with H2A.Bbd, the protein is also present in mature sperm and it was proposed to be involved in higher order organization of sperm chromatin (Hoyer-Fender *et al.*, 2000).

During mammalian spermiogenesis, histones at the onset of the differentiation process are gradually replaced by transition proteins and protamines (Oliva and Dixon, 1991; Unni and Meistrich, 1992) and although the replacement is almost complete in most species, in humans approximately 15% of the mature sperm chromatin remains associated with histone variants (Gatewood *et al.*, 1987). *In vitro* studies of H2A.Bbd have shown that it participates in chromatin destabilization and unfolding (Bao *et al.*, 2004; Eirin-Lopez *et al.*, 2008; Gautier *et al.*, 2004). Therefore, it is possible to envisage how this variant may play a critical role in assisting the displacement of histones by protamines and in facilitating the transition from a nucleohistone to a nucleoprotamine chromatin organization during the late stages of mammalian spermiogenesis. The presence of H2A.Bbd within the histone complement that remains bound to DNA in mature human sperm is very intriguing (Wykes and Krawetz, 2003). The role of these remaining histones is currently the focus of intense investigation. Evidence exists for both structural (Zalenskaya and Zalensky, 2002) and functional (Hammoud *et al.*, 2009) involvement and a recent study indicates that these histones could have potential implications for fertility (Singleton *et al.*, 2007b).

Chapter 4. Characterization of nucleosomes consisting of the human testis/sperm-specific histone H2B variant (hTSH2B)

Adapted from Li *et al.* for the purpose of this thesis (Li *et al.*, 2005b).

Li A's contribution to the work : all of the experimental work, preparation of the figures and writing. Zalensky contributed the *E.coli* expressed recombinant hTSH2B.

Abstract

We have reported earlier the occurrence of a specific histone H2B variant in human testis and sperm. In this chapter, we have structurally characterized this protein, its association with the rest of the histone octamer and its effects on the nucleosome structure. We show that a reconstituted octamer consisting of hTSH2B and a stoichiometric complement of histones H2A, H3, and H4 exhibits a lower stability compared to the reconstituted native counterpart consisting of H2B. In contrast, the hTSH2B containing octamers are able to form nucleosome core particles which are structurally and dynamically indistinguishable from those reconstituted with octamers consisting of only native histones. Furthermore, the presence of hTSH2B in the nucleosome does not affect its ability to bind to linker histones.

Introduction

Replacement histone variants are coming of age as the function and structure of several H2A and H3 variants are elucidated (Ausió and Abbott, 2002; Malik and Henikoff, 2003). Histone H2A.X in its phosphorylated form, has been shown to play a critical role in DNA repair, in meiosis and perhaps in other important cellular processes (Bonner, 2003; Ismail and Hendzel, 2008; Lewis *et al.*, 2003d; Mahadevaiah *et al.*, 2001b). The function of histone H2A.Z is underscored by its indispensability for survival in many organisms (Clarkson *et al.*, 1999) and this variant is at the center of controversial structural and functional studies (Abbott *et al.*, 2001; Dryhurst *et al.*, 2004; Krogan *et al.*, 2003; Meneghini *et al.*, 2003; Mizuguchi *et al.*, 2004; Park, 2004). Other members of the H2A family of variants, macroH2A and H2A.Bbd (Pehrson and Fried, 1992), have also been the focus of attention of recent studies of function and structure (Abbott *et al.*, 2004; Angelov *et al.*, 2003; Changolkar and Pehrson, 2002; Meneghini *et al.*, 2003; Thambirajah *et al.*, 2009). In a similar fashion, the physiological implications of histone H3.3 have started to be more clear in the past few years (Malik and Henikoff, 2003; Orsi *et al.*, 2009). As the functional role of these variants is being clarified, their structural implications still remain largely elusive (Ausió and Abbott, 2004).

The structural variation that differentiates replacement core histone variants from their canonical counterparts can affect different regions of the histone molecule to different extents (Ausió and Abbott, 2002). For instance, in histone H2A.Z, the main sequence departure takes place at the C-terminal end of the molecule, which is the part that has been shown to be indispensible (Clarkson *et al.*, 1999). Macro H2A contains a large non-histone domain which extends from its C-terminal end (Pehrson and Fried,

1992). Histone H3.3 is different from H3.1 and H3.2 in only a few amino acids that mainly affect the histone fold domain of the molecule. CENP-A, a histone variant related to H3 which is part of the centromeric chromatin, exhibits an extensive amount of sequence variation at its N-terminal domain and to a lesser extent throughout the rest of the molecule (Palmer *et al.*, 1991). In contrast to H2A and H3, few histone variants have been characterized for either core histone H2B or core histone H4.

In the course of vertebrate spermatogenesis, the somatic histones, which are present at the onset of the differentiation process, undergo several transitions. These transitions occur in those organisms in which the main protein chromosomal component consists of protamines in their mature spermatozoa (Lewis *et al.*, 2003a; Oliva and Dixon, 1991). This involves the replacement by different testis-specific histone variants (Churikov *et al.*, 2004; Lewis *et al.*, 2003d; Meistrich *et al.*, 1978) before they are finally replaced by protamines at the end of spermatogenesis. Human spermatogenesis is different in that the spermatozoa, in addition to protamine presence, retain a 10-15 % of specific core histone variants (Gatewood *et al.*, 1990; Gusse *et al.*, 1986; Tanphaichitr *et al.*, 1978) with unknown biological function. One such histone (hTSH2B) has been characterized (Zalensky *et al.*, 2002). The main sequence difference between hTSH2B and human somatic H2B occurs at the N-terminal end of the molecule where three of the four proline amino acids that are present in the somatic counterpart of this histone are replaced by phosphorylatable serine/threonine amino acids.

In this chapter, I report the structural characterization of hTSH2B and of the complexes resulting from its association with other core histones (histone octamer) and in the nucleosome.

Materials and Methods

Protein expression and purification

Recombinant hTSH2B was expressed in *E. coli* and purified as described in Chapter 2.

Gel electrophoresis

SDS-PAGE was performed as described by Laemmli (Laemmli, 1970). Two-dimensional gel electrophoresis was carried out as described elsewhere (Ausió, 1986). Approximately 20 μg of histones were separated by an AU-PAGE gel in the first dimension. Then, the lane on AU-PAGE gel containing the histones was cut, fitted into a 15% SDS-PAGE with a wide well, and sealed with 1% agarose. The histones were separated by SDS-PAGE (second dimension) at 100 V in a direction that is perpendicular to the first dimension. Native 4.5 % PAGE in 20 mM sodium acetate, 1 mM EDTA, 40 mM Tris-HCl (pH 7.2) buffer for the analysis of nucleosome core particles was carried out according to Yager and van Holde (Yager and van Holde, 1984). In some instances the buffer was changed to 0.5x TBE (45 mM Tris-borate, 1 mM EDTA (pH 8.3)). Analysis of the restriction fragments in the nucleosome positioning experiments was carried out in 8% PAGE (20:1 acrylamide:bisacrylamide) and 8.3 M urea in 1xTBE (90 mM Tris-borate, 2 mM EDTA (pH 8.3)) as described previously (Howe and Ausió, 1998). DNase I footprinting analysis was carried out in 8% PAGE (10:1 acrylamide:bisacrylamide) and 7 M urea in 1xTBE (Ausió *et al.*, 1989) .

Circular dichroism

Circular dichroism (CD) analysis of chicken histone H2B and hTSH2B in 100 mM NaCl, 10 mM Tris-HCl (pH 7.5) buffer was carried out at 20ºC on a Jasco – J720 spectropolarimeter as described previously (Frehlick *et al.*, 2007). Measurements were carried out in thermostated cells with 1cm path length at room temperature. Both samples had an A_{260} of approximately 0.8. The spectrum for the buffer was recorded for buffer contribution and sample spectrum was corrected by subtracting buffer base-line from sample spectrum. Molar ellipticity, [ɵ], determined using the formula, [ɵ] = (CD signal) (Average MW x $Ɛ_{230}$)/(A_{230} x10xl). In the formula, CD signal is collected from CD spectrum, Average MW is the mean residue weight (the molecular weight of H2B/hTSH2B divided by the number of amino acids), $Ɛ_{230}$ is the extinction coefficient in water at 230 nm (3.9 for both H2B and hTSH2B) and l is the path length of the cell in cm. The amount of α-helix was determined using the formula, % α helix = 8.9 – (2.47 x $[ɵ]_{222nm}$ x 10^{-3}) (Verdaguer *et al.*, 1993).

Secondary structure prediction

The secondary structure of histones was predicted by SOPM (self-optimized prediction method) (Geourjon and Deleage, 1994) available at the ExPASy Molecular Biology Server (http://au.expasy.org/).

Histone octamer reconstitution

Histone octamers were reconstituted from native chicken erythrocyte histones and purified recombinant hTSH2B following the procedure described in (Ausió and Moore,

1998) and as described in Chapter 2. Histones (H2B/hTSH2B, H2A, H3 and H4) in stoichiometric amounts were lyophilized and resuspended at 2 mg/ml in a 6 M guanidinium-hydrochloride, 20 mM β-mercaptoethanol, 50 mM Tris-HCl (pH 7.5) buffer. After incubation for 30 min at room temperature, the samples were dialyzed against dsH_2O for 2 hours at 4°C. The dialysis bag was then transferred to another container containing 2 M NaCl, 50 mM Tris-HCl (pH 7.5), 1 mM EDTA, 1 mM DTT buffer and dialyzed overnight at 4°C. After reconstitution, the octamers (~500 μg) were fractionated by gel filtration, in 2 M NaCl, 10 mM Tris-HCl (pH 7.5) buffer, using a 1.2 x 120 cm Sephacryl S-300-HR column eluted at 4 °C at 5 ml/4 fractions/h with 2 M NaCl, 10 mM Tris-HCl (pH 7.5) buffer.

Nucleosome reconstitution

Recombinant human hTSH2B was mixed with chicken native H2A, H3 and H4 histones in stoichiometric amounts and histone octamers were reconstituted onto either a random sequence 146 bp obtained from chicken erythrocyte nucleosome core particles (Ausió *et al.*, 1989) or onto a 196 bp fragment with defined sequence. The latter was obtained by *Eco* RI digestion of a 208-12 DNA construct consisting of 12 identical copies of a 196 bp fragment of the 5S rRNA gene from *L. variegatus* connected by a 12 bp DNA linker consisting of an *Eco* RI site at each end (Simpson *et al.*, 1985). After digestion with *Eco* RI, the 196 bp DNA was HPLC purified using a 75x7.5 mm Bio-Gel DEAE-5-PW (Bio-Rad Hercules, CA). Reconstitution was carried out by a 2 M to 0 M step-wise salt gradient dialysis (Ausió and Moore, 1998) in 10 mM Tris-HCl (7.5), 0.1 mM EDTA (8.0) as described in Chapter 2. The reconstituted chromatin particles thus obtained (at a

concentration of 40-50 μg/mL) were dialyzed against the appropriate buffers (Ausió *et al.*, 1989; Garcia Ramirez *et al.*, 1992) and used for subsequent analytical ultracentrifuge analysis (Ausió, 2000; Ausió *et al.*, 1984).

Sucrose gradient purification

Reconstituted hTSH2B nucleosome core particles in 10 mM Tris-HCl (pH 7.5), 0.1 mM EDTA were loaded onto a 5% to 20% sucrose gradient in 25 mM NaCl, 10 mM Tris (pH 7.5), 0.1 mM EDTA and centrifuged at 134,400 x *g* for 19 hrs in a Beckman SW41 rotor at 4^{o}C. Fractions (0.5 ml) were collected and analyzed by SDS-PAGE.

Analytical ultracentrifuge

Reconstituted hTSH2B nucleosomes were dialyzed against buffers of varying ionic strength as described in Ausió *et al.* (Ausió *et al.*, 1989). Sedimentation velocity runs were performed in a Beckman XL-A ultracentrifuge using an An-55 Al aluminum rotor as described in Chapter 2. Data was analyzed by the van Holde and Weischet method also as described in Chapter 2.

DNase I footprinting

DNase I footprinting of reconstituted nucleosomes was carried out as described previously (Ausió *et al.*, 1989). γ^{32}P-labelled nucleosomes, method described in Chapter 2, at a concentration of approximately 0.14 μg/μl were digested with 0.1 u/μl of DNaseI (Invitrogen) (800 u DNase I/mg of DNA). The digestion was carried out for 0, 5, 10 and 20 mins in 12.5 mM NaCl, 4.5 mM Tris-HCl, (pH 7.5), 1 mM $MgCl_2$. The reaction was

stopped by addition of EDTA to a final 25 mM and boiling for 1 min. Proteinase K (1.2 ng/µl) was then added and the solution was incubated for 60 mins at 37°C. After digestion the samples were mixed with an equal volume of 98% deionized formamide, 0.4 % bromophenol blue, 0.4 % xylene cyanol, 10 mM EDTA and loaded on 8% polyacrylamide sequencing gel containing urea. The dried gel was exposed overnight.

Nucleosome positioning

The hTSH2B/H2B-containing nucleosomes reconstituted onto the 196 bp DNA fragment of the 5S rRNA gene of the sea urchin *L. variegates* (Simpson *et al.*, 1985) were adjusted to 1 mM $CaCl_2$ and digested with MNase. The reaction was stopped with the addition of EDTA to the final concentration of 25 mM. The MNase-resistant DNA fragment was then deproteinated with Proteinase K and phenol/chloroform extracted. Following this, the DNA was precipitated, gel-purified from a 4% polyacrylamide gel and end-labelled with γ ^{32}P ATP and polynucleotide kinase. After the DNA fragments were end labelled, The DNA was cut with 5 units of restriction enzyme in 20 µl of appropriate restriction buffer for 4 hrs at 37°C. Then, the fragments were phenol/chloroform extracted and precipitated. The resuspended DNA was denatured at 90°C for 2 min and separated on a 8% polyacrylamide gel (20:1 acrylamide: bisacrylamide) containing 8.3 M urea and 1x TBE (0.1 mM Tris-HCl (pH7.5), 0.1 mM Boric acid and 2 mM EDTA).

Histone H1 binding

γ ^{32}P-labelled 196 bp nucleosomes were titrated with increasing amounts of chicken erythrocyte histone H1 as described in Chapter 2. The H1 to mononucleosomes molar ratios used were: 0, 0.5, 1.0, 2.0, 4.0 and 8.0. The electrophoretic mobility shift resulting from histone H1 binding was analyzed by native 4.5 % PAGE.

Results

Histone hTSH2B exhibits a higher helical organization than histone H2B

The sequence of histone hTSH2B is shown in comparison to human H2B and chicken H2B (Fig. 18). Chicken H2B has been used in the experimental part of this work as a non-variant counterpart to hTSH2B. The most significant primary structural difference between the main human/chicken somatic H2B variants and hTSH2B occurs at the N-terminal domain of the molecule (Fig. 18A). It involves only nine amino acids in the N-terminal domain in addition to four amino acid replacements throughout the rest of molecule that involve G→S, N→S and N→T transitions.

The primary structure changes allow the prediction of a slight increase in the amount of secondary structure at the N-terminal end of hTSH2B (Fig. 18B). In fact, circular dichroism demonstrates a 6 % increase in the α-helical content (Fig. 19) as determined from the change in ellipticity at 222 nm (Bradbury *et al.*, 1975). Careful inspection of the primary structure of hTSH2B (Fig. 18A) shows that there is a replacement of two helix breaker residues (proline), which are present in both chicken and human somatic H2B, in the N-terminal domain of the hTSH2B.

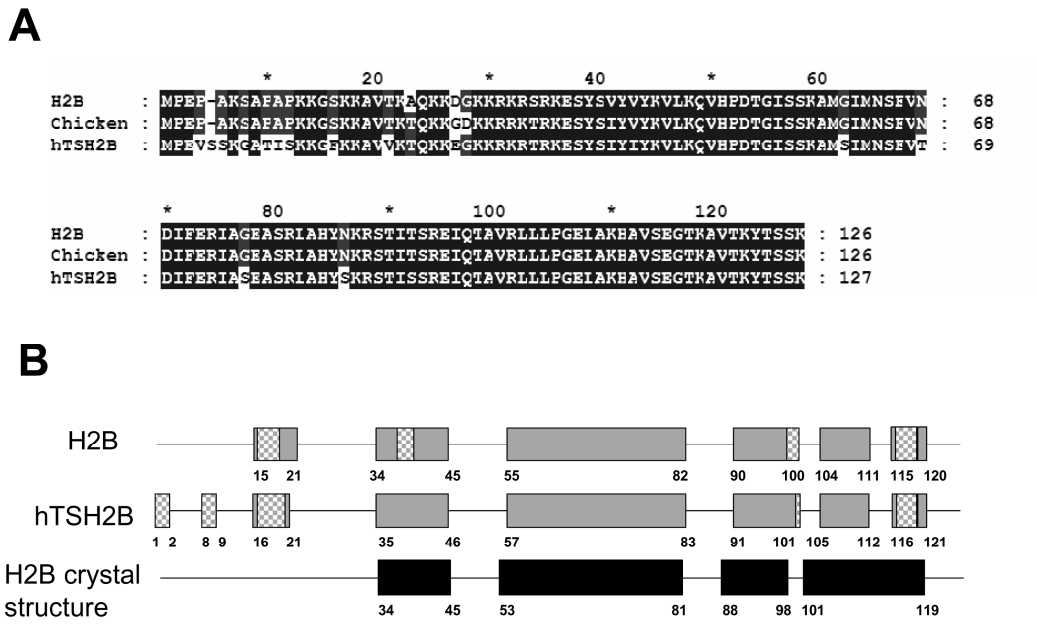

Figure 18. Alignment and secondary structure comparison of somatic human H2B, somatic chicken H2B and hTSH2B.

A) Protein sequence comparison of somatic human histone H2B (Ohe *et al.*, 1979), chicken histone H2B (Grandy *et al.*, 1982) and human hTSH2B sperm histone variant (Zalensky *et al.*, 2002). B) Schematic representation of the secondary structure of the human H2B histone variants. Shown in black are the α-helical regions of H2B determined from the crystallographic analysis of the histone octamer (Arents *et al.*, 1991) and the nucleosome (Luger *et al.*, 1997). Also shown are the α-helical (grey) and β-sheet (checkered pattern) regions predicted from the primary structure of the protein (Geourjon and Deleage, 1994). The numbers indicate the amino acid location in the sequences shown in A).

The hTSH2B reconstituted histone octamer exhibits a lower stability than the chicken H2B reconstituted histone octamer

Histone octamers were reconstituted using stoichiometric amounts of native chicken erythrocyte H2A, H3 and H4 and either native chicken H2B or hTSH2B and the stability of the resulting complexes was assessed by gel filtration chromatography in 2 M NaCl (Fig. 20) (Eickbush and Moudrianakis, 1978). With the experimental protocol followed, histone octamers elute first followed by H2A/H2B dimers and finally H3/H4 complexes (see Fig. 20A and C). In 2 M NaCl, the native histone octamer [$(H3\text{-}H4)_2$ 2(H2A-H2B)] is in equilibrium with histone hexamers [$(H3\text{-}H4)_2$ (H2A-H2B)], tetramers [$(H3\text{-}H4)_2$] and dimers [(H2A-H2B)]. This equilibrium depends on the concentration of the starting sample, as well as on the pH and temperature (Eickbush and Moudrianakis, 1978). Whereas most of the complex reconstituted with native chicken histones elutes from the column as octamers, the histone complexes consisting of hTSH2B are eluted as a mixture in which the hTSH2B-H2A and H3-H4 complexes are the predominant forms (Fig. 20). These results indicate that the hTSH2B reconstituted histone complexes exhibit a reduced stability in 2 M NaCl at pH 7.5 and 4 °C when compared to the complexes consisting of the H2B counterpart.

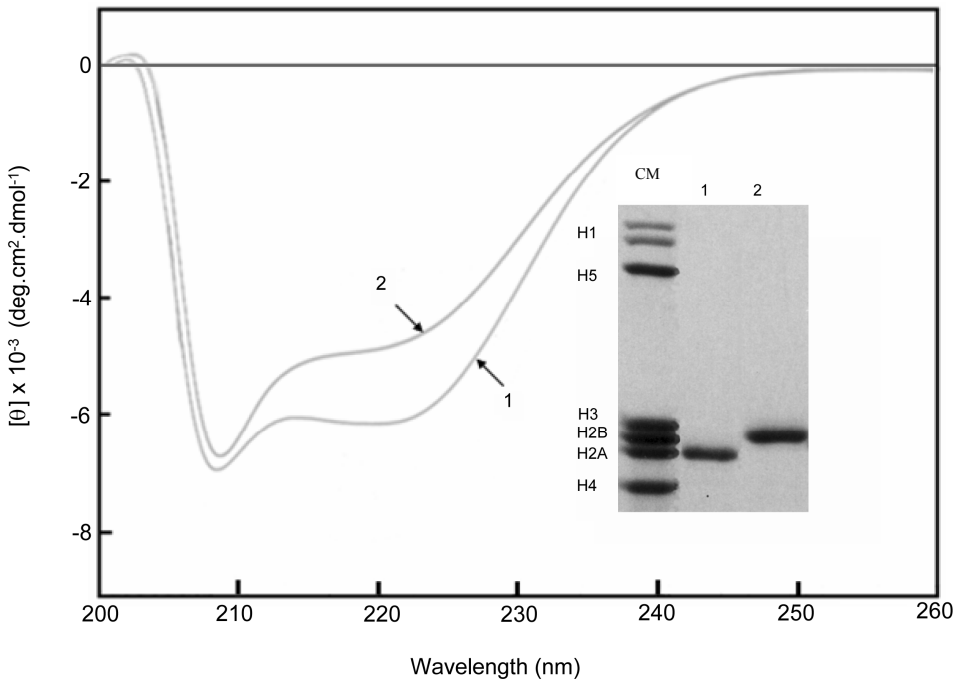

Figure 19. The α-helical content of hTSH2B is increased compared to that of the somatic chicken H2B.

Circular dichroism spectra of histone H2B from chicken (line 2) in comparison to recombinant hTSH2B (line 1). The inset shows an SDS-PAGE of chicken hTSH2B (lane 1) in comparison to H2B (lane 2). CM is a chicken erythrocyte histone marker. Please note that hTSH2B co-migrates with H2A on SDS-PAGE (Zalensky *et al.*, 2002).

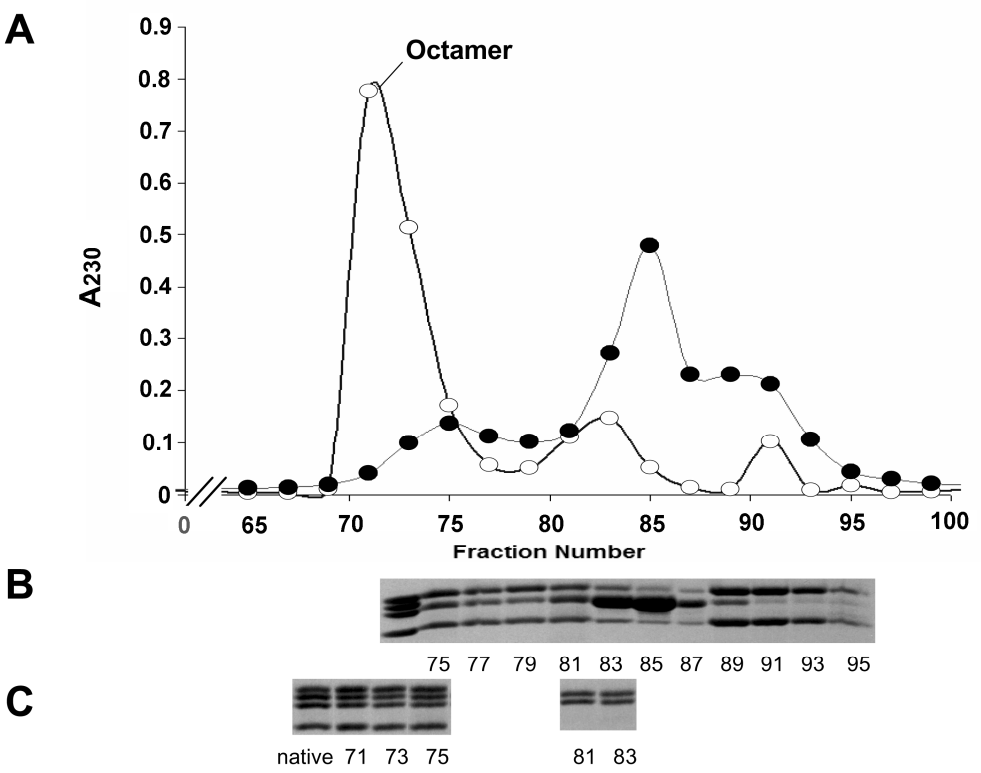

Figure 20. The hTSH2B reconstituted histone octamer exhibits a lower stability than the chicken H2B reconstituted histone octamer.

A) Gel filtration chromatography of reconstituted histone octamer complexes. The black circles correspond to complexes reconstituted with hSTH2B and the open circles correspond to complexes reconstituted from native histones. B) and C) are the SDS-PAGE electrophoretic analysis of some of the fractions corresponding to the hTSH2B (B) and native histone (C) reconstituted complexes, respectively. The numbers under the lanes are those of the fractions analyzed.

Association of stoichiometric amounts of hTSH2B, H2A, H3 and H4 with 146 bp DNA produces stable nucleosome core particles

In contrast to the results described above, when stoichiometric amounts of histones in 2 M NaCl were mixed with 146 bp random sequence DNA in the same salt concentration and sequentially dialyzed down to low ionic strength (Ausió and Moore, 1998), nucleoprotein complexes were obtained that exhibit the same electrophoretic mobility in native gels as nNCP (Fig. 21A). Furthermore, the reconstituted nucleoprotein complexes sedimented in sucrose gradients as nNCP (Fig.22A and B) and exhibited a stoichiometric histone composition (Fig. 21B and Fig. 22C).

Sedimentation velocity analysis in the analytical ultracentrifuge confirmed these results (Fig. 23). As seen in this figure, the sedimentation coefficient of the nucleosome core particles reconstituted from hTSH2B exhibits a very similar ionic strength dependence to that of the nucleosomes reconstituted with the native H2B counterpart or with nNCP (Ausió *et al.*, 1989). Furthermore, the DNase I footprinting analysis (Fig. 24) shows that hTSH2B-containing nucleosomes are structurally similar to nucleosomes reconstituted with the native H2B counterpart or nNCP.

Histone hTSH2B does not affect the mobility of the histone octamer in the nucleosome and does not affect the binding of histone H1 to the nucleosome.

It has been shown that the nucleosomes consisting of histones bearing *sin* mutations and H2A.Z histone variants affect the mobility of the histone octamer (Flaus *et al.*, 2004). It has also been shown that the N-terminal tail of histone H2B plays a role in

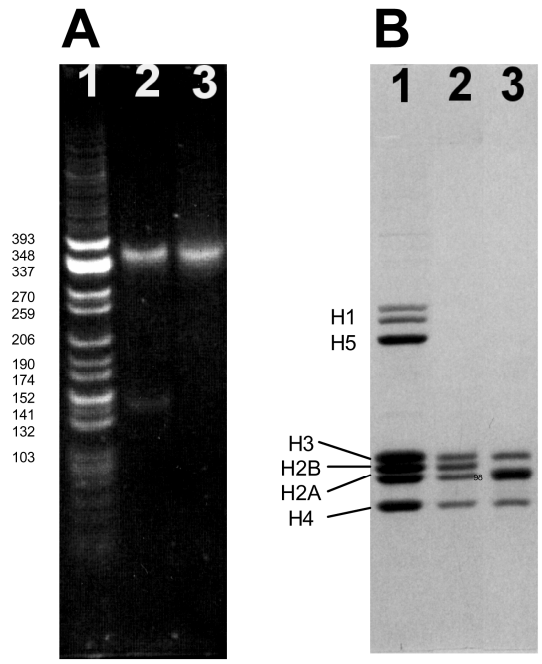

Figure 21. Electrophoretic analysis of H2B- or hTSH2B-containing nucleosomes. A) Native 4.5 % PAGE analysis of nucleosomes reconstituted with native histone octamers (lane2) or with hSTH2B (lane 3). Lane 1 is a *Cfo* I cut pBR 322 marker. The native PAGE gel is stained with ethidium bromide. B) SDS-PAGE analysis of the histones from the reconstituted nucleosome core particles shown in A). The assignment of lanes 2 and 3 is the same as in A). Lane 1 is chicken erythrocyte histones used as a marker. The SDS-PAGE gel is stained with Coomassie Blue.

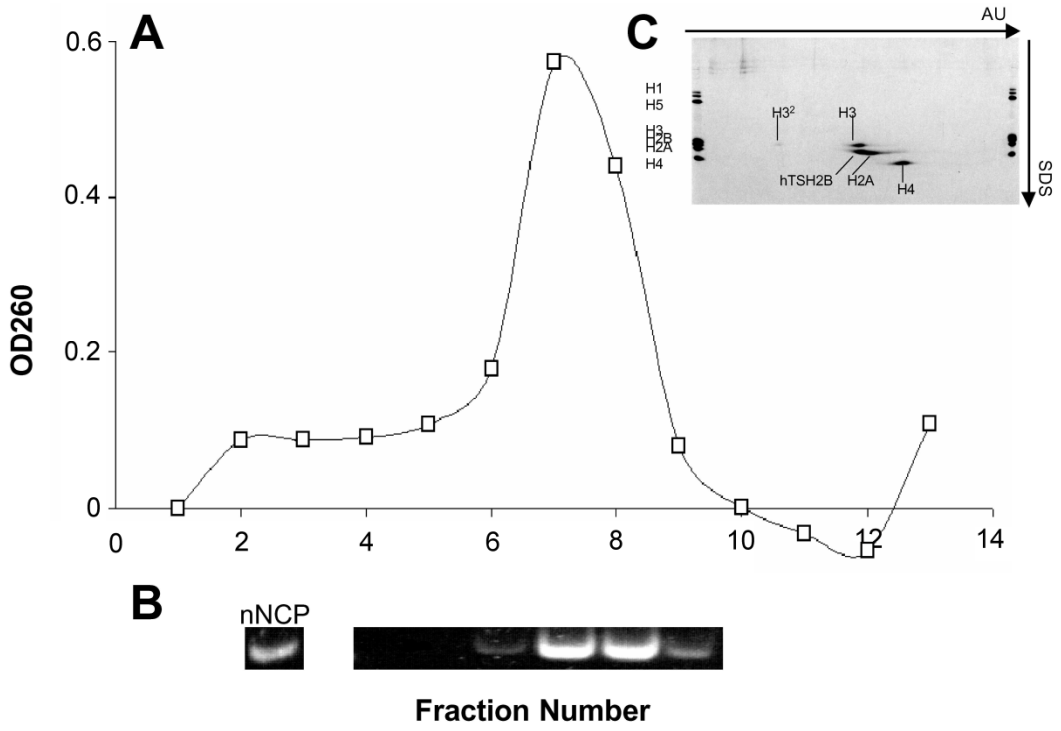

Figure 22. Electrophoretic analysis of hTSH2B reconstituted nucleosome core particle fractions collected from a sucrose gradient.

A) Sucrose gradient fractionation of hTSH2B reconstituted nucleosome core particles. B) Several fractions from the main peak were analyzed by native 4.5% PAGE and exhibited identical mobility to nNCP isolated from chicken erythrocyte chromatin. **C)** Two-dimensional PAGE analysis of fractions 7+8. The first dimension was run in an acetic acid-urea PAGE (AU) and the second dimension was run in a SDS-PAGE (SDS).

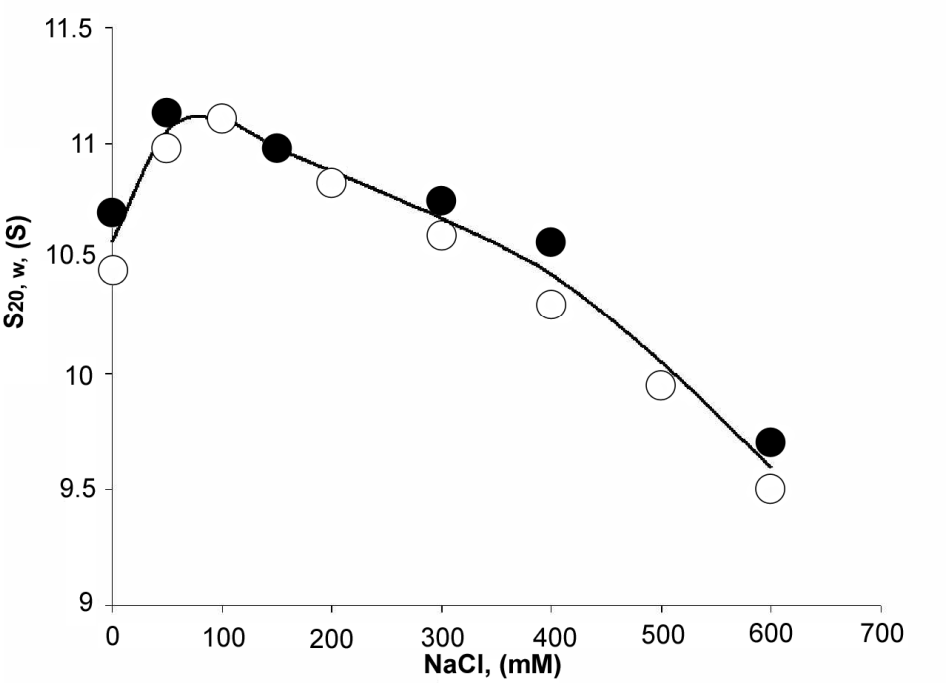

Figure 23. The sedimentation coefficient of the nucleosome core particles reconstituted from hTSH2B exhibits similar ionic strength dependence compared to that of the nucleosomes reconstituted with the native H2B counterpart.

NaCl-dependence of the sedimentation coefficient ($s_{20,w}$) of nucleosomes reconstituted with native histone octamers (open circles) or with hSTH2B (black circles). Sedimentation velocity experiments were carried out at 40,000 rpm at 20 °C at different NaCl concentrations in 10 mM Tris-HCl, 0.1 mM EDTA (pH 7.5) buffer.

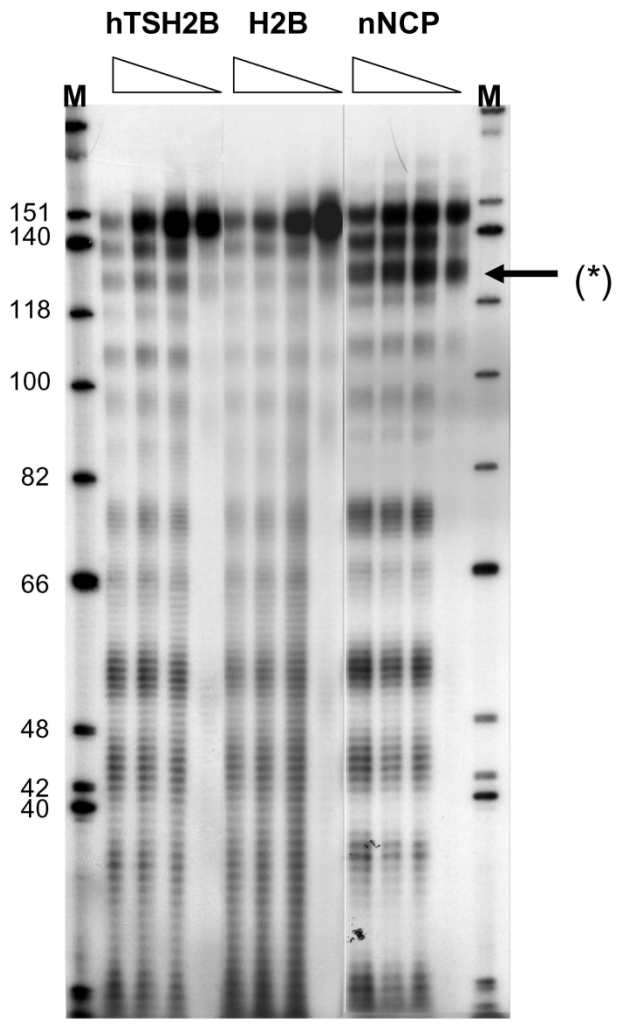

Figure 24. hTSH2B-containing nucleosomes are structurally similar to nucleosomes reconstituted with the native H2B counterpart or nNCP.

DNase I footprinting analysis of nucleosomes reconstituted with native histone (H2B) or with hTSH2B (hSTH2B) octamers, in comparison to chicken erythrocyte native nucleosome core particles (nNCP). The open triangles indicate the increasing time of digestion. M= ΦX174 *Hinf* I digested marker. The numbers on the left hand side represent the base pair numbers. The asterisk on the right hand side points to an artifact band in nNCP resulting from the occurrence of partial (at 125 bp) subnucleosome core particle contamination resulting from overdigestion of DNA during the process of nucleosome core particle preparation.

the sliding of histone octamers reconstituted onto linear DNA templates (Hamiche *et al.*, 2001) and in the structural and dynamic polymorphism of nucleosomes reconstituted onto circular DNA templates (Sivolob *et al.*, 2003). As the largest extent of variation in hTSH2B occurs at the N-terminal end of the molecule (Fig. 18), we therefore decided to examine whether or not any of these parameters are affected by the presence of this H2B variant.

To examine if nucleosome positioning was affected by the presence of the histone variant hTSH2B, nucleosomes were reconstituted onto a 196 bp DNA fragment of the 5S rRNA gene from the sea urchin *L. variegates* (Simpson *et al.*, 1985). The nucleosome positioning was then compared to that of a nucleosome reconstituted on the same DNA template but consisting of native H2B. The results are shown in Fig. 25. In native PAGE, both nucleosomes (see Fig. 25A, lanes 3 and 4) appeared to consist of a major band and some minor bands with lower electrophoretic mobility (one for the native nucleosome and two for the variant nucleosome) corresponding to alternative positions. A major and minor positioning was confirmed in both instances when the positioning was more accurately determined (Fig. 25B, see also Fig. 25C). The major position (approx. 90 %) was found to be 5±2 bp to 151±2 bp and the minor position (approx. 10 %) was 47±2 bp to 193±2 bp (see Fig. 25C) in agreement with previous results (Howe *et al.*, 1998; Meersseman *et al.*, 1991).

Because of this lack of effect of hTSH2B variant on the trajectory of the DNA entering and exiting the nucleosome, it was not surprising to find that binding of histone H1 (linker histones) to the nucleosome is not affected by the presence of hTSH2B. Gel

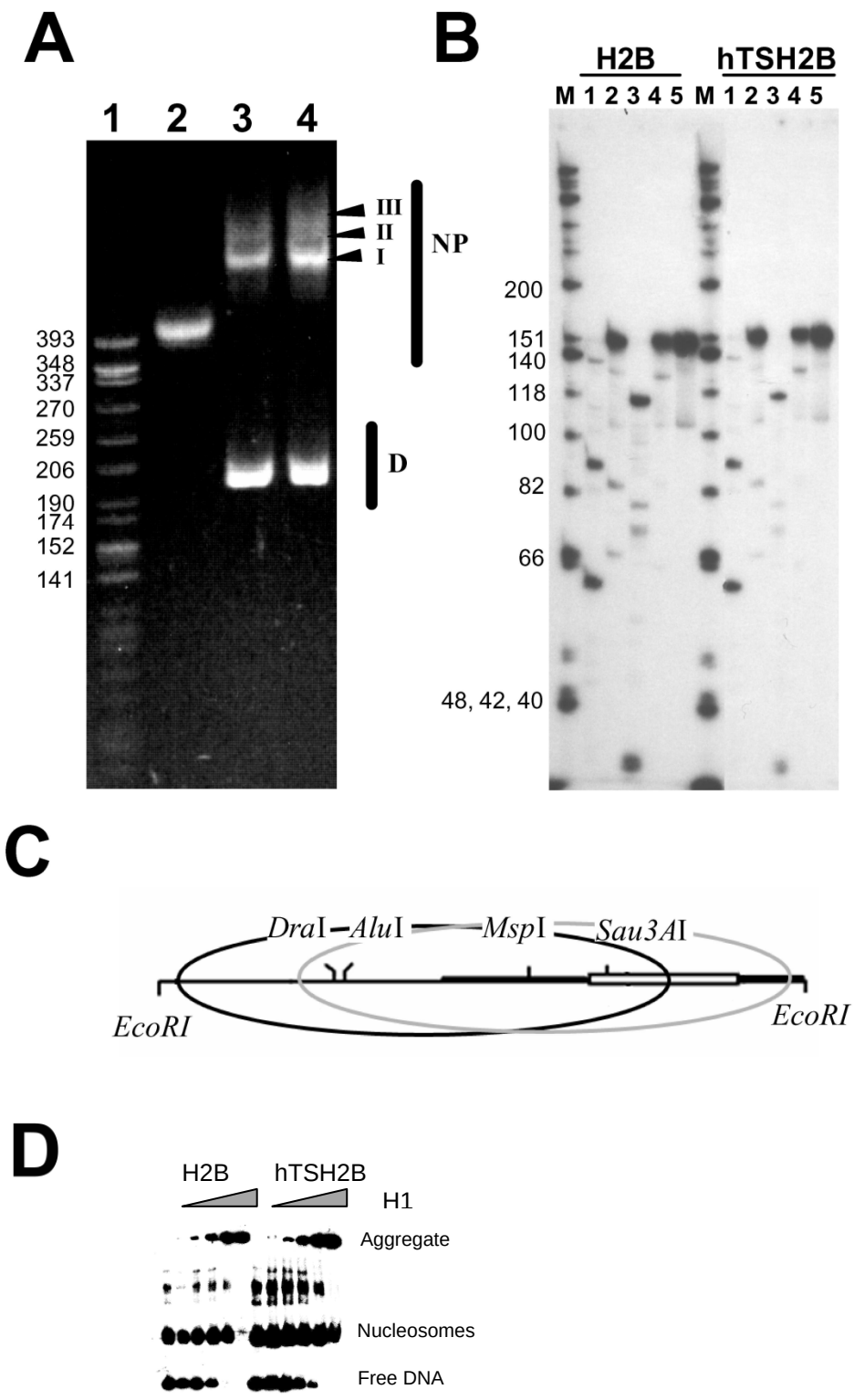
A
1 2 3 4
III
II
I
NP
D
393
348
337
270
259
206
190
174
152
141
B
H2B
hTSH2B
M 1 2 3 4 5 M 1 2 3 4 5
200
151
140
118
100
82
66
48, 42, 40
C
DraI
AluI
MspI
Sau3AI
EcoRI
EcoRI
D
H2B
hTSH2B
H1
Aggregate
Nucleosomes
Free DNA

Figure 25. H2B- or hTSH2B- containing nucleosome exhibit similar translational positioning on the 196 bp positioning DNA fragment and exhibit similar H1 binding affinity.

A) Native 4.5 % PAGE (0.5x TBE) analysis of nucleosomes reconstituted onto a 196 bp fragment of the 5S rRNA sea urchin gene using native H2B (lane 3) or hSTH2B (lane 4) reconstituted histone octamers in comparison to nNCP (lane 2). Lane 1 is a *Cfo* I cut pBR 322 marker. The numbers on the left hand side of the picture indicate the base pair size of the DNA fragments. The roman numerals point to different translational positions of the histone octamer. NP: nucleosome particle; D: free DNA. B) Determination of the translational positioning of the native H2B and hSTH2B reconstituted nucleosomes on the 196 bp DNA fragment. The region of DNA directly associated with the histone octamer was determined by digestion of a gel purified, end-labeled, deproteinized 146 bp MNase-resistant fragment with different restriction enzymes: *Dra* I (lane 1); *Alu* I (lane 2); *Msp* I (lane 3); *Sau* 3A1 (lane 4). Lane 5 is the 146 bp MNase-resistant undigested fragment. M = ΦX174 *Hinf* I digested marker. The numbers indicate the base pair size of the DNA fragments. C) Schematic representation of the main translational nucleosome positions on the reconstituted 196 bp DNA fragment. The ellipsoid black line represents the predominant position and a weaker position is depicted by the grey line ellipsoid. The heavy line indicates the 5S rRNA coding sequence, and the open box indicates the intragenic TFIIIA binding site. D) Nucleosomes reconstituted with H2B /hTSH2B and γP^{32}-ATP-labelled DNA were titrated with increasing amounts of histone H1 and analysed by 4% native gel electrophoresis. The histone H1 to nucleosome molar ratios used were 0, 1.0, 2.0, 4.0 and 8.0. The image shows an autoradiograph of the gel.

shift analysis showed that H1 binds to the reconstituted nucleosomes with the same affinity and stoichiometry regardless of the presence or absence of hTSH2B (Fig. 25D).

Discussion

Our sequence alignment shows the limited extent of the variation between hTSH2B and human/chicken somatic H2B and thus, it would allow the classification of hTSH2B as a homeomorphous replacement histone variant (Ausió *et al.*, 2001; West and Bonner, 1980). The replacement of two helix breaker residues (proline) in the N-terminal domain, which are present in both chicken and human somatic H2B, may explain the increase in secondary structure of hTSH2B as predicted by online predictive methods and determined by CD. However, the predictive methods suggest that only an increase in β-turns occurs as a result of these substitutions (Fig. 18B) and that the subtle increase in the α-helical content of this H2B variant determined by CD may indeed occur in the histone fold.

Our results indicate that the human sperm histone variant, hTSH2B, can be reconstituted to form nucleosomes that exhibit an almost identical structural conformation with nNCP. Thus, it is very likely that this variant exists in a nucleosome organization in the selected chromatin loci with which it appears to be associated within the human sperm nuclei (Zalensky *et al.*, 2002). The lack of stability of the hTSH2B histone octamer in the absence of DNA contrasts with the otherwise indistinguishable properties of nucleosome core particles reconstituted with these octamers. While this observation is puzzling, it is interesting to note that two of the mutations in hTSH2B at position 77 (G→S) and 86 (N→S) are in the histone fold domain and remarkably close to

the Y→G *Sin* mutation at position 86 of yeast histone H2B. Importantly, this mutation has been shown to bypass the requirement for Swi-Snf in yeast (Recht and Osley, 1999). Thus, it is possible that the transitions observed in the histone fold of the H2B variant have a similar behaviour. Furthermore, the interaction between the different histones is primarily determined by their histone fold domains. Within these regions, hTSH2B exhibits a sequence similar to that of H2B (Fig. 18). Therefore, in the absence of a crystallographic structure of the nucleosome (Luger *et al.*, 1997; Suto *et al.*, 2000) for this variant, it is difficult to establish the reasons for the observed lower stability of the hTSH2B-containing octamer. However, the possibility that this be the result of yet unclear interactions between the various core histone tails, cannot be disregarded (Hansen *et al.*, 1998).

It may be proposed that most of the structural effects associated to the chromatin regions enriched with hTSH2B could be the result of PTMs most likely phosphorylation at several sites that are unique to this variant (Zalensky *et al.*, 2002). These modifications may affect the physical parameters (stability, dynamics) of the chemically modified nucleosome or create an alternative histone code.

Chapter 5. C-terminal Phosphorylation of Murine Testis-specific Histone H1t in Elongating Spermatids

Li A's contribution to the work: extraction and purification of H1t from rat and mouse, preparation of the figures, writing and organizing data from different collaborators. Rose KL's contribution: writing and analysing mass spectrometry data. Meistrich ML contributed spermatid separation, protein isolation, alkaline treament, ^{32}P-labelling and analysis. Adapted from for the Rose *et al.* purpose of this thesis (Rose *et al.*, 2008).

Abstract

Previous studies gave differing results as to whether the testis-specific histone H1t was phosphorylated during rodent spermatogenesis. We show that histones extracted from germ cell populations enriched with spermatids at different stages of development in rat testis reveal an electrophoretic shift in the position of H1t to slower mobilities in elongating spermatids as compared to that from earlier stages. Alkaline phosphatase treatment and radioactive labelling with ^{32}P demonstrated that the electrophoretic shift is due to phosphorylation. Mass spectrometric analysis of histone H1t purified from sexually mature mice and rat testis confirmed the occurrence of singly-, doubly-, and triply-phosphorylated species, with phosphorylation sites predominantly found at the C-terminus of the molecule. Furthermore, using collision-activated dissociation (CAD) and electron transfer dissociation (ETD), we have been able to identify the major phosphorylation sites. These include a new, previously unidentified putative H1t-specific cdc2 phosphorylation site in linker histones. The presence of phosphorylation at the C-terminal end of H1t and the timing of its appearance suggest that this post-translational modification is involved in the reduction of H1t binding strength to DNA. It is proposed that this could participate in the opening of the chromatin fiber in preparation for histone displacement by transition proteins in the next phase of spermiogenesis.

Introduction

Mammalian linker histones bind to the linker DNA regions that connect adjacent nucleosomes along the chromatin fiber and in doing so, participate in the modulation of the folding dynamics of the fiber (Ausio, 2006; Bustin *et al.*, 2005). They encompass a highly heterogeneous family of histones, also known as the histone H1 family, which in mammals consists of at least 12 functionally identified components. Common to all the protein members of this family is a tertiary structure organization consisting of a central winged fold domain (Ramakrishnan *et al.*, 1993), that is flanked by N-and C-terminal tails that are highly unstructured in solution. It has been shown that C-terminal regions can, under certain circumstances and upon interaction with DNA, adopt a helical organization (Clark *et al.*, 1988; Roque *et al.*, 2005; Vila *et al.*, 2001; Vila *et al.*, 2000). The C-terminal domain is also critical for the folding of the chromatin fiber (Allan *et al.*, 1986; Th'ng *et al.*, 2005). Phosphorylation of histone H1 at this domain has been shown to significantly weaken the interaction with the chromatin fiber and reduce its binding affinity (Hendzel *et al.*, 2004).

Histone H1 and its related chromosomal proteins play an important role in the organization of sperm chromatin in different organisms (Eirín-López *et al.*, 2006). In mammals, the somatic-like histones, which are present at the onset of spermatogenesis, are partially replaced by testis-specific histones, including a highly specific histone H1t (Seyedin and Kistler, 1980). The histones are almost completely replaced by the transition nuclear proteins and then the protamines as the mature sperm are formed.

During mammalian spermatogenesis (Meistrich, 1989), the transcription of numerous haploid specific genes is initiated during the round spermatid (RS) phase (steps

1-8 in the rat) and is followed by a cessation of all transcription in the elongating spermatids (steps 9-12). Profound chromatin reorganization occurs as the histones are initially replaced by transition proteins (Kistler *et al.*, 1973) in the condensing spermatids (steps 12-15) followed by their eventual replacement by protamines in condensed spermatids (steps 16-19). The mechanisms by which histones are displaced and transition proteins and protamines are deposited are not known. Acetylation of core histones appears to be involved in this process. In particular, histone H4 has been shown to be highly acetylated in spermatids, and *in vitro* studies showed that H4 acetylation resulted in an enhanced ability of protamines to displace histones from chromatin (Oliva and Dixon, 1991).

I characterize, in this chapter, the modification of histone H1t during the steps of spermiogenesis just prior to histone displacement. H1t is first synthesized during the primary spermatocyte stage; in the round spermatids H1t is the predominant form of linker histones (Bucci *et al.*, 1982), where it accounts for approximately 55% of the histone H1 complement. H1a represents about 26 % and the other somatic types (H1b, c, d and e) are more minor contributors.

There has been some disagreement in the literature as to whether or not H1t is phosphorylated during spermatogenesis. In studies of adult mouse testis, it was first reported using two dimensional AU-SDS gels that H1t exhibited several more slowly migrating spots that disappeared upon treatment with alkaline phosphatase (Lennox and Cohen, 1984). An additional band in a corresponding position was also shown for adult rat testis and a decrease in H1t mobility was detected in elongating spermatids of vitamin A synchronized rats (Meistrich *et al.*, 1994). In contrast, in a study of testis from 40-day

old rats, it was reported that H1t was not phosphorylated based on absence of detectable ^{32}P incorporation into the band corresponding to H1t (Khadake *et al.*, 1994).

In this chapter, I have revisited this problem and show that in both mice and rats H1t is phosphorylated and that the phosphorylation occurs in elongating spermatids and mainly affects the C-terminal region of the molecule. A powerful mass spectrometric approach utilizing both CAD and ETD mass spectrometry has been used to identify the main phosphorylation sites involved.

Materials and Methods

Histone H1t purification

The testis from either rat or mouse were homogenized using a Kinematica Polytron in 150 mM NaCl, 20 mM Tris-HCl (pH 7.5), 0.1 mM EDTA buffer containing a protease inhibitor mixture ("Complete" from Roche Diagnostics, Laval, QC) at the ratio of 1 tablet per 100 mL buffer. After homogenization, the samples were centrifuged at 2,000 x *g* for 10 min at 4ºC. The pellet was then resuspended in 0.6 N HCl (at approximately 6 mL per gram of starting tissue), homogenized and centrifuged as above. The HCl supernatant extracts were precipitated with 6 volumes of acetone at -20ºC overnight and then centrifuged at 2,000 x *g* for 10 min at 4ºC. The acetone pellets were dried using a speedvac concentrator. The dried pellets were re-suspended in approximately 1 mL of water. An equal volume (1mL) of 10% perchloric acid (PCA) was added to reach a final concentration of 5% PCA. The 5% PCA solution was incubated on ice for 5 min and then centrifuged at 12 000 x *g* for 10 min. HCl was added to the supernatant to a final concentration of 0.25 N HCl. The HCl supernatant extracts were

precipitated with 6 volumes of acetone at -20ºC overnight. The acetone pellet was dried as above. The dried pellet after PCA extraction was resuspended in water, filtered through a 0.45 µm Nanosep centrifugal device (Pall, Ann Arbor, MI) and injected onto a 4.6 x 250 mm Vydac C_{18} RP-HPLC column (Grace Vydac, St. Hesperia, CA). Histone H1s were eluted starting from a 0.1 % trifluoroacetic acid (TFA) solution and an increasing acetonitrile (ACN) shallow gradient: 1-5 % ACN for 1 min, 5-25 % ACN for 10 min, 30-40 % for 40 min.

Cell separation and protein isolation

In general, cell suspensions prepared from testis of adult Sprague-Dawley rats (Harlan-Sprague-Dawley, Indianapolis, IN) were separated by centrifugal elutriation (Meistrich, 1977; Unni and Meistrich, 1992) to obtain fractions enriched in round spermatids (steps 1-8) and elongating spermatids (steps 9-12). In the round spermatid fraction, the round spermatids accounted for 73% of histones, with early spermatocytes and somatic cells each contributing 11%. It is difficult to purify elongating (step 9-12) spermatids by a single step of centrifugal elutriation (Meistrich *et al.*, 1994). In the elongating spermatids fraction, these cells contributed 42% of the histones, with somatic cells, which resembled macrophages and white blood cells from the interstitial region, contributing 50%.

In one experiment, highly purified fractions of round and elongating spermatids at specific steps of development were prepared from vitamin A synchronized rats by centrifugal elutriation followed by equilibrium density centrifugation (Meistrich *et al.*, 1994).

Nuclei were prepared by lysis in hypotonic buffer containing Triton X-100 (Meistrich *et al.*, 1992; Platz *et al.*, 1977) with PMSF, p-chloromercuriphenyl sulfonic acid, and, in some cases, iodoacetamide, as protease, phosphatase, and isopeptidase inhibitors, respectively. Proteins were extracted from nuclei with 0.25 N HCl and precipitated with trichloroacetic acid (TCA). TCA precipitations were done with either 25% TCA or in two steps: 4% TCA to remove the core histones and most non-histone proteins followed by 25% TCA precipitation to collect the H1 histones. All of the bands shown here were observed both in the 25% precipitate and the 4%-25% cut, which is consistent with them representing H1 histones.

Alkaline phosphatase treatment of histones

The incubation mixture contained bacterial alkaline phosphatase (60 units per milligram, Sigma Chemical Co, St Louis, MO) at 100 µg/ml, nuclear protein extracted from spermatids, and PMSF in a volume of 150 µl of 100 mM Tris-HCl (pH 8.0). The mixture was incubated for 1 hour at 37 ºC. To control for the possibility that the observed result was due to some possible non-specific reaction of the enzyme or a contaminant in the preparation, a different alkaline phosphatase from calf intestine (Worthington Biochemical Corp. Freehold, Lakewood, NJ) was used in one experiment. The enzyme concentration was 400 µg/ml (2100 U/ml) in 100 µl of the same buffer but with the addition of 1 mM para-aminobenzoic acid and 10 µg/ml leupeptin. Reaction was incubated at 37 ºC for 1.5 hours. Proteins were collected by TCA precipitation.

Radioactive labeling with ^{32}P

Prior to and during the preparation of the cell suspension by the trypsin method (Meistrich, 1977), 10 mCi of ^{32}P-orthophosphate was added to 200 ml of PBS and distributed among 4 flasks. The free ^{32}P was removed during the centrifugation of the cell suspension prior to elutriation.

Gel electrophoresis and detection of proteins

The nuclear proteins were usually analyzed by AU-PAGE (15 % acrylamide, 2.5 M urea) (Ausió, 1992; Panyim and Chalkley, 1969). In some cases, SDS-PAGE (Laemmli, 1970) or AUT-PAGE (Frehlick *et al.*, 2006; Trostle-Weige *et al.*, 1984) were used. Gels were stained with either Coomassie blue or amido black. H1t bands were identified by Western-blotting with a polyclonal antiserum to H1t (Markose and Rao, 1985) used at a dilution of 1:200. Autoradiography was performed by drying the gel and exposure to Kodak AR film for 3 days.

Mass spectrometric Analysis

Upon purification of murine H1t as described above, the H1t-containing HPLC fraction was lyophilized and then resuspended in 50 µL H_2O. An aliquot (5% of the resuspended fraction) was diluted 3-fold with 100 mM ammonium bicarbonate, pH 8. The aliquot of H1t was then digested with AspN protease (Roche Diagnostics) at a substrate-to-enzyme ratio of 20:1 for 7 hrs at 37°C and the resulting peptide mixture was acidified to pH 3.5 with glacial acetic acid. An aliquot (5%) of AspN-digested H1t was

pressure-loaded (200 PSI) onto a precolumn (360 µm O.D. x 75 um I.D., Polymicro Technologies, Phoenix, AZ) packed with 4 cm of C_{18} resin (5-20 µm diameter, 120 Å pore size, YMC Inc. Milford, MA). The precolumn was washed for 5 mins with 0.1% acetic acid at 1 µL/min. The precolumn was then connected to an analytical column (360 µm O.D. x 50 µm I.D. fused silica) packed with 7 cm of C_{18} resin (5 µm diameter, 120 Å pore size, YMC Inc., Milford, MA) (Schroeder *et al.*, 2004). H1t peptides were eluted using nanoflow HPLC with an 1100 series binary HPLC pump (Agilent Technologies, Santa Clara, CA) coupled to an electrospray ionization source, modified for nanospray, on a LTQ-Orbitrap mass spectrometer (Thermo Scientific, Waltham, MA). A splitter enabled the excess solvent to flow to waste through a stainless steel union where the high-voltage was applied for electrospray ionization (Martin *et al.*, 2000). The gradient consisted of 0-60 % B in solvent A in 60 min and 60-100 % B in 10 min, where solvent A and solvent B were 0.1 M acetic acid and 0.1 M acetic acid in 70 % acetonitrile, respectively. Full scan (*m/z* 300-2000) mass spectra were acquired with the Orbitrap.

A second aliquot (5 %) of purified H1t was again diluted 3-fold with 100 mM ammonium bicarbonate (pH 8). H1t was then treated with propionic anhydride to derivatize endogenously monomethylated or unmodified ε-amino groups of lysine residues. Chemical derivatization with propionic anhydride converts amino groups of lysines to their corresponding propionyl amides and has been detailed previously (Garcia *et al.*, 2007). Briefly, equal volumes of propionylation reagent and protein were reacted, and derivatization was repeated three times to ensure full conversion of amino groups. H1t was then digested with trypsin (Promega, Madison, WI) at a substrate-to-enzyme ratio of 20:1 for 6 hrs at 37°C. Trypsin cleaved C-terminal to arginine residues only since

lysine residues were derivatized and blocked from cleavage. The resulting H1t peptide mixture was acidified with glacial acetic acid. Similar to as described above, an aliquot of the H1t peptide mixture was loaded onto a reverse phase capillary column and H1t peptides were analyzed via tandem mass spectrometry (MS/MS) using a hybrid quadrupole linear ion trap Fourier transform (LTQ-FT) mass spectrometer (Thermo Scientific, Waltham, MA). Precursor ions selected for MS/MS were fragmented via collision-activated dissociation (CAD) and MS/MS scans were acquired using the ion trap as the analyzer.

An aliquot of trypsin-digested H1t was also analyzed on a LTQ (Thermo Scientific, Waltham, MA) equipped with a Thermo upgrade for electron transfer dissociation (ETD) (Syka *et al.*, 2004). Trypsin-digested H1t peptides were again analyzed via LC-MS/MS, and specific *m/z* values corresponding to precursors of singly- and doubly-phosphorylated peptides of H1t were targeted for isolation and fragmentation via ETD.

The HPLC fraction containing rat H1t was resuspended in 100 μL H_2O. An aliquot (5% of the fraction) was diluted 4-fold with 100 mM ammonium bicarbonate. Rat H1t was digested with AspN at a substrate-to-enzyme ratio of 20:1 for 7 hrs at 37°C and the resulting peptide mixture was acidified with glacial acetic acid. Similar to that described above for murine H1t, AspN-digested rat H1t was analyzed via nanoflow LC-MS/MS on the LTQ Orbitrap.

Results

Histone H1t is phosphorylated in rat

Histones from specific stages of highly purified spermatids obtained by vitamin A synchronization, elutriation, and density gradient centrifugation were analyzed by AUT-PAGE. The results (Fig. 26A) showed that highly purified spermatids contained almost exclusively H1t and H1a; hence the majority of the somatic forms [b, c, d, e following the nomenclature of Seyedin and Kistler (Seyedin and Kistler, 1979)] seen in moderately enriched round spermatid populations must have been largely derived from contaminating cells. Although H1a and H1t are poorly separated on these gels, they can be distinguished by the metachromasia of staining with amido black; H1a stains black while H1t stains blue. Within the band marked H1a/t in steps 1-8, spermatids with both black (slowly migrating) and blue components were seen (Fig. 26A). At steps 9-10, this band was black, representing H1a, and at steps 11-12, it was absent. Concurrently, an additional distinctively blue, more slowly migrating component (P) was observed weakly in steps 7-8 and as a more major component in steps 9-10 and 11-12 in spermatids. Thus, H1t was essentially the only form of H1 present in steps 11-12 in spermatids and all the H1t had a modified mobility in these cells. Subsequent experiments done with moderately enriched cells subjected to elutriation only were interpreted using this information. Histones from moderately enriched populations of spermatids at different stages of development were analyzed by SDS-PAGE. The results (Fig. 26B) confirmed the presence of H1t as the major linker histone in the elongating spermatids. Most of the H1c, H1bde, and H1º was likely a result of the somatic cell contamination in this fraction.

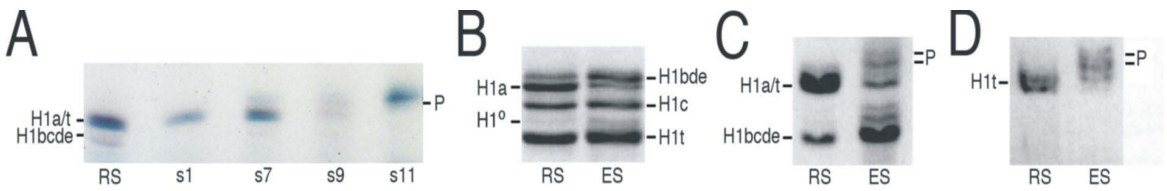

Figure 26. Histone H1t is the main histone H1 component of spermatids and exhibits a decreased electrophoretic mobility in elongating spermatids.

A) The H1 region of an amido-black stained AUT gel of nuclear protein extracted from the following cell types: RS, round spermatids enriched by elutriation; and highly purified s1, step1-2; s7, step7-8; s9, step 9-10; s11, step 11-12 spermatids. B)-D) Protein profiles of the H1 region of nuclear proteins extracted from moderately enriched populations of round spermatids (RS) or elongating spermatids (ES). B) SDS gel (Coomassie blue stain). C) AU gel (Coomassie blue stain). D) Immunoblot of AU gel reacted with antibodies to H1t. The putative phosphorylated forms of H1t are marked with P.

H1a levels were quite low in the elongating spermatids. Next, histones were separated by AU-PAGE using long gels (Fig. 26C). In the fraction enriched in elongating spermatids, a series of four bands was observed extending from the position of H1a/t to slower mobilities; some of these clearly had slower migrations than the bands in the round spermatid fraction. The identity of the shifted bands as modified forms of H1t was confirmed by Western blotting with antibodies to H1t (Fig. 26D). The slowly migrating bands were observed in the 4-25 % TCA cut as well as in the 25% TCA precipitate, ruling out the possibility that transition protein 4 (TP4), which also migrates slower than H1t, but is precipitated by 4 % TCA (Unni and Meistrich, 1992), contributes to these bands. The shifted bands were demonstrated to be phosphorylated forms of H1t by their disappearance after treatment of the preparations with alkaline phosphatases (Fig. 27). In the samples not treated with alkaline phosphatase, four bands were present in the H1a/t region, but after treatment with alkaline phosphatase, only the fastest two bands are observed (Fig. 27B). The loss of the more slowly migrating forms is clearly shown in the scan of the gel (Fig. 27A). Identical results were obtained by treatment with calf intestinal alkaline phosphatase (not shown). Immunostaining with antibodies to H1t shows that the slowest two bands represent phosphorylated H1t (Fig. 27C).

To further investigate whether the modified form of H1t was due to phosphorylation, we examined the incorporation of ^{32}P into histones. There was a more than two-fold increase in the specific activity of H1t detected as the spermatids matured (Table 2). This increase in labelling was observed in the H1t region in SDS and AU gels

(Fig. 28), and it supports the interpretation that H1t is phosphorylated in elongating spermatids.

Purification of mouse and rat Histone H1t

The results provided in the preceding section show that, like mouse H1t, rat H1t is also phosphorylated. The core histones of unfractionated testis from both mouse and rat consist of a heterogeneous mixture of variants including H2A.X, H2A.Z, and the testis-specific H2Bt as visualized by AUT PAGE (Fig. 29A). Gel electrophoresis by either AUT- or SDS-PAGE (Fig. 29A-B) of the 5% PCA extracts show that the linker histones also exhibit compositional complexity with 4-5 clearly distinctive bands. These bands can be chromatographically resolved into at least 8 distinctive elution peaks by RP-HPLC (Fig. 29C). As a result, it is possible to obtain an electrophoretically pure H1t fraction that is amenable to mass spectrometry analysis for the identification of the sites of phosphorylation of H1t.

Murine histone H1t is mainly phosphorylated at the C-terminus

Because H1t is a lysine-rich protein, a conventional peptide analysis utilizing trypsin for protein digestion would provide minimal sequence coverage of H1t. Therefore, derivatization of H1t with propionic anhydride was performed to convert the ε-amino groups of lysine residues into their corresponding propionyl amides and limit histone. Cdc2 is a mitotic kinase that is a well-known participant in the phosphorylation of histone H1(Nurse, 1991). The other identified phosphorylation sites are putative

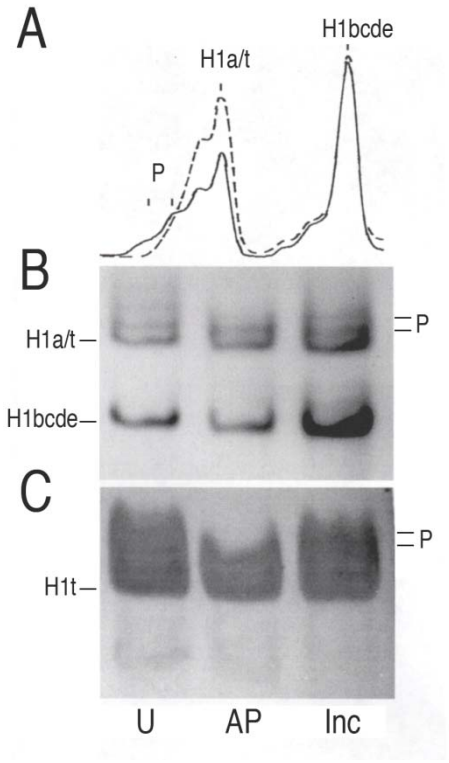

Figure 27. Effect of treatment with alkaline phosphatase on mobility of H1 proteins extracted from the elongating spermatid fraction in an AU gel.

A) Scan of the gel. Dashed line is protein treated with alkaline phosphatase; solid line is protein incubated without the enzyme. B) Coomassie blue stained gel. U, untreated proteins; AP, protein treated with bacterial alkaline phosphatase; Inc, protein incubated as in previous lane but without the enzyme. C) Immunoblot with antibodies to H1t. (Note: the Immunoblot was overstained spreading the bands, but differences between the AP-treated sample and the others can still be observed.)

Table 3. Relative specific activity of ^{32}P-labelled histones in enriched fractions of testicular cells resolved using SDS gels.

Histone Variant	Round Spermatid Fraction	Elongating Spermatid Fraction
H1t	9	22
H1abcde	10	12
H2A	100	54

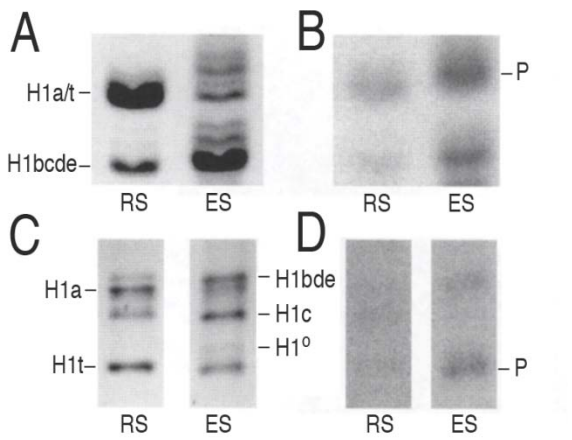

Figure 28. Incorporation of ^{32}P into H1 proteins extracted from fractions enriched in round spermatids (RS) and elongating spermatids (ES).

A) Stained AU gel. B) Autoradiogram of AU gel. C) Stained SDS gel. D) Autoradiogram of SDS gel. The bands in the autoradiogram corresponding to the phosphorylated forms of H1t are marked with P.

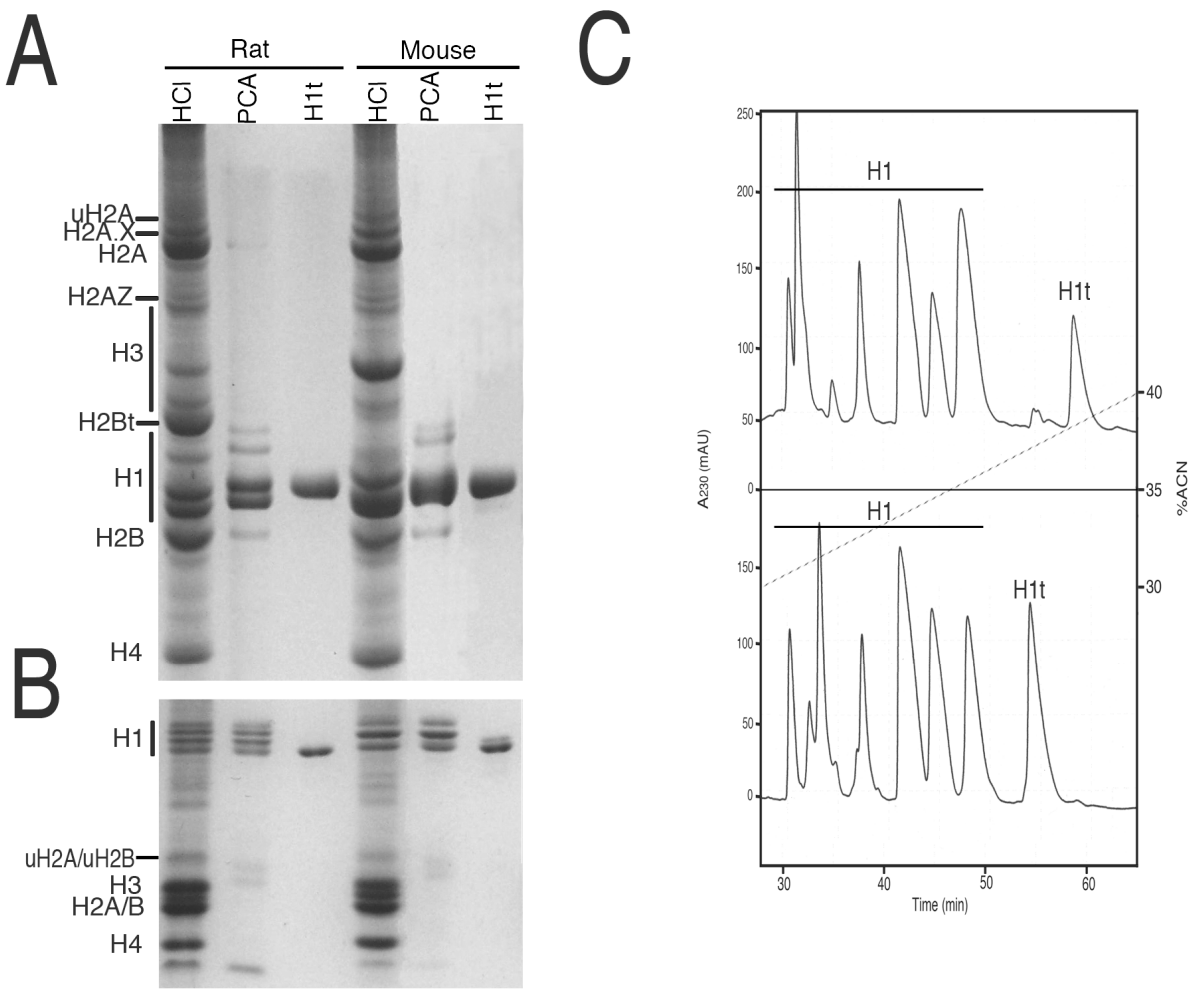

Figure 29. Purification of histone H1t.

A)-B) Protein composition of rat and mouse testis histones after different purification steps: HCl, hydrochloric acid extracted histones; PCA, perchloric acid extracted histones; H1t, histone H1t purified by RP-HPLC fractionation. A) AUT gel. B) SDS gel. C) RP-HPLC elution profile of rat (upper plot) and mouse (lower plot) PCA histone extracts.

tryptic cleavage to arginine residues (Garcia *et al.*, 2007). Mouse H1t derivatization and subsequent treatment with trypsin resulted in the generation of peptides that were more readily retained on a reverse phase column for analysis via LC-coupled tandem mass spectrometry (MS/MS).

Both CAD and ETD were employed to fragment mouse H1t peptides. ETD was necessary to unambiguously assign phosphorylation sites on these peptides as peptide fragmentation via ETD is indifferent to the presence of labile modifications such as phosphorylation (Chi *et al.*, 2007; Syka *et al.*, 2004). This ETD-based method is a sensitive technique which can be combined with LC-MS/MS and facilitated the identification of multiple phosphorylation sites on mouse H1t from femtomole amounts of material. Four sites of phosphorylation at the C-terminal region of H1t were identified on residues S140, T155, S162, and S177 (Fig. 30). The relative abundances of the phosphorylation sites, S140, S177, S162, and T155, are in the ratio of 8:4:2:1. Furthermore, LC-MS/MS analysis employing ETD facilitated the interrogation of doubly-phosphorylated H1t peptides, and the various forms of phosphorylated H1t peptides are shown in Fig. 30B. Phosphorylation of S140 was found to coexist with T155 or S162 phosphorylation. Interestingly, T155 represents a putative cdc2-dependent phosphorylation site that is not conserved within any other linker substrates of Cdc2, PKA or PKC as these H1t residues are present within regions that resemble recognition motifs for these kinases. PKA and PKC have long been suspected to be involved in the phosphorylation of spermiogenic chromosomal proteins because of the presence of basic amino acids in their phosphorylation recognition motifs (Meetei *et al.*, 2002; Pirhonen *et al.*, 1994).

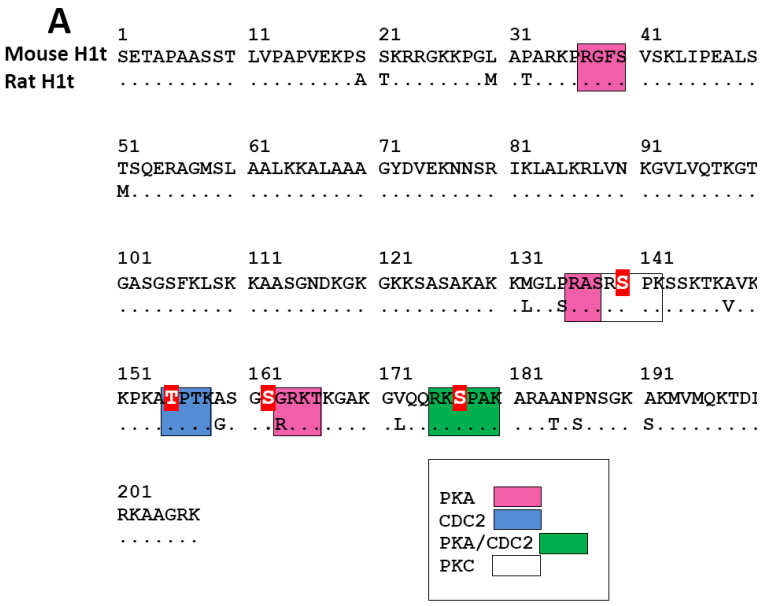

Figure 30. A schematic representation of amino acid sequence alignment of mourse and rat H1t and the phosphorylated peptides observed by mass spectrometry.
A) Amino acid sequence alignment of mouse and rat H1t. The boxed amino acid sequences correspond to the predicted kinase phosphorylation consensus sequences. The serines highlighted in red represent the novel phosphorylation sites that were identified by mass spectrometry. B) Singly- and doubly- phosphorylated peptides observed following LC-MS/MS analysis of trypsin-digested H1t.

While singly- and doubly-phosphorylated H1t peptides were successfully interrogated following tryptic digestion, digestion with endoproteinase Asp-N was utilized to generate larger peptides compared to that from the tryptic digestion and also enabled the detection of H1t peptides concurrently modified with multiple phosphate groups. The C-terminal peptide of murine H1t generated with Asp-N is an 82-residue peptide (residues 117-198) and harbours all four residues that were found to be phosphorylated upon LC-MS/MS analysis of trypsin-digested H1t. Of all the forms of 117-198 that were detected, approximately 70% of the H1t peptide was unmodified, while the various phosphorylated forms were present at a combined 30% relative abundance and include forms harbouring one to four phosphate groups. The multi-enzyme approach, utilizing both trypsin and Asp-N, followed by mass spectrometric analysis of H1t peptides allowed for the interrogation of 90% of the murine H1t sequence and facilitated the interrogation of 94% of the serine, threonine, and tyrosine residues that are present within H1t.

In order to determine the location of phosphorylation occurring on rat H1t, Asp-N digestion and subsequent LC-MS analysis was performed on rat H1t. Similar to that found for murine H1t, the major phosphorylation sites of rat H1t were located within the C-terminal region and were detected on the 82-residue rat H1t peptide generated with the Asp-N protease. The notable similarity in the phosphorylation patterns of mouse and rat H1t is demonstrated in the MS spectra shown in Fig. 31. The C-terminal peptide comprised of residues 117-198 of rat H1t were detected unphosphorylated and phosphorylated, harbouring one to four phosphate groups. These phosphorylated species of rat H1t are analogous to the phosphorylated species identified in murine H1t.

In summary, this mass spectrometric approach enabled the identification of novel phosphorylation sites within H1t, with these sites being located in the C-terminal region of both mouse and rat H1t.

Discussion

Histone H1t is ubiquitously phosphorylated in elongating spermatids of murine species

The results in this chapter support and extend the observation of phosphorylation of H1t in spermatids of the mouse (Lennox and Cohen, 1984) to the rat. The first appearance of phosphorylated forms at 4 weeks of age in the mouse and their increase at 16 weeks indicated that the phosphorylation was occurring in spermatids. In this chapter, we confirmed these results in the rat and localized this event to elongating spermatids. Since the phosphorylation is localized to the elongating spermatids, the failure to observe such phosphorylation in 40-day old rat testis might be explained. Normal elongating spermatids first appear in the testis at day 36 in the rat, but initially their numbers constitute a smaller percentage in the testis than at maturation, which in the rat occurs later (Ekwall *et al.*, 1984).

Post-translational modifications of murine histone H1t

The post-translational modifications of somatic linker histones have been studied extensively in recent years (Deterding *et al.*, 2004; Garcia *et al.*, 2004; Garcia *et al.*, 2006; Sarg *et al.*, 2006; Wisniewski *et al.*, 2007) [see (Godde and Ura, 2008) for review]. However, little attention has been paid to the developmental-specific histones such as the testis-specific H1t.

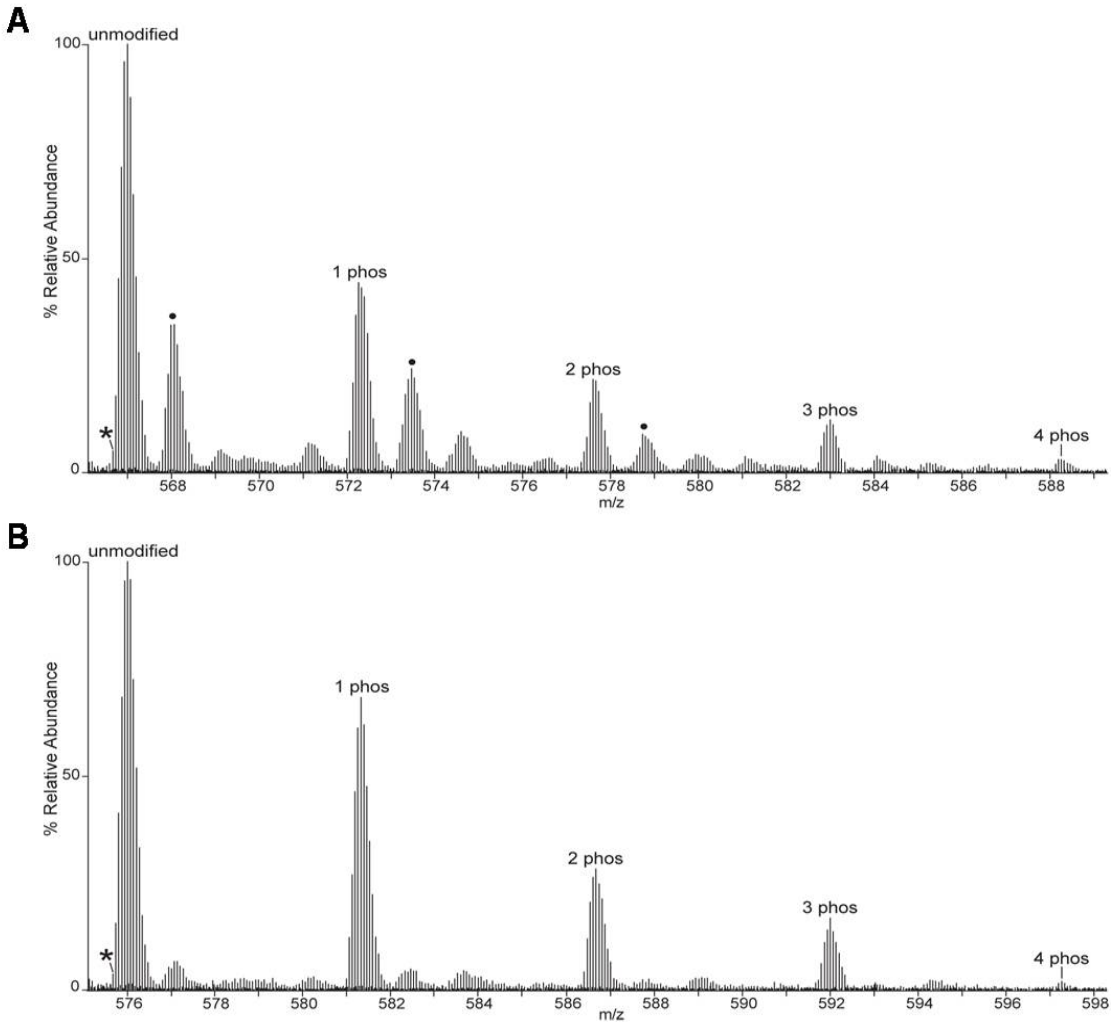

Figure 31. MS spectra of the C-terminal peptides (residues 117-198) derived from mouse (A) and rat (B) H1t.

The monoisotopic ions of the unphosphorylated mouse and rat peptides are denoted with asterisks and consist of m/z 566.6645 and m/z 575.6696, respectively. Note the remarkable similarity in relative abundances of the phosphorylated murine and rat peptides. The species indicated with filled circles are oxidized forms (present at ≥10% relative abundance) of the H1t peptides. Oxidation was more prominent in the mouse H1t sample.

As is typical of other members of the histone H1 family (Garcia *et al.*, 2004; Rall and Cole, 1971; Wisniewski *et al.*, 2007), histone H1t was also described to be N-terminally acetylated (Cole *et al.*, 1984). This also appears to be the case for both mouse and rat H1t. Upon ETD MS/MS analysis of trypsin-digested mouse H1t, the N-terminal peptide identified was SETAPAASSTLVPAPVEKPSSKR (residues 1-23). This peptide was observed to have a 42 Dalton increase compared to the expected molecular weight, which is consistent with acetylation at the N-terminus of the H1t protein. In addition, an N-terminal peptide was observed with the sequence SETAPAASSTLVPAPVEEKPSSKR (residues 1-24), which indicates the presence of a second, lower-abundant isoform of mouse H1t. Note the addition of a glutamic acid residue, which is underlined in the peptide sequence above. The molecular weight and ETD MS/MS information acquired of the H1t peptide 1-24 is also consistent with N-terminal acetylation. Furthermore, the observed masses of the N-terminal mouse H1t peptides derived using AspN (H1t 1-72 or 1-73) contained a 42-Dalton shift, consistent with acetylation. This shift in mass was also observed upon LC-MS analysis of AspN-derived rat H1t 1-72. Following N-terminal acetylation, phosphorylation appears to be the next most prominent post-translational modification (PTM) present on H1t.

Phosphorylation of a somatic histone H1 has been extensively characterized both in the past [see (Hohmann, 1983) for a review] and more recently through MS analysis (Garcia *et al.*, 2004; Garcia *et al.*, 2006; Sarg *et al.*, 2006; Wisniewski *et al.*, 2007). It was initially shown that its distribution along the molecule (in CHO cells) depended on the stage of the cell cycle with the C-terminus becoming increasingly phosphorylated as the cell cycle progressed from G1 to mitosis. In the mitotic chromosome, H1 became

additionally phosphorylated at its N-terminal end (Hohmann, 1983). This pattern is non-random, and in humans, distinct serine- and threonine-specific kinases participate in different cell cycle stages (Sarg *et al.*, 2006).

As a result of the global proteomic analysis of linker histones, histone H1t was detected to be present in low amounts in mouse spleen extracts (Wisniewski *et al.*, 2007) and in HeLa cells (Olsen *et al.*, 2006) where a KPRApTpTPK peptide, which corresponds to T155 and T157 of the mouse sequence shown in Fig. 30, was identified. However, this peptide was identified from a mixture of thousands of phosphopeptides using a data-base searching algorithm and the MS/MS data were not manually examined as we have done here. The occurrence of minute amounts of H1t in somatic cells, which probably is the result of gene "leaking" (Wisniewski *et al.*, 2007), is not surprising. Hence, the physiological relevance, if any, of the presence of H1t and its two putative phosphorylation sites in somatic cells remains to be determined.

Phosphorylation of H1t and the replacement of histones by transition proteins

The C-terminal localization of the main phosphorylation sites of H1t obtained from mature testis of murine species is interesting in different regards. Firstly, the pattern of phosphorylation observed is similar to that which is found at the C-termini of other somatic histone H1s in what appears to be a consensus region (Godde and Ura, 2008). This consensus region is approximately 20 amino acids away from the winged helix domain and 20-30 amino acids upstream from the C-terminus. This is the region that is mainly involved in the participation of histone H1 in the folding of the chromatin fiber (Lu and Hansen, 2004). Furthermore, a serine to glutamic acid substitution, used as a

phosphorylation mimic at S183 of human histone H1d, dramatically impaired its binding to chromatin (Hendzel *et al.*, 2004). Based on primary sequence alignment, phosphorylation of S183 in human H1d is equivalent to S177 phosphorylation in murine H1t, the latter of which was identified in this chapter. This is a site that is also present in murine somatic linker histones and which appears to have been quite conserved throughout mammalian evolution. Thus, it is likely that phosphorylation of H1t in spermatids is associated with the decondensation of chromatin.

This suggestion raises the question as to what is the possible function of chromatin decondensation in elongating murine spermatids. H1t phosphorylation cannot be related to transcriptional activity because transcription has already ceased earlier in round spermatids. Instead, we propose that the phosphorylation of H1t in conjunction with the hyperacetylation of histone H4 that is observed in elongating spermatids (Meistrich *et al.*, 1992) are part of a process of loosening the histone-DNA interactions in preparation for the displacement of the histones by transition proteins (Kistler *et al.*, 1996; Meistrich, 1989). The fact that pS177 is a prominent phosphorylation site together with the relevance of this site in lowering the DNA-binding affinity at an equivalent position in a somatic linker histone counterpart (Hendzel *et al.*, 2004) would explain why this tissue-specific histone H1 is not indispensible for normal spermatogenesis in mice (Lin *et al.*, 2000). The compensatory effect of the somatic histone H1 complement that increases upon depletion of H1t (Lin *et al.*, 2000) could be possibly explained by the phosphorylatable RKSPAK sequence around S177 of H1t (Fig. 30). This sequence is present at a similar position in all somatic mouse and human H1 variants and for which evidence of phosphorylation has been well documented (Garcia *et al.*, 2004; Sarg *et al.*,

2006; Wisniewski *et al.*, 2007). Interestingly, this sequence can be a target for both the sperm ubiquitous PKA and cdc2. The presence of the other specific phosphorylation sites detected here as well as the more open conformation conferred by H1t to chromatin (De Lucia *et al.*, 1994), while not strictly required, may contribute to enhancing the efficiency of the spermiogenic process.

Global Conclusion

Spermatogenesis is the differentiation processes that leads to the formation of male gametes. At the onset, spermatogonia undergo several rounds of mitosis to produce primary spermatocytes. These cells then go through two cycles of meiosis and spermiogenesis to produce spermatozoa (Fig. 32). Spermiogenesis is a part of spermatogenesis where chromatin from spermatids undergoes a dramatic reorganization. During this stage, histones are replaced by protamines and DNA is compacted. At the onset of spermiogenesis, histone H4 and H3 are hyperacetylated and the spermatid chromatin forms 200 Å granular structures (Kurtz *et al.*, 2009). It is possible that this chromatin conformation initiates the replacement of histones by transition proteins. The replacement of transition proteins by protamines results in a different chromatin structure. Protamines bind to the minor groove of DNA without inducing coiling of the DNA (Ward and Coffey, 1991). Therefore, the sperm chromatin is packaged in a side-by-side linear array in which sperm DNA is condensed six fold compared to somatic chromatin (Ward and Coffey, 1991).

It has become increasingly clear that the presence of histone variants and histone PTMs play a critical role in the chromatin transitions that take place during spermatogenesis (Lewis *et al.*, 2003b). In addition, in most mammals a fraction of chromatin remains associated with histones in the mature sperm (Tanphaichitr *et al.*, 1978). Although the nature of this phenomenon is not well understood, it has been suggested that these histones associate with genes that are important for the events that take place immediately after fertilization (Vastenhouw *et al.*, 2010).

Histone variants and histone PTMs have been shown to act as a signal for the recruitment of proteins (Li *et al.*, 2005a; Thambirajah *et al.*, 2009). The structural contribution of histone variants and their PTMs to chromatin cannot be overlooked. Hypotheses were put forward in this thesis and also in the literature (Downs *et al.*, 2000; Li *et al.*, 2005a) to account for their structural contribution. The hypothesis proposed in this thesis was that the four histone variants studied, H2A.X, H2A.Bbd, hTSH2B and H1t, and their PTMs play an important role in the various stages of spermatogenesis partly through their ability to alter chromatin structure. In this thesis, I provided evidence for the structural contributions of the four histone variants and their PTMs to chromatin. Although most of the experiments showing the structural contributions of histone variants performed were *in vitro*, my data provided valuable information for further *in vivo* investigations. The interactions of histone variants during the different stages of spermatogenesis and their contributions to chromatin structure *in vivo* should be the focus of future investigations.

H2A.X and its phosphorylated form are enriched in primary spermatocytes due to the presence of DNA DSB during homologous recombination in meiosis (Meistrich *et al.*, 1985) (Fig. 32). More specifically, H2A.X expression peaks at leptotene stage during prophase I of Meiosis I where DSBs are initiated (Meistrich *et al.*, 1985). Although the phosphorylation of H2A.X in DNA DSB repair in somatic cells is well known, H2A.X and its modifications are not well understood in spermatogenesis. The fact that the initiation of DNA DSB during Meiosis I coincides with the enrichment of H2A.X during leptotene stage implies a DNA repair role for H2A.X during spermatogenesis. In Chapter 1, I proposed a putative model for the role of H2A.X during DNA DSB repair, including

the repair of DSB during meiosis. The phosphorylation of H2A.X could serves as an epigenetic signal for the recruitment of DNA DSB repair machineries. In addition, phosphorylated H2A.X could also have a structural role which allows the chromatin to adopt a more open conformation. Chapter 2 of this thesis provided evidence for the role of phosphorylated H2A.X in destabilizing the nucleosome. The phosphorylation of T136 and S139 at the C-terminus of H2A.X, which is at the entry and exit sites of DNA in the nucleosomes, relaxes the chromatin fibre and affects the association of linker histones to chromatin in this region. Although H2A.X expression peaks during prophase I, it is present throughout spermatogenesis from spermatogonia to spermatozoa. As described in Chapter 1, H2A.X have shown to be present in cellular processes not related to DNA DSB repair, such as transcription and replication. It is possible that the role of H2A.X during spermatogenesis is multifaceted and it may help destabilize chromatin to facilitate the histone to protamine transition.

Chapter 3 describes for the first time the occurrence of native H2A.Bbd in cells during spermiogenesis. This histone is present at the later stages of spermiogenesis when histone H4 is hyperacetylated and histones are actively being replaced by transition proteins (Fig. 32). Since both H2A.Bbd and H2A.X have shown to be involved in the destabilization of nucleosomes [(Gonzalez-Romero *et al.*, 2008) and Chapter 2], the presence of these two histone H2A variants and hyperacetylated H4 in spermiogenesis may affect chromatin synergistically causing the displacement of histones from chromatin and thus, facilitating the replacement of histone by transition proteins and protamines. Interestingly, both H2A.Bbd and H2A.X are still present in the nucleosomes that remain associated with mature spermatozoa in humans (Chapter 3 and data not

shown). It is appreciated that mature spermatozoa DNA is highly condensed resulting in the absence of cellular metabolism. The presence of minute amounts H2A.X-containing and H2A.Bbd-containing nucleosomes interspersed in the protamine compacted DNA in spermatozoa may also play an important role in the events that occur in early development immediately after fertilization. Very little information is available on the role of histone variants after fertilization due to the limited amount of material that can be collected from eggs for this type of research. It would be of great interest to study the involvement of histone variants in these processes, which also involve DNA DSB (Marchetti *et al.*, 2007).

A homomorphous H2B variant, hTSH2B, was first characterized by Zalensky and colleagues in 2002 (Zalensky *et al.*, 2002). The major differences between hTSH2B and H2B are at the N-terminal of the histones where proline residues in the somatic H2B are replaced by phosphorylatable serines/threonines in hTSH2B. The expression of hTSH2B takes place exclusively in human male germ cells and in only 20% of spermatozoa (Singleton *et al.*, 2007a; Zalensky *et al.*, 2002) (Fig. 32). The contribution of hTSH2B to the octamer described in Chapter 4 suggests that the regions of DNA associated with hTSH2B may have a different mechanism than those that have no hTSH2B. Although the presence of hTH2B has been implicated in spermatozoa motility (Singleton *et al.*, 2007a), the role of this H2B variant in fertilization is not known. The investigation of whether spermatozoa with hTSH2B are more fertile compared to that without hTSH2B would be valuable to researches in fertilization processes. Furthermore, the chromatin structural effects of post-translationally modified hTSH2B, such as phosphorylation at sites that are unique to this variant, still needs to be investigated.

Histone H1 is known to play a critical role in chromatin folding. A variant of H1, H1t, is the focus of Chapter 5 in this thesis. It is first synthesized in primary spermatocytes and it is the predominant form of linker histone in round spermatids (Bucci *et al.*, 1982). Its presence in Meiosis I suggest a potential involvement in homologous recombination. Histone H1 phosphorylation has been shown to weaken the interaction of this histone with chromatin (Hendzel *et al.*, 2004). While the phosphorylation of somatic H1 has been well characterized, there has been disagreement as to whether or not H1t is phosphorylated during spermatogenesis. The data presented in Chapter 5 shows that H1t is phosphorylated during spermatogenesis and the specific locations of these PTMs. The phosphorylation of H1t at specific sites may inhibit its association with chromatin, thereby altering the chromatin conformation. It is possible that, during spermiogenesis, the phosphorylation of H1t together with the phosphorylation of H2A.X and the presence of H2A.Bbd in spermatids could act synergistically to alter the conformation of spermatid chromatin to facilitate the replacement of histones by transition proteins. Interestingly, the formation of the 200 Å chromatin granule during spermiogenesis coincides with the H4 and H3 acetylation and the phosphorylation of H1t. This chromatin granule conformation is reminiscent of the relaxed acetylated chromatin seen in the absence of histone H1 (Garcia Ramirez *et al.*, 1995) and further suggests that the phosphorylation of H1t inhibits its association with chromatin.

In addition to the histone variants discussed in this thesis, the role other histone variants, such as H3.3 and macroH2A, and other histone PTMs, such as phosphorylation of H3 and hyperacetylation of H4, have also been implicated at different stages in

mammalian spermatogenesis (Lewis *et al.*, 2003b). While H3.3 is implicated in meiosis-specific gene transcription, macroH2A is linked to transcriptional inactivation (Akhmanova *et al.*, 1997; Pehrson *et al.*, 1997). The phosphorylation of H3 is involved in chromatin condensation (Kaszas and Cande, 2000). In contrast, the extensive acetylation of H4 during spermiogenesis results in the displacement of histones during spermiogenesis (Oliva and Dixon, 1991). The four variants and their PTMs studied in this thesis encompass an important part of the repertoire of histone variants and histone modifications that are critical for spermatogenesis. With the recent advances in laboratory techniques, such as ChIP-Seq, high throughput sequencing and Covalent Attachment of Tags to Capture Histones and Identify Turnover (CATCH-IT), it should be possible to better define the interactions of these variants and PTMs at various stages of spermatogenesis in the future. Such information will be critical in elucidating the epigenetic regulation involved in the progression of this important cellular differentiation process.

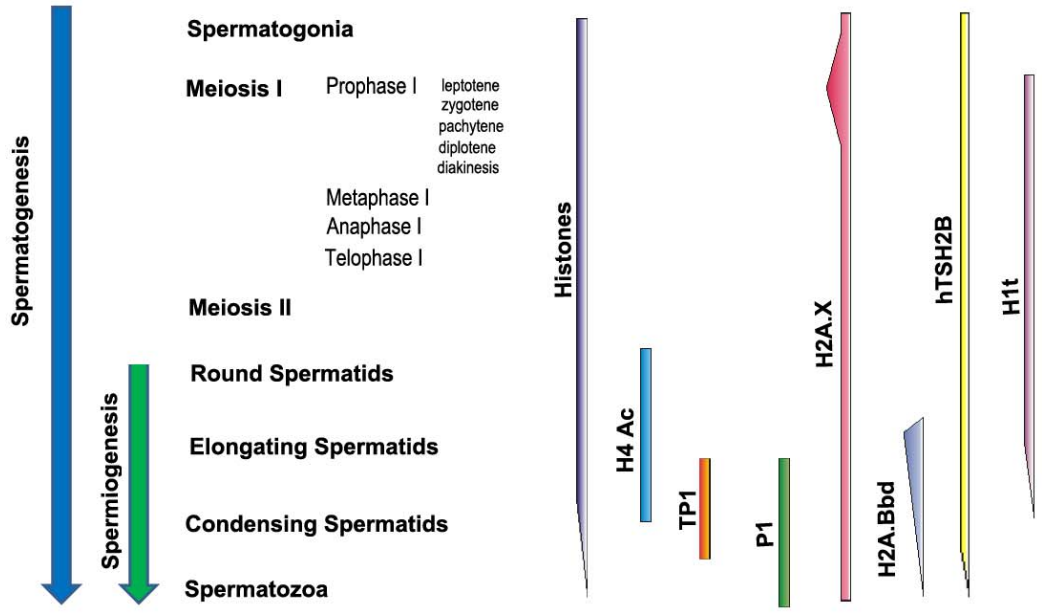

Figure 32. Schematic representation of histones and non-histone proteins at different stages of mammalian spermatogenesis.

On the left, the stages of spermatogenesis are shown. The color filled bars on the right represents the presence of histone variants, modified histones, transition proteins and protamine at different stages of spermatogenesis.

Bibliography

Abbott, D. W., Chadwick, B. P., Thambirajah, A. A., and Ausio, J. (2005). Beyond the Xi: macroH2A chromatin distribution and post-translational modification in an avian system. J Biol Chem *280*, 16437-16445.

Abbott, D. W., Ivanova, V. S., Wang, X., Bonner, W. M., and Ausió, J. (2001). Characterization of the stability and folding of H2A.Z chromatin particles: implications for transcriptional activation. J Biol Chem *276*, 41945-41949.

Abbott, D. W., Laszczak, M., Lewis, J. D., Su, H., Moore, S. C., Hills, M., Dimitrov, S., and Ausio, J. (2004). Structural characterization of macroH2A containing chromatin. Biochemistry *43*, 1352-1359.

Akhmanova, A., Miedema, K., Wang, Y., van Bruggen, M., Berden, J. H., Moudrianakis, E. N., and Hennig, W. (1997). The localization of histone H3.3 in germ line chromatin of Drosophila males as established with a histone H3.3-specific antiserum. Chromosoma *106*, 335-347.

Allan, J., Mitchell, T., Harborne, N., Bohm, L., and Crane-Robinson, C. (1986). Roles of H1 domains in determining higher order chromatin structure and H1 location. J Mol Biol *187*, 591-601.

Allfrey, V. G., Faulkner, R., and Mirsky, A. E. (1964). Acetylation and Methylation of Histones and Their Possible Role in the Regulation of Rna Synthesis. Proc Natl Acad Sci U S A *51*, 786-794.

Alvelo-Ceron, D., Niu, L., and Collart, D. G. (2000). Growth regulation of human variant histone genes and acetylation of the encoded proteins. Mol Biol Reports *27*, 61-71.

Angelov, D., Bondarenko, V. A., Almagro, S., Menoni, H., Mongelard, F., Hans, F., Mietton, F., Studitsky, V. M., Hamiche, A., Dimitrov, S., and Bouvet, P. (2006). Nucleolin is a histone chaperone with FACT-like activity and assists remodeling of nucleosomes. Embo J *25*, 1669-1679.

Angelov, D., Molla, A., Perche, P. Y., Hans, F., Cote, J., Khochbin, S., Bouvet, P., and Dimitrov, S. (2003). The Histone Variant MacroH2A Interferes with Transcription Factor Binding and SWI/SNF Nucleosome Remodeling. Mol Cell *11*, 1033-1041.

Angelov, D., Verdel, A., An, W., Bondarenko, V., Hans, F., Doyen, C. M., Studitsky, V. M., Hamiche, A., Roeder, R. G., Bouvet, P., and Dimitrov, S. (2004). SWI/SNF remodeling and p300-dependent transcription of histone variant H2ABbd nucleosomal arrays. Embo J *23*, 3815-3824.

Annunziato, A. T., and Hansen, J. C. (2000). Role of histone acetylation in the assembly and modulation of chromatin structures. Gene Expr *9*, 37-61.

Arents, G., Burlingame, R. W., Wang, B. C., Love, W. E., and Moudrianakis, E. N. (1991). The nucleosomal core histone octamer at 3.1 A resolution: a tripartite protein assembly and a left-handed superhelix. Proc Natl Acad Sc *88*, 10148-10152.

Arents, G., and Moudrianakis, E. N. (1995). The histone fold: a ubiquitous architectural motif utilized in DNA compaction and protein dimerization. Proc Natl Acad Sc *92*, 11170-11174.

Arnaudeau, C., Lundin, C., and Helleday, T. (2001). Replication forks are predominantly repaired by homoglogous recombination involving an exchange mechanism in mammalian cells. J Mol Biol *307*, 1235-1245.

Arpanahi, A., Brinkworth, M., Iles, D., Krawetz, S. A., Paradowska, A., Platts, A. E., Saida, M., Steger, K., Tedder, P., and Miller, D. (2009). Endonuclease-sensitive regions of human spermatozoal chromatin are highly enriched in promoter and CTCF binding sequences. Genome Res *19*, 1338-1349.

Ausio, J. (2006). Histone variants--the structure behind the function. Brief Funct Genomic Proteomic *5*, 228-243.

Ausió, J. (1986). Structural variability and compositional homology of the protamine-like components of the sperm from bivalve molluscs. Comp Biochem Physio *85 B*, 439-449.

Ausió, J. (1992). Presence of a highly specific histone H1-like protein in the chromatin of the sperm of the bivalve mollusks. Mol Cell Biochem *115*, 163-172.

Ausió, J. (2000). Analytical ultracentrifugation and the characterization of chromatin structure. Biophy Chem *86*, 141-153.

Ausio, J., and Abbott, D. W. (2002). The many tales of a tail: carboxyl-terminal tail heterogeneity specializes histone H2A variants for defined chromatin function. Biochemistry *41*, 5945-5949.

Ausio, J., and Abbott, D. W. (2004). The role of histone variability in chromatin stability and folding. In *Chromatin Structure and Dynamics: State-of-the-Art*, J. Zlatanova, and S.H. Leuba, eds. (Elsevier B.V.), pp. 241-290.

Ausió, J., Abbott, D. W., Wang, X., and Moore, S. C. (2001). Histone variants and histone modifications: a structural perspective. Biochemistry and Cell Biology = Biochimie Et Biologie Cellulaire *79*, 693-708.

Ausió, J., Dong, F., and van Holde, K. E. (1989). Use of selectively trypsinized nucleosome core particles to analyze the role of the histone "tails" in the stabilization of the nucleosome. J Mol Biol *206*, 451-463.

Ausió, J., and Moore, S. C. (1998). Reconstitution of chromatin complexes from high-performance liquid chromatography-purified histones. Methods (San Diego, Calif) *15*, 333-342.

Ausio, J., Seger, D., and Eisenberg, H. (1984). Nucleosome core particle stability and conformational change. Effect of temperature, particle and NaCl concentrations, and crosslinking of histone H3 sulfhydryl groups. J Mol Biol *176*, 77-104.

Ausió, J., Seger, D., and Eisenberg, H. (1984). Nucleosome core particle stability and conformational change. Effect of temperature, particle and NaCl concentrations, and crosslinking of histone H3 sulfhydryl groups. J Mol Biol *176*, 77-104.

Ausió, J., and van Holde, K. E. (1986). Histone hyperacetylation: its effects on nucleosome conformation and stability. Biochemistry *25*, 1421-1428.

Bakkenist, C. J., and Kastan, M. B. (2003). DNA damage activates ATM through intermolecular autophosphorylation and dimer dissociation. Nature *421*, 499-506.

Balajee, A. S., and Geard, C. R. (2004). Replication protein A and γ-H2AX foci assembly is triggered by cellular response to DNA double-strand breaks. Exp Cell Res *300*, 320-334.

Bao, Y., Konesky, K., Park, Y. J., Rosu, S., Dyer, P. N., Rangasamy, D., Tremethick, D. J., Laybourn, P. J., and Luger, K. (2004). Nucleosomes containing the histone variant H2A.Bbd organize only 118 base pairs of DNA. Embo J *23*, 3314-3324.

Bassing, C. H., Suh, H., Ferguson, D. O., Chua, K. F., Manis, J., Eckersdorff, M., Gleason, M., Bronson, R., Lee, C., and Alt, F. W. (2003). Histone H2AX: a dosage-dependent suppressor of oncogenic translocations and tumors. Cell *114*, 359-370.

Bewersdorf, J., Bennett, B. T., and Knight, K. L. (2006). H2AX chromatin structures and their response to DNA damage revealed by 4Pi microscopy. Proc Natl Acad Sci U S A *103*, 18137-18142.

Bird, A. W., Yu, D. Y., Pray-Grant, M. G., Qiu, Q., Harmon, K. E., Megee, P. C., Grant, P. A., Smith, M. M., and Christman, M. F. (2002). Acetylation of histone H4 by Esa1 is required for DNA double-strand break repair. Nature *419*, 411-415.

Bonner, W. M. (2003). Low-dose radiation: thresholds, bystander effects, and adaptive responses. Proc Natl Acad Sci *100*, 4973-4975.

Boudreault, A. A., Cronier, D., Selleck, W., Lacoste, N., Utley, R. T., Allard, S., Savard, J., Lane, W. S., Tan, S., and Cote, J. (2003). Yeast enhancer of polycomb defines global Esa1-dependent acetylation of chromatin. Genes Dev *17*, 1415-1428.

Bradbury, E. M., Cary, P. D., Crane_Robinson, C., Rattle, H. W., Boublik, M., and Sautiere, P. (1975). Conformations and interactions of histone H2A (F2A2, ALK). Biochemistry *14*, 1876-1885.

Bucci, L. R., Brock, W. A., and Meistrich, M. L. (1982). Distribution and synthesis of histone 1 subfractions during spermatogenesis in the rat. Exp Cell Res *140*, 111-118.

Burma, S., Chen, B. P., Murphy, M., Kurimasa, A., and Chen, D. J. (2001). ATM phosphorylates histone H2AX in response to DNA double-strand breaks. J Biol Chem *276*, 42462-42467.

Bustin, M., Catez, F., and Lim, J. H. (2005). The dynamics of histone H1 function in chromatin. Mol Cell *17*, 617-620.

Calestagne-Morelli, A., and Ausio, J. (2006). Long-range histone acetylation: biological significance, structural implications, and mechanisms. Biochem Cell Biol *84*, 518-527.

Celeste, A., Fernandez-Capetillo, O., Kruhlak, M. J., Pilch, D. R., Staudt, D. W., Lee, A., Bonner, R. F., Bonner, W. M., and Nussenzweig, A. (2003). Histone H2AX phosphorylation is dispensable for the initial recognition of DNA breaks. Nat Cell Biol *5*, 675-679.

Celeste, A., Petersen, S., Romanienko, P. J., Fernandez Capetillo, O., Chen, H. T., Sedelnikova, O. A., Reina San Martin, B., Coppola, V., Meffre, E., Difilippantonio, M. J.*, et al.* (2002). Genomic instability in mice lacking histone H2AX. Science *296*, 922-927.

Chadwick, B. P., and Willard, H. F. (2001). A novel chromatin protein, distantly related to histone H2A, is largely excluded from the inactive X chromosome. J Cell Biol *152*, 375-384.

Changolkar, L. N., and Pehrson, J. R. (2002). Reconstitution of nucleosomes with histone macroH2A1.2. Biochemistry *41*, 179-184.

Chen, H. T., Bhandoola, A., Difilippantonio, M. J., Zhu, J., Brown, M. J., Tai, X., Rogakou, E. P., Brotz, T. M., Bonner, W. M., Ried, T., and Nussenzweig, A. (2000). Response to RAG-mediated VDJ cleavage by NBS1 and gamma-H2AX. Science *290*, 1962-1965.

Chi, A., Huttenhower, C., Geer, L. Y., Coon, J. J., Syka, J. E., Bai, D. L., Shabanowitz, J., Burke, D. J., Troyanskaya, O. G., and Hunt, D. F. (2007). Analysis of phosphorylation

sites on proteins from Saccharomyces cerevisiae by electron transfer dissociation (ETD) mass spectrometry. Proc Natl Acad Sci U S A *104*, 2193-2198.

Chodaparambil, J. V., Barbera, A. J., Lu, X., Kaye, K. M., Hansen, J. C., and Luger, K. (2007). A charged and contoured surface on the nucleosome regulates chromatin compaction. Nat Struct Mol Biol *14*, 1105-1107.

Churikov, D., Zalenskaya, I. A., and Zalensky, A. O. (2004). Male germline-specific histones in mouse and man. Cytogenet Genome Res *105*, 203-214.

Clark, D. J., Hill, C. S., Martin, S. R., and Thomas, J. O. (1988). Alpha-helix in the carboxy-terminal domains of histones H1 and H5. Embo J *7*, 69-75.

Clarkson, M. J., Wells, J. R., Gibson, F., Saint, R., and Tremethick, D. J. (1999). Regions of variant histone His2AvD required for Drosophila development. Nature *399*, 694-697.

Cole, K. D., York, R. G., and Kistler, W. S. (1984). The amino acid sequence of boar H1t, a testis-specific H1 histone variant. J Biol Chem *259*, 13695-13702.

Cole, R. D. (1984). A minireview of microheterogeneity in H1 histone and its possible significance. Anal Biochem *136*, 24-30.

Costes, S. V., Chiolo, I., Pluth, J. M., Barcellos-Hoff, M. H., and Jakob, B. (2010). Spatiotemporal characterization of ionizing radiation induced DNA damage foci and their relation to chromatin organization. Mutat Res.

Cowell, I. G., Sunter, N. J., Singh, P. B., Austin, C. A., Durkacz, B. W., and Tilby, M. J. (2007). gammaH2AX foci form preferentially in euchromatin after ionising-radiation. PloS one *2*, e1057.

Dalton, S., Robins, A. J., Harvey, R. P., and Wells, J. R. (1989). Transcription from the intron-containing chicken histone H2A.F gene is not S-phase regulated. Nucleic Acids Res *17*, 1745-1756.

Daniel, R., Ramcharan, J., Rogakou, E., Taganov, K. D., Greger, J. G., Bonner, W. M., Nussenzweig, A., Katz, R. A., and Skalka, A. M. (2004). Histone H2AX is phosphorylated at sites of retroviral DNAintegration but is dispensable for postintegration repair. J Biol Chem *279*, 45810-45814.

De Lucia, F., Faraone-Mennella, M. R., D'Erme, M., Quesada, P., Caiafa, P., and Farina, B. (1994). Histone-induced condensation of rat testis chromatin: testis-specific H1t versus somatic H1 variants. Biochem Biophys Res Commun *198*, 32-39.

Demeler, B. (2005). UltrScan A Comprehensive Data Analysis Software Package for Analytical Ultracentrifugation Experiments. Modern Analytical Ultracentrifugation:

Techniques and Methods. . In, D.J. Scott, Hardfing, S.E., Rowe, A.J., ed. (UK: Royal Society of Chemistry), pp. 210 - 229.

Deterding, L. J., Banks, G. C., Tomer, K. B., and Archer, T. K. (2004). Understanding global changes in histone H1 phosphorylation using mass spectrometry. Methods *33*, 53-58.

Downs, J. A., Allard, S., Jobin-Robitaille, O., Javaheri, A., Auger, A., Bouchard, N., Kron, S. J., Jackson, S. P., and Cote, J. (2004a). Binding of chromatin-modifying activities to phosphorylated histone H2A at DNA damage sites. Mol Cell *16*, 979-990.

Downs, J. A., Allard, S., Jobin-Robitaille, O., Javaheri, A., Auger, A., Bouchard, N., Kron, S. J., Jackson, S. P., and Cote, J. (2004b). Binding of chromatin-modifying activities to phosphorylated histone H2A at DNA damage sites. Mol Cell *16*, 979-990.

Downs, J. A., Kosmidou, E., Morgan, A., and Jackson, S. P. (2003). Suppression of homologous recombination by the *Saccharomyces cerevisiae* linker histone. Mol Cell *11*, 1685-1692.

Downs, J. A., Lowndes, N. F., and Jackson, S. P. (2000). A role for Saccharomyces cerevisiae histone H2A in DNA repair. Nature *408*, 1001-1004.

Doyen, C. M., Montel, F., Gautier, T., Menoni, H., Claudet, C., Delacour-Larose, M., Angelov, D., Hamiche, A., Bednar, J., Faivre-Moskalenko, C.*, et al.* (2006). Dissection of the unusual structural and functional properties of the variant H2A.Bbd nucleosome. Embo J *25*, 4234-4244.

Doyon, Y., Selleck, W., Lane, W. S., Tan, S., and Cote, J. (2004). Structural and functional conservation of the NuA4 histone acetyltransferase complex from yeast to humans. Mol Cell Biol *24*, 1884-1896.

Drouet, J., Delteil, C., Lefrancois, J., Concannon, P., Salles, B., and Calsou, P. (2004). DNA-PK and XRCC4/DNA ligase IV Mobilization in the cell in response to DNA double-strand breaks. J Biol Chem.

Dryhurst, D., Thambirajah, A. A., and Ausio, J. (2004). New twists on H2A.Z: a histone variant with a controversial structural and functional past. Biochem Cell Biol *82*, 490-497.

Eickbush, T. H., and Moudrianakis, E. N. (1978). The histone core complex: an octamer assembled by two sets of protein-protein interactions. Biochemistry *17*, 4955-4964.

Eirín-López, J. M., Frehlick, L. J., and Ausió, J. (2006). Protamines, in the footsteps of linker histone evolution. J Biol Chem *281*, 1-4.

Eirin-Lopez, J. M., Ishibashi, T., and Ausio, J. (2008). H2A.Bbd: a quickly evolving hypervariable mammalian histone that destabilizes nucleosomes in an acetylation-independent way. Faseb J *22*, 316-326.

Ekwall, H., Jansson, A., Sjoberg, P., and Ploen, L. (1984). Differentiation of the rat testis between 20 and 120 days of age. Arch Androl *13*, 27-36.

Fernandez-Capetillo, O., Allis, C. D., and Nussenzweig, A. (2004). Phosphorylation of histone H2B at DNA double-strand breaks. J Exp Med *199*, 1671-1677.

Fink, M., Imholz, D., and Thoma, F. (2007). Contribution of the serine 129 of histone H2A to chromatin structure. Mol Cell Biol *27*, 3589-3600.

Flaus, A., Rencurel, C., Ferreira, H., Wiechens, N., and Owen_Hughes, T. (2004). Sin mutations alter inherent nucleosome mobility. The Embo Journal *23*, 343-353.

Frehlick, L. J., Eirin-Lopez, J. M., Jeffery, E. D., Hunt, D. F., and Ausio, J. (2006). The characterization of amphibian nucleoplasmins yields new insight into their role in sperm chromatin remodeling. BMC Genomics *7*, 99.

Frehlick, L. J., Prado, A., Calestagne-Morelli, A., and Ausio, J. (2007). Characterization of the PL-I-Related SP2 Protein from Xenopus. Biochemistry *46*, 12700-12708.

Garcia, B. A., Busby, S. A., Barber, C. M., Shabanowitz, J., Allis, C. D., and Hunt, D. F. (2004). Characterization of phosphorylation sites on histone H1 isoforms by tandem mass spectrometry. J Proteome Res *3*, 1219-1227.

Garcia, B. A., Joshi, S., Thomas, C. E., Chitta, R. K., Diaz, R. L., Busby, S. A., Andrews, P. C., Ogorzalek Loo, R. R., Shabanowitz, J., Kelleher, N. L.*, et al.* (2006). Comprehensive phosphoprotein analysis of linker histone H1 from Tetrahymena thermophila. Mol Cell Proteomics *5*, 1593-1609.

Garcia, B. A., Mollah, S., Ueberheide, B. M., Busby, S. A., Muratore, T. L., Shabanowitz, J., and Hunt, D. F. (2007). Chemical derivatization of histones for facilitated analysis by mass spectrometry. Nat Protoc *2*, 933-938.

Garcia Ramirez, M., Dong, F., and Ausió, J. (1992). Role of the histone "tails" in the folding of oligonucleosomes depleted of histone H1. J Biol Chem *267*, 19587-19595.

Garcia Ramirez, M., Rocchini, C., and Ausió, J. (1995). Modulation of chromatin folding by histone acetylation. J Biol Chem *270*, 17923-17928.

Gatewood, J. M., Cook, G. R., Balhorn, R., Bradbury, E. M., and Schmid, C. W. (1987). Sequence-specific packaging of DNA in human sperm chromatin. Science *236*, 962-964.

Gatewood, J. M., Cook, G. R., Balhorn, R., Schmid, C. W., and Bradbury, E. M. (1990). Isolation of four core histones from human sperm chromatin representing a minor subset of somatic histones. J Biol Chem *265*, 20662-20666.

Gautier, T., Abbott, D. W., Molla, A., Verdel, A., Ausio, J., and Dimitrov, S. (2004). Histone variant H2ABbd confers lower stability to the nucleosome. EMBO Rep *5*, 715-720.

Geourjon, C., and Deleage, G. (1994). SOPM: a self-optimized method for protein secondary structure prediction. Prot Eng *7*, 157-164.

Godde, J. S., and Ura, K. (2008). Cracking the Enigmatic Linker Histone Code. J Biochem.

Gonzalez-Romero, R., Mendez, J., Ausio, J., and Eirin-Lopez, J. M. (2008). Quickly evolving histones, nucleosome stability and chromatin folding: all about histone H2A.Bbd. Gene *413*, 1-7.

Goodarzi, A. A., and Lees-Miller, S. P. (2004). Biochemical characterization of the ataxia-telangiectasia mutated (ATM) protein from human cells. DNA Repair (Amst) *3*, 753-767.

Govin, J., Caron, C., Lestrat, C., Rousseaux, S., and Khochbin, S. (2004). The role of histones in chromatin remodelling during mammalian spermiogenesis. Eur J Biochem *271*, 3459-3469.

Grandy, D. K., Engel, J. D., and Dodgson, J. B. (1982). Complete nucleotide sequence of a chicken H2b histone gene. J Biol Chem *257*, 8577-8580.

Gusse, M., Sautiere, P., Belaiche, D., Martinage, A., Roux, C., Dadoune, J. P., and Chevaillier, P. (1986). Purification and characterization of nuclear basic proteins of human sperm. Biochimica Et Biophysica Acta *884*, 124-134.

Hall, T. A. (1999). BioEdit: a user friendly biological sequence alignment editor and analysis program for Windows 95/98/NT. Nucleic Acids Symposium Series *41*, 95-98.

Hamer, G., Roepers-Gajadien, H. L., van Duyn-Goedhart, A., Gademan, I. S., Kal, H. B., van Buul, P. P., and de Rooij, D. G. (2003). DNA double-strand breaks and gamma-H2AX signaling in the testis. Biol Reprod *68*, 628-634.

Hamiche, A., Kang, J. G., Dennis, C., Xiao, H., and Wu, C. (2001). Histone tails modulate nucleosome mobility and regulate ATP-dependent nucleosome sliding by NURF. Proc Natl Acad Sci USA *98*, 14316-14321.

Hammoud, S. S., Nix, D. A., Zhang, H., Purwar, J., Carrell, D. T., and Cairns, B. R. (2009). Distinctive chromatin in human sperm packages genes for embryo development. Nature *460*, 473-478.

Hansen, J. C., Tse, C., and Wolffe, A. P. (1998). Structure and function of the core histone N-termini: more than meets the eye. Biochemistry *37*, 17637-17641.

Harvey, A. C., Jackson, S. P., and Downs, J. A. (2005). Saccharomyces cerevisiae histone H2A Ser122 facilitates DNA repair. Genetics *170*, 543-553.

Hendzel, M. J., Lever, M. A., Crawford, E., and Th'ng, J. P. (2004). The C-terminal domain is the primary determinant of histone H1 binding to chromatin in vivo. J Biol Chem *279*, 20028-20034.

Henikoff, S., Henikoff, J. G., Sakai, A., Loeb, G. B., and Ahmad, K. (2008). Genome-wide profiling of salt fractions maps physical properties of chromatin. Genome Res.

Heo, K., Kim, H., Choi, S. H., Choi, J., Kim, K., Gu, J., Lieber, M. R., Yang, A. S., and An, W. (2008). FACT-mediated exchange of histone variant H2AX regulated by phosphorylation of H2AX and ADP-ribosylation of Spt16. Mol Cell *30*, 86-97.

Hohmann, P. (1983). Phosphorylation of H1 histones. Mol Cell Biochem *57*, 81-92.

Howe, L., and Ausió, J. (1998). Nucleosome translational position, not histone acetylation, determines TFIIIA binding to nucleosomal Xenopus laevis 5S rRNA genes. Mol Cell Biol *18*, 1156-1162.

Howe, L., Iskandar, M., and Ausió, J. (1998). Folding of chromatin in the presence of heterogeneous histone H1 binding to nucleosomes. J Bioll Chem *273*, 11625-11629.

Hoyer-Fender, S., Singh, P. B., and Motzkus, D. (2000). The murine heterochromatin protein M31 is associated with the chromocenter in round spermatids and is a component of mature spermatozoa. Exp Cell Res *254*, 72-79.

Hua, S., Kallen, C. B., Dhar, R., Baquero, M. T., Mason, C. E., Russell, B. A., Shah, P. K., Liu, J., Khramtsov, A., Tretiakova, M. S.*, et al.* (2008). Genomic analysis of estrogen cascade reveals histone variant H2A.Z associated with breast cancer progression. Mol Syst Biol *4*, 188.

Huen, M. S., Grant, R., Manke, I., Minn, K., Yu, X., Yaffe, M. B., and Chen, J. (2007). RNF8 transduces the DNA-damage signal via histone ubiquitylation and checkpoint protein assembly. Cell *131*, 901-914.

Hunter, N., Valentin Borner, G., Lichten, M., and Kleckner, N. (2001). Gamma-H2AX illuminates meiosis. Nature Genet *27*, 236-238.

Huyen, Y., Zgheib, O., Ditullio, R. A., Jr., Gorgoulis, V. G., Zacharatos, P., Petty, T. J., Sheston, E. A., Mellert, H. S., Stavridi, E. S., and Halazonetis, T. D. (2004). Methylated lysine 79 of histone H3 targets 53BP1 to DNA double-strand breaks. Nature *432*, 406-411.

Ikura, T., Ogryzko, V. V., Grigoriev, M., Groisman, R., Wang, J., Horikoshi, M., Scully, R., Qin, J., and Nakatani, Y. (2000). Involvement of the TIP60 histone acetylase complex in DNA repair and apoptosis. Cell *102*, 463-473.

Ikura, T., Tashiro, S., Kakino, A., Shima, H., Jacob, N., Amunugama, R., Yoder, K., Izumi, S., Kuraoka, I., Tanaka, K.*, et al.* (2007). DNA damage-dependent acetylation and ubiquitination of H2AX enhances chromatin dynamics. Mol Cell Biol *27*, 7028-7040.

Ishibashi, T., Dryhurst, D., Rose, K. L., Shabanowitz, J., Hunt, D. F., and Ausio, J. (2009a). Acetylation of vertebrate H2A.Z and its effect on the structure of the nucleosome. Biochemistry *48*, 5007-5017.

Ishibashi, T., Li, A., Eirin-Lopez, J. M., Zhao, M., Missiaen, K., Abbott, D. W., Meistrich, M., Hendzel, M. J., and Ausio, J. (2009b). H2A.Bbd: an X-chromosome-encoded histone involved in mammalian spermiogenesis. Nucleic Acids Res.

Ismail, I. H., and Hendzel, M. J. (2008). The gamma-H2A.X: is it just a surrogate marker of double-strand breaks or much more? Environ Mol Mutagen *49*, 73-82.

Jason, L. J., Finn, R. M., Lindsey, G., and Ausio, J. (2005). Histone H2A ubiquitination does not preclude histone H1 binding, but it facilitates its association with the nucleosome. J Biol Chem *280*, 4975-4982.

Javaheri, A., Wysocki, R., Jobin-Robitaille, O., Altaf, M., Cote, J., and Kron, S. J. (2006). Yeast G1 DNA damage checkpoint regulation by H2A phosphorylation is independent of chromatin remodeling. Proc Natl Acad Sci U S A *103*, 13771-13776.

Kao, G. D., McKenna, W. G., Guenther, M. G., Muschel, R. J., Lazar, M. A., and Yen, T. J. (2003). Histone deacetylase 4 interacts with 53BP1 to mediate the DNA damage response. J Cell Biol *160*, 1017-1027.

Kaszas, E., and Cande, W. Z. (2000). Phosphorylation of histone H3 is correlated with changes in the maintenance of sister chromatid cohesion during meiosis in maize, rather than the condensation of the chromatin. J Cell Sci *113*, 3217-3226.

Khadake, J. R., Markose, E. R., and Rao, M. R. (1994). Testis-specific histone (H1t) is not phosphorylated and has a weak interaction with chromatin. Indian J Biochem Biophys *31*, 335-338.

Kim, J. A., Kruhlak, M., Dotiwala, F., Nussenzweig, A., and Haber, J. E. (2007). Heterochromatin is refractory to gamma-H2AX modification in yeast and mammals. J Cell Biol *178*, 209-218.

Kistler, W. S., Geroch, M. E., and Williams-Ashman, H. G. (1973). Specific basic proteins from mammalian testes. Isolation and properties of small basic proteins from rat testes and epididymal spermatozoa. J Biol Chem *248*, 4532-4543.

Kistler, W. S., Henriksen, K., Mali, P., and Parvinen, M. (1996). Sequential expression of nucleoproteins during rat spermiogenesis. Exp Cell Res *225*, 374-381.

Krebs, J. E. (2007). Moving marks: dynamic histone modifications in yeast. Mol Biosyst *3*, 590-597.

Krogan, N. J., Keogh, M. C., Datta, N., Sawa, C., Ryan, O. W., Ding, H., Haw, R. A., Pootoolal, J., Tong, A., Canadien, V*., et al.* (2003). A Snf2 family ATPase complex required for recruitment of the histone H2A variant Htz1. Mol Cell *12*, 1565-1576.

Krogh, B. O., and Symington, L. S. (2004). Recombination Proteins in Yeast. Annu Rev Genet *38*, 233-271.

Kumar, S., and Hedges, S. B. (1998). A molecular timescale for vertebrate evolution. Nature *392*, 917-920.

Kurimasa, A., Ouyang, H., Dong, L., Wang, S., Li, X., Cordon-Cardo, C., Chen, D. J., and Li, G. C. (1999). Catalytic subunit of DNA-dependent protein kinase: impact on lymphocyte development and tumorigenesis. Proc Natl Acad Sci USA *96*, 1403-1408.

Kurtz, K., Saperas, N., Ausio, J., and Chiva, M. (2009). Spermiogenic nuclear protein transitions and chromatin condensation. Proposal for an ancestral model of nuclear spermiogenesis. J Exp Zoolog B Mol Dev Evol.

Kusch, T., Florens, L., MacDonald, W. H., Swanson, S. K., Glaser, R. L., Yates III, J. R., Abmaryr, S. M., Washburn, M. P., and Workman, J. L. (2004). Acetylation by Tip60 is required for selective histone variant exchange at DNA lesions. Science *306*, 2084-2087.

Kysela, B., Chovanec, M., and Jeggo, P. A. (2005). Phosphorylation of linker histones by DNA-dependent protein kinase is required for DNA ligase IV-dependent ligation in the presence of histone H1. Proc Natl Acad Sci USA *102*, 1877-1882.

Laemmli, U. K. (1970). Cleavage of structural proteins during the assembly of the head of bacteriophage T4. Nature *227*, 680-685.

Lennox, R. W., and Cohen, L. H. (1984). The alterations in H1 histone complement during mouse spermatogenesis and their significance for H1 subtype function. Dev Biol *103*, 80-84.

Lewis, J., Song, Y., de Jong, M., Bagha, S., and Ausió, J. (2003a). A walk though vertebrate and invertebrate protamines. Chromosoma *111*, 473-482.

Lewis, J. D., Abbott, D. W., and Ausio, J. (2003b). A haploid affair: core histone transitions during spermatogenesis. Biochem Cell Biol *81*, 131-140.

Lewis, J. D., Abbott, D. W., and Ausio, J. (2003c). A haploid affair: core histone transitions during spermatogenesis. Biochem Cell Biol *81*, 131-140.

Lewis, J. D., Abbott, D. W., and Ausio, J. (2003d). A haploid affair: core histone transitions during spermatogenesis. Biochemistry and Cell Biology = Biochimie Et Biologie Cellulaire *81*.

Lewis, J. D., Song, Y., de Jong, M. E., Bagha, S. M., and Ausio, J. (2003e). A walk though vertebrate and invertebrate protamines. Chromosoma *111*, 473-482.

Li, A., Eirin-Lopez, J. M., and Ausio, J. (2005a). H2AX: tailoring histone H2A for chromatin-dependent genomic integrity. Biochem Cell Biol *83*, 505-515.

Li, A., Maffey, A. H., Abbott, W. D., Conde e Silva, N., Prunell, A., Siino, J., Churikov, D., Zalensky, A. O., and Ausio, J. (2005b). Characterization of nucleosomes consisting of the human testis/sperm-specific histone H2B variant (hTSH2B). Biochemistry *44*, 2529-2535.

Lin, Q., Sirotkin, A., and Skoultchi, A. I. (2000). Normal spermatogenesis in mice lacking the testis-specific linker histone H1t. Mol Cell Biol *20*, 2122-2128.

Lu, X., and Hansen, J. C. (2004). Identification of specific functional subdomains within the linker histone H10 C-terminal domain. J Biol Chem *279*, 8701-8707.

Luger, K., Mader, A. W., Richmond, R. K., Sargent, D. F., and Richmond, T. J. (1997). Crystal structure of the nucleosome core particle at 2.8 A resolution. Nature *389*, 251-260.

Maffey, A. H., Ishibashi, T., He, C., Wang, X., White, A. R., Hendy, S. C., Nelson, C. C., Rennie, P. S., and Ausio, J. (2007). Probasin promoter assembles into a strongly positioned nucleosome that permits androgen receptor binding. Mol Cell Endocrinol.

Mahadevaiah, S. K., Turner, J. M., Baudat, F., Rogakou, E. P., de Boer, P., Blanco-Rodriguez, J., Jasin, M., Keeney, S., Bonner, W. M., and Burgoyne, P. S. (2001a). Recombinational DNA double strand breaks in mice precede synapsis. Nat Genet *27*, 271-276.

Mahadevaiah, S. K., Turner, J. M., Baudat, F., Rogakou, E. P., de_Boer, P., Blanco_Rodriguez, J., Jasin, M., Keeney, S., Bonner, W. M., and Burgoyne, P. S.

(2001b). Recombinational DNA double-strand breaks in mice precede synapsis. Nature Genetics *27*, 271-276.

Mahaney, B. L., Meek, K., and Lees-Miller, S. P. (2009). Repair of ionizing radiation-induced DNA double-strand breaks by non-homologous end-joining. Biochem J *417*, 639-650.

Mailand, N., Bekker-Jensen, S., Faustrup, H., Melander, F., Bartek, J., Lukas, C., and Lukas, J. (2007). RNF8 ubiquitylates histones at DNA double-strand breaks and promotes assembly of repair proteins. Cell *131*, 887-900.

Malik, H. S., and Henikoff, S. (2003). Phylogenomics of the nucleosome. Nature Struct Biol *10*, 882-891.

Mannironi, C., Bonner, W. M., and Hatch, C. L. (1989). H2A.X, a histone isoprotein with a conserved C-terminal sequence, is encoded by a novel mRNA with both DNA replication type and polyA 3' processing signals. Nucleic Acids Res *17*, 9113-9126.

Marchetti, F., Essers, J., Kanaar, R., and Wyrobek, A. J. (2007). Disruption of maternal DNA repair increases sperm-derived chromosomal aberrations. Proc Natl Acad Sci U S A *104*, 17725-17729.

Marino-Ramirez, L., Kann, M. G., Shoemaker, B. A., and Landsman, D. (2005). Histone structure and nucleosome stability. Expert Rev Proteomics *2*, 719-729.

Markose, E. R., and Rao, M. R. (1985). Testis-specific histone H1t is antigenically distinct among H1 subtypes. J Biol Chem *260*, 16263-16268.

Martin, S. E., Shabanowitz, J., Hunt, D. F., and Marto, J. A. (2000). Subfemtomole MS and MS/MS peptide sequence analysis using nano-HPLC micro-ESI fourier transform ion cyclotron resonance mass spectrometry. Anal Chem *72*, 4266-4274.

Marushige, K. (1976). Activation of chromatin by acetylation of histone side chains. Proc Natl Acad Sci U S A *73*, 3937-3941.

Masumoto, H., Hawke, D., Kobayashi, R., and Verreault, A. (2005). A role for cell-cycle-regulated histone H3 lysine 56 acetylation in the DNA damage response. Nature *436*, 294-298.

McManus, K. J., and Hendzel, M. J. (2005). ATM-dependent DNA damage-independent mitotic phosphorylation of H2AX in normally growing mammalian cells. Mol Biol Cell *16*, 5013-5025.

Meek, K., Dang, V., and Lees-Miller, S. P. (2008). DNA-PK: the means to justify the ends? Adv Immunol *99*, 33-58.

Meersseman, G., Pennings, S., and Bradbury, E. M. (1991). Chromatosome positioning on assembled long chromatin. Linker histones affect nucleosome placement on 5 S rDNA. J Mol Biol *220*, 89-100.

Meetei, A. R., Ullas, K. S., Vasupradha, V., and Rao, M. R. (2002). Involvement of protein kinase A in the phosphorylation of spermatidal protein TP2 and its effect on DNA condensation. Biochemistry *41*, 185-195.

Meistrich, M. L. (1977). Separation of spermatogenic cells and nuclei from rodent testes. Met Cell Biol *15*, 15-54.

Meistrich, M. L. (1989). Histone and basic nuclear prtein transitions in mammalian spermatogenesis (Boca Raton FL: CRC Press).

Meistrich, M. L., Brock, W. A., Grimes, S. R., Platz, R. D., and Hnilica, L. S. (1978). Nuclear protein transitions during spermatogenesis. Fed Proc *37*, 2522-2525.

Meistrich, M. L., Bucci, L. R., Trostle-Weige, P. K., and Brock, W. A. (1985). Histone variants in rat spermatogonia and primary spermatocytes. Dev Biol *112*, 230-240.

Meistrich, M. L., Trostle-Weige, P. K., Lin, R., Bhatnagar, Y. M., and Allis, C. D. (1992). Highly acetylated H4 is associated with histone displacement in rat spermatids. Mol Reprod Dev *31*, 170-181.

Meistrich, M. L., Trostle-Weige, P. K., and Van Beek, M. E. (1994). Separation of specific stages of spermatids from vitamin A-synchronized rat testes for assessment of nucleoprotein changes during spermiogenesis. Biol Reprod *51*, 334-344.

Meneghini, M. D., Wu, M., and Madhani, H. D. (2003). Conserved histone variant H2A.Z protects euchromatin from the ectopic spread of silent heterochromatin. Cell *112*, 725-736.

Millar, C. B., Guy, J., Sansom, O. J., Selfridge, J., MacDougall, E., Hendrich, B., Keightley, P. D., Bishop, S. M., Clarke, A. R., and Bird, A. (2002). Enhanced CpG mutability and tumorigenesis in MBD4-deficient mice. Science *297*, 403-405.

Mizuguchi, G., Shen, X., Landry, J., Wu, W. H., Sen, S., and Wu, C. (2004). ATP-driven exchange of histone H2AZ variant catalyzed by SWR1 chromatin remodeling complex. Science *303*, 343-348.

Montel, F., Fontaine, E., St-Jean, P., Castelnovo, M., and Faivre-Moskalenko, C. (2007). Atomic force microscopy imaging of SWI/SNF action: mapping the nucleosome remodeling and sliding. Biophys J *93*, 566-578.

Moore, J. D., and Krebs, J. E. (2004). Histone modifications and DNA double-strand break repair. Biochem Cell Biol *82*, 446-452.

Moore, J. D., Yazgan, O., Ataian, Y., and Krebs, J. E. (2007). Diverse roles for histone H2A modifications in DNA damage response pathways in yeast. Genetics *176*, 15-25.

Morrison, A. J., Highland, J., Krogan, N. J., Arbel-Eden, A., Greenblatt, J. F., Haber, J. E., and Shen, X. (2004). INO80 and gamma-H2AX interaction links ATP-dependent chromatin remodeling to DNA damage repair. Cell *119*, 767-775.

Morrison, A. J., and Shen, X. (2005). DNA repair in the context of chromatin. Cell Cycle *4*, 568-571.

Murr, R., Loizou, J. I., Yang, Y. G., Cuenin, C., Li, H., Wang, Z. Q., and Herceg, Z. (2006). Histone acetylation by Trrap-Tip60 modulates loading of repair proteins and repair of DNA double-strand breaks. Nature cell biology *8*, 91-99.

Nazarov, I., Schlyachtenko, L., Lyubchenko, Y., Zalenskaya, I., and Zalensky, A. (2008). Characterization of soluble chromatin released from human sperm nuclei. Arch Androl : J Rep Syst *54*, 1-10.

Nazarov, I. B., Smirnova, A. N., Krutilina, R. I., Solovjeva, L. V., Nikiforov, A. A., Oei, S.-L., Zalenskaya, I. A., Yau, P. M., Bradbury, E. M., and Tomilin, N. V. (2003). Dephosphorylation of Histone γ-H2AX during Repair of DNA Double-Strand Breaks in Mammalian Cells and its Inhibition by Calyculin A. Rad Res *160*, 309-317.

Nurse, P. (1991). The Florey Lecture, 1990. How is the cell division cycle regulated? Philos Trans R Soc Lond B Biol Sci *332*, 271-276.

Ohe, Y., Hayashi, H., and Iwai, K. (1979). Human spleen histone H2B. Isolation and amino acid sequence. J Biochem (Tokyo) *85*, 615-624.

Okuwaki, M., Kato, K., Shimahara, H., Tate, S. I., and Nagata, K. (2005). Assembly and Disassembly of Nucleosome Core Particles Containing Histone Variants by Human Nucleosome Assembly Protein I. Mol Cell Biol *25*, 10639-10651.

Oliva, R., and Dixon, G. H. (1991). Vertebrate protamine genes and the histone-to-protamine replacement reaction. Progress in Nucleic Acid Research and Molecular Biology *40*, 25-94.

Olsen, J. V., Blagoev, B., Gnad, F., Macek, B., Kumar, C., Mortensen, P., and Mann, M. (2006). Global, in vivo, and site-specific phosphorylation dynamics in signaling networks. Cell *127*, 635-648.

Orsi, G. A., Couble, P., and Loppin, B. (2009). Epigenetic and replacement roles of histone variant H3.3 in reproduction and development. Int J Dev Biol *53*, 231-243.

Osley, M. A. (2004). H2B ubiquitylation: the end is in sight. Biochimica Et Biophysica Acta *1677*, 74-78.

Palmer, D. K., O_Day, K., Trong, H. L., Charbonneau, H., and Margolis, R. L. (1991). Purification of the centromere-specific protein CENP-A and demonstration that it is a distinctive histone. Proc Natl Acad Sci USA *88*, 3734-3738.

Panyim, S., and Chalkley, R. (1969). High resolution acrylamide gel electrophoresis of histones. Arch Biochem Biophys *130*, 337-346.

Park, E., Chan, D. W., Park, J., Oettinger, M. A., and Kwon, J. (2003a). DNA-PK is activated by nucleosomes and phosphorylates H2AX within the nucleosomes in an acetylation-dependent manner. Nucleic Acids Res *31*, 6819-6827.

Park, E. J., Chan, D. W., Park, J. H., Oettinger, M. A., and Kwon, J. (2003b). DNA-PK is activated by nucleosomes and phosphorylates H2AX within the nucleosomes in an acetylation-dependent manner. Nucleic Acids Res *31*, 6819-6827.

Park, Y.-J., Dyer, P.N., Tremethick, D.J., and Luger, K. (2004). A new FRET approach demonstrates that the histone variant H2A.Z stabilizes the histone octamer within the nucleosome. J Biol Chem.

Paull, T. T., Rogakou, E. P., Yamazaki, V., Kirchgessner, C. U., Gellert, M., and Bonner, W. M. (2000). A critical role for histone H2AX in recruitment of repair factors to nuclear foci after DNA damage. Curr Biol *10*, 886-895.

Pehrson, J. R., Costanzi, C., and Dharia, C. (1997). Developmental and tissue expression patterns of histone macroH2A1 subtypes. J Cell Biochem *65*, 107-113.

Pehrson, J. R., and Fried, V. A. (1992). MacroH2A, a core histone containing a large nonhistone region. Science *257*, 1398-1400.

Perry, M., and Chalkley, R. (1982). Histone acetylation increases the solubility of chromatin and occurs sequentially over most of the chromatin. A novel model for the biological role of histone acetylation. J Biol Chem *257*, 7336-7347.

Pilch, D. R., Sedelnikova, O., Redon, C., Celeste, A., Nussenzweig, A., and Bonner, W. M. (2003a). Characteristics of γ-H2AX foci at DNA double-strand breaks sites. Biochem Cell Biol *81*, 123-129.

Pilch, D. R., Sedelnikova, O. A., Redon, C., Celeste, A., Nussenzweig, A., and Bonner, W. M. (2003b). Characteristics of gamma-H2AX foci at DNA double-strand breaks sites. Biochem Cell Biol *81*, 123-129.

Pineiro, M., Puerta, C., and Palacian, E. (1991). Yeast nucleosomal particles: structural and transcriptional properties. Biochemistry *30*, 5805-5810.

Pinto, D. M., and Flaus, A. Structure and Function of Histone H2AX. Sub-cellular biochemistry *50*, 55-78.

Pirhonen, A., Linnala-Kankkunen, A., and Menpaa, P. H. (1994). P2 protamines are phosphorylated in vitro by protein kinase C, whereas P1 protamines prefer cAMP-dependent protein kinase. A comparative study of five mammalian species. Eur J Biochem *223*, 165-169.

Platz, R. D., Meistrich, M. L., and Grimes, S. R., Jr. (1977). Low-molecular-weight basic proteins in spermatids. Methods Cell Biol *16*, 297-316.

Rall, S. C., and Cole, R. D. (1971). Amino acid sequence and sequence variability of the amino-terminal regions of lysine-rich histones. J Biol Chem *246*, 7175-7190.

Ramakrishnan, V., Finch, J. T., Graziano, V., Lee, P. L., and Sweet, R. M. (1993). Crystal structure of globular domain of histone H5 and its implications for nucleosome binding. Nature *362*, 219-223.

Rattner, J. B., Hendzel, M. J., Furbee, C. S., Muller, M. T., and Bazett-Jones, D. P. (1996). Topoisomerase II alpha is associated with the mammalian centromere in a cell cycle- and species-specific manner and is required for proper centromere/kinetochore structure. J Cell Biol *134*, 1097-1107.

Recht, J., and Osley, M. A. (1999). Mutations in both the structured domain and N-terminus of histone H2B bypass the requirement for Swi-Snf in yeast. The Embo Journal *18*, 229-240.

Retief, J. D., Winkfein, R. J., Dixon, G. H., Adroer, R., Queralt, R., Ballabriga, J., and Oliva, R. (1993). Evolution of protamine P1 genes in primates. J Mol Evol *37*, 426-434.

Rogakou, E. P., Boon, C., Redon, C., and Bonner, W. M. (1999). Megabase chromatin domains involved in DNA double-strand breaks in vivo. J Cell Biol *146*, 905-916.

Rogakou, E. P., Nieves-Neira, W., Boon, C., Pommier, Y., and Bonner, W. M. (2000a). Initiation of DNA fragmentation during apoptosis induces phosphorylation of H2AX histone at serine 139. J Biol Chem *275*, 9390-9395.

Rogakou, E. P., Nieves-Neira, W., Boon, C., Pommier, Y., and Bonner, W. M. (2000b). Initiation of DNA fragmentation during apoptosis induces phosphorylation of H2AX histone at serine 139. J Biol Chem *275*, 9390-9395.

Rogakou, E. P., Pilch, D. R., Orr, A. H., Ivanova, V. S., and Bonner, W. M. (1998). DNA double-stranded breaks induce histone H2AX phosphorylation on serine 139. J Biol Chem *273*, 5858-5868.

Roque, A., Iloro, I., Ponte, I., Arrondo, J. L., and Suau, P. (2005). DNA-induced secondary structure of the carboxyl-terminal domain of histone H1. J Biol Chem *280*, 32141-32147.

Rose, K. L., Li, A., Zalenskaya, I., Zhang, Y., Unni, E., Hodgson, K. C., Yu, Y., Shabanowitz, J., Meistrich, M. L., Hunt, D. F., and Ausio, J. (2008). C-Terminal Phosphorylation of Murine Testis-Specific Histone H1t in Elongating Spermatids. J Proteome Res.

Sanders, M. M. (1978). Fractionation of nucleosomes by salt elution from micrococcal nuclease-digested nuclei. J Cell Biol *79*, 97-109.

Saperas, N., Chiva, M., Casas, M. T., Campos, J. L., Eirin-Lopez, J. M., Frehlick, L. J., Prieto, C., Subirana, J. A., and Ausio, J. (2006). A unique vertebrate histone H1-related protamine-like protein results in an unusual sperm chromatin organization. Febs J *273*, 4548-4561.

Sarcinella, E., Zuzarte, P. C., Lau, P. N., Draker, R. R., and Cheung, P. (2007). Monoubiquitylation of H2A.Z distinguishes its association with euchromatin or facultative heterochromatin. Mol Cell Biol.

Sarg, B., Helliger, W., Talasz, H., Forg, B., and Lindner, H. H. (2006). Histone H1 phosphorylation occurs site-specifically during interphase and mitosis: identification of a novel phosphorylation site on histone H1. J Biol Chem *281*, 6573-6580.

Scherthan, H. (2003). Knockout mice provide novel insights into meiotic chromosome and telomere dynamics. Cytogenet Genome Res *103*, 235-244.

Schneider, T. D., and Stephens, R. M. (1990). Sequence logos: a new way to display consensus sequences. Nucleic Acids Research *18*, 6097-6100.

Schroeder, M. J., Shabanowitz, J., Schwartz, J. C., Hunt, D. F., and Coon, J. J. (2004). A neutral loss activation method for improved phosphopeptide sequence analysis by quadrupole ion trap mass spectrometry. Anal Chem *76*, 3590-3598.

Seyedin, S. M., and Kistler, W. S. (1979). H1 histone subfractions of mammalian testes. 2. Organ specificity in mice and rabbits. Biochemistry *18*, 1376-1379.

Seyedin, S. M., and Kistler, W. S. (1980). Isolation and characterization of rat testis H1t. An H1 histone variant associated with spermatogenesis. J Biol Chem *255*, 5949-5954.

Shechter, D., Chitta, R. K., Xiao, A., Shabanowitz, J., Hunt, D. F., and Allis, C. D. (2009). A distinct H2A.X isoform is enriched in Xenopus laevis eggs and early embryos and is phosphorylated in the absence of a checkpoint. Proc Natl Acad Sci USA *106*, 749-754.

Siino, J. S., Nazarov, I. B., Svetlova, M. P., Adamson, R. H., Zalenskaya, I. A., Yau, P. M., Bradbury, E. M., and Tomilin, N. V. (2002a). Photobleaching of GFP-labeled H2AX in chromatin: H2AX has low diffusional mobility in the nucleus. Biochem Biophys Res Commun *297*, 1318-1323.

Siino, J. S., Nazarov, I. B., Svetlova, M. P., Solovjeva, L. V., Adamson, R. H., Zalenskaya, I. A., Yau, P. M., Bradbury, E. M., and Tomilin, N. V. (2002b). Photobleaching of GFP-labeled H2AX in chromatin: H2AX has low diffusional mobility in the nucleus. Biochem Biophys Res Commun *297*, 1318-1323.

Simon, R. H., and Felsenfeld, G. (1979). A new procedure for purifying histone pairs H2A + H2B and H3 + H4 from chromatin using hydroxylapatite. Nucleic Acids Res *6*, 689-696.

Simpson, R. T., Thoma, F., and Brubaker, J. M. (1985). Chromatin reconstituted from tandemly repeated cloned DNA fragments and core histones: a model system for study of higher order structure. Cell *42*, 799-808.

Sims, R. J., 3rd, Belotserkovskaya, R., and Reinberg, D. (2004). Elongation by RNA polymerase II: the short and long of it. Genes Dev *18*, 2437-2468.

Singleton, S., Mudrak, O., Morshedi, M., Oehninger, S., Zalenskaya, I., and Zalensky, A. (2007a). Characterisation of a human sperm cell subpopulation marked by the presence of the TSH2B histone. Reprod Fertil Dev *19*, 392-397.

Singleton, S., Zalensky, A., Doncel, G. F., Morshedi, M., and Zalenskaya, I. A. (2007b). Testis/sperm-specific histone 2B in the sperm of donors and subfertile patients: variability and relation to chromatin packaging. Hum Reprod *22*, 743-750.

Sivolob, A., Lavelle, C., and Prunell, A. (2003). Sequence-dependent nucleosome structural and dynamic polymorphism. Potential involvement of histone H2B N-terminal tail proximal domain. J Mol Biol *326*, 49-63.

Stewart, G. S., Wang, B., Bignell, C. R., Taylor, A. M. R., and Elledge, S. J. (2004). MDC1 is a mediator of the mammalian DNA damage checkpoint. Nature *421*, 961-966.

Stiff, T., O'Driscoll, M., Rief, N., Iwabuchi, K., Lobrich, M., and Jeggo, P. A. (2004a). ATM and DNA-PK function redundantly to phosphorylate H2AX after exposure to ionizing radiation. Cancer Res *64*, 2390-2396.

Stiff, T., O'Driscoll, M., Rief, N., Iwabuchi, K., Lobrich, M., and Jeggo, P. A. (2004b). ATM and DNA-PK function redundantly to phosphorylate H2AX after exposure to ionizing radiation. Cancer Res, 2390-2396.

Strahl, B. D., and Allis, C. D. (2000). The language of covalent histone modifications. Nature *403*, 41-45.

Suto, R. K., Clarkson, M. J., Tremethick, D. J., and Luger, K. (2000). Crystal structure of a nucleosome core particle containing the variant histone H2A.Z. Nature Structural Biology *7*, 1121-1124.

Syka, J. E., Coon, J. J., Schroeder, M. J., Shabanowitz, J., and Hunt, D. F. (2004). Peptide and protein sequence analysis by electron transfer dissociation mass spectrometry. Proc Natl Acad Sci U S A *101*, 9528-9533.

Tamburini, B. A., and Tyler, J. K. (2005). Localized histone acetylation and deacetylation triggered by the homologous recombination pathway of double-strand DNA repair. Mol Cell Biol *25*, 4903-4913.

Tanphaichitr, N., Sobhon, P., Taluppeth, N., and Chalermisarachai, P. (1978). Basic nuclear proteins in testicular cells and ejaculated spermatozoa in man. Exp Cell Res *117*, 347-356.

Taylor, A. M. R., Groom, A., and Byrd, P. J. (2004). Ataxia-telangiectasia-like disorder (ATLD)--its clinical presentation and molecular basis. DNA Repair *3*, 1219-1225.

Th'ng, J. P., Sung, R., Ye, M., and Hendzel, M. J. (2005). H1 family histones in the nucleus. Control of binding and localization by the C-terminal domain. J Biol Chem *280*, 27809-27814.

Thambirajah, A. A., Li, A., Ishibashi, T., and Ausio, J. (2009). New developments in post-translational modifications and functions of histone H2A variants. Biochem Cell Biol *87*, 7-17.

Thelestam, M., and Frisan, T. (2004). Cytolethal distending toxins. Rev Physiol Biochem Pharmacol *152*, 111-133.

Torgerson, D. G., and Singh, R. S. (2003). Sex-linked mammalian sperm proteins evolve faster than autosomal ones. Mol Biol Evol *20*, 1705-1709.

Trostle-Weige, P. K., Meistrich, M. L., Brock, W. A., and Nishioka, K. (1984). Isolation and characterization of TH3, a germ cell-specific variant of histone 3 in rat testis. J Biol Chem *259*, 8769-8776.

Unni, E., and Meistrich, M. L. (1992). Purification and characterization of the rat spermatid basic nuclear protein TP4. J Biol Chem *267*, 25359-25363.

van Attikum, H., Fritsch, O., Hohn, B., and Gasser, S. M. (2004a). Recruitment of the INO80 complex by H2A phosphorylation links ATP-dependent chromatin remodeling with DNA double-strand break repair. Cell *119*, 777-788.

van Attikum, H., Fritsch, O., Hohn, B., and Gasser, S. M. (2004b). Recruitment of the INO80 complex by H2A phosphorylation links ATP-dependent chromatin remodeling with DNA double-strand break repair. Cell *119*, 777-788.

van Holde, K. E., and Weischet, W.O. (1978). Boundary analysis of sedimentation velocity experiments with monodisperse and paucidisperse solutes. Biopolymers *17*, 1387-1403.

Vasireddy, R. S., Karagiannis, T. C., and El-Osta, A. (2009). gamma-radiation-induced gammaH2AX formation occurs preferentially in actively transcribing euchromatic loci. Cell Mol Life Sci.

Vastenhouw, N. L., Zhang, Y., Woods, I. G., Imam, F., Regev, A., Liu, X. S., Rinn, J., and Schier, A. F. (2010). Chromatin signature of embryonic pluripotency is established during genome activation. Nature *464*, 922-926.

Verdaguer, N., Perello, M., Palau, J., and Subirana, J. A. (1993). Helical structure of basic proteins from spermatozoa. Comparison with model peptides. Eur J Biochem *214*, 879-887.

Vila, R., Ponte, I., Collado, M., Arrondo, J. L., and Suau, P. (2001). Induction of secondary structure in a COOH-terminal peptide of histone H1 by interaction with the DNA: an infrared spectroscopy study. J Biol Chem *276*, 30898-30903.

Vila, R., Ponte, I., Jimenez, M. A., Rico, M., and Suau, P. (2000). A helix-turn motif in the C-terminal domain of histone H1. Protein Sci *9*, 627-636.

Wang, X., Moore, S. C., Laszckzak, M., and Ausió, J. (2000). Acetylation increases the alpha-helical content of the histone tails of the nucleosome. J Biol Chem *275*, 35013-35020.

Ward, I. M., and Chen, J. (2001). Histone H2AX is phosphorylated in an ATR-dependent manner in response to replicational stress. J Biol Chem *276*, 47759-47762.

Ward, I. M., Minn, K., Jorda, K. G., and Chen, J. (2003). Accumulation of checkpoint protein 53BP1 at DNA breaks involves its binding to phosphorylated histone H2AX. J Biol Chem *278*, 19579-19582.

Ward, W. S., and Coffey, D. S. (1991). DNA packaging and organization in mammalian spermatozoa: comparison with somatic cells. Biol Reprod *44*, 569-574.

West, M. H., and Bonner, W. M. (1980). Histone 2A, a heteromorphous family of eight protein species. Biochemistry *19*, 3238-3245.

Wisniewski, J. R., Zougman, A., Kruger, S., and Mann, M. (2007). Mass spectrometric mapping of linker histone H1 variants reveals multiple acetylations, methylations, and

phosphorylation as well as differences between cell culture and tissue. Mol Cell Proteomics *6*, 72-87.

Wyatt, H. R., Liaw, H., Green, G. R., and Lustig, A. J. (2003). Multiple roles for *Saccharomyces cerevisiae* histone H2A in telomere position effect, Spt phenotypes and double-strand-break repair. Genetics *164*, 47-64.

Wykes, S. M., and Krawetz, S. A. (2003). The structural organization of sperm chromatin. J Biol Chem *278*, 29471-29477.

Xiao, A., Li, H., Shechter, D., Ahn, S. H., Fabrizio, L. A., Erdjument-Bromage, H., Ishibe-Murakami, S., Wang, B., Tempst, P., Hofmann, K.*, et al.* (2009). WSTF regulates the H2A.X DNA damage response via a novel tyrosine kinase activity. Nature *457*, 57-62.

Xu, Y., Ashley, T., Brainerd, E. E., Bronson, R. T., Meyn, M. S., and Baltimore, D. (1996). Targeted disruption of ATM leads to growth retardation, chromosomal fragmentation during meiosis, immune defects, and thymic lymphoma. Genes Dev *10*, 2411-2422.

Yager, J. D., and Davidson, N. E. (2006). Estrogen carcinogenesis in breast cancer. N Engl J Med *354*, 270-282.

Yager, T. D., and van Holde, K. E. (1984). Dynamics and equilibria of nucleosomes at elevated ionic strength. J Biol Chem *259*, 4212-4222.

Zalenskaya, I. A., Bradbury, E. M., and Zalensky, A. O. (2000). Chromatin structure of telomere domain in human sperm. Biochem Biophys Res Commun *279*, 213-218.

Zalenskaya, I. A., and Zalensky, A. O. (2002). Telomeres in mammalian male germline cells. Intl Rev Cyt *218*, 37-67.

Zalensky, A. O., Siino, J. S., Gineitis, A. A., Zalenskaya, I. A., Tomilin, N. V., Yau, P., and Bradbury, E. M. (2002). Human testis/sperm-specific histone H2B (hTSH2B). Molecular cloning and characterization. J Biol Chem *277*, 43474-43480.

Zhang, H., Roberts, D. N., and Cairns, B. R. (2005). Genome-wide dynamics of Htz1, a histone H2A variant that poises repressed/basal promoters for activation through histone loss. Cell *123*, 219-231.

Zhang, Y., Griffin, K., Mondal, N., and Parvin, J. D. (2004). Phosphorylation of histone H2A inhibits transcription on chromatin templates. J Biol Chem *279*, 21866-21872.

Zhao, M., Rohozinski, J., Sharma, M., Ju, J., Braun, R. E., Bishop, C. E., and Meistrich, M. L. (2007). Utp14b: a unique retrogene within a gene that has acquired multiple promoters and a specific function in spermatogenesis. Dev Biol *304*, 848-859.

Zhao, M., Shirley, C. R., Hayashi, S., Marcon, L., Mohapatra, B., Suganuma, R., Behringer, R. R., Boissonneault, G., Yanagimachi, R., and Meistrich, M. L. (2004). Transition nuclear proteins are required for normal chromatin condensation and functional sperm development. Genesis *38*, 200-213.

Zhou, J., Fan, J. Y., Rangasamy, D., and Tremethick, D. J. (2007). The nucleosome surface regulates chromatin compaction and couples it with transcriptional repression. Nat Struct Mol Biol *14*, 1070-1076.

Zimmerman, E. S., Chen, J., Andersen, J. L., Ardon, O., DeHart, J. L., Blackett, J., Choudhary, S. K., Camerini, D., Nghiem, P., and Planelles, V. (2004). Human immunodeficiency virus type 1 Vpr-mediated G2 arrest requires Rad17 and Hus1 and induces nuclear BRCA1 and γ-H2AX focus Formation. Mol Cell Biol *24*, 9286-9294.